UNIVERSITY OF CALIFORNIA, SAN DIEGO

Nanoparticle Cloaking of Viral Vectors for Enhanced Gene Delivery

A dissertation submitted in partial satisfaction of the
requirements for the degree
Doctor of Philosophy

in

Bioengineering

by

Ajay Ajit Sapre

Committee in charge:

Professor Adam J. Engler, Chair
Professor Sadik C. Esener, Co-Chair
Professor Dennis A. Carson
Professor Michael J. Heller
Professor Yu-Tsueng Liu

2018

The dissertation of Ajay Ajit Sapre is approved, and it is acceptable in quality and form for publication on microfilm and electronically:

_____

_____

_____

_____
Co-Chair

_____
Chair

University of California, San Diego

2018

DEDICATION

To mom for her endless support.

TABLE OF CONTENTS

LIST OF FIGURES

LIST OF TABLES

ACKNOWLEDGEMENTS

First, I would like to thank Jared Fischer, PhD for his incredible hard work and dedication to all the *in vivo* experiments performed. The depth of experiments would not have been possible without his curiosity to try new things and his drive to perform numerous experiments. He was a pleasure to work with.

I would like to thank Sadik Esener, PhD for taking me in as first year graduate student looking to change labs. His hands off approach allowed me to grow as an independent researcher. The other graduate students in the lab were also very supportive and I learned a lot from Ya-San Yeh, PhD. Justin Plaut was another student who was a great sounding board for ideas. Though not technically part of the Esener lab, Laura Ruff PhD was great resource for all things molecular biology and her boss, Brad Messmer PhD, was always there to constructively tear down ideas and make beer bets. Dr. Y.T. Liu was always there to bounce ideas off and chat while at Moores Cancer Center. My graduate school experience was fulfilling because of some great friendships through UCSD. Gary Johnston never said no to go on an adventure in the mountains. Colton Llyod and Mehmet Badur shared some great coffee breaks. I would also like to thank Jan Lenington for sorting out all the administrative issues associated with moving mid-PhD.

At OHSU, Jonny Flores, Zeynep Sayar, Kyle Gustafson, Stephen Palani, and Anna Brown were great co-workers and friends. At the Knight Cancer Center for Early Detection Advanced Research Jakki Martinez was a wonderful lab manager

and helped with luciferase imaging and connecting us with Anupriya Agarwal, who assisted in running the serum cytokine assay. I would also like to thank the Sahay lab and Sun lab for being great lab neighbors.

My journey to and through graduate school would not have been complete without the total support of Lashanda Korley, PhD. Dr. Korley was a caring and thoughtful mentor throughout my undergraduate studies and during my time working in her lab. She has been very supportive and I cherish her mentorship.

Chapter 2 & 3, in part, is currently being prepared for submission for publication of the material. A. Sapre, G. Yong, Y. Yeh, L. Ruff, Z. Sayar, J. Plaut, J. Martinez, T. Nguyen, A. Agarwal, YT. Liu, B. Messmer, S. Esener, J. Fischer, "Silica Cloaking of Adenovirus Enhances Gene Delivery while Reducing Immunogenicity." *Nature Nanotechnology.* The dissertation author is the primary investigator and author of this material.

VITA

2010	B.S. in Biomedical Engineering *suma cum laude*, Case Western Reserve University, Cleveland, OH
2010	Graduate of National Outdoor Leadership School (NOLS), Patagonia, Chile
2011-2013	Chemist, Akzo Nobel Coatings, Strongsville, OH
2013	Chemist II, Akzo Nobel Coatings, Strongsville, OH
2013-2016	Graduate Research Assistant, University of California, San Diego, CA
2016-2018	Junior Investigator, Oregon Health Sciences University, Portland, OR
2018	Ph.D. in Bioengineering, University of California, San Diego, CA

PUBLICATIONS

A. Sapre, G. Yong, Y. Yeh, L. Ruff, Z. Sayar, J. Plaut, J. Martinez, T. Nguyen, A. Agarwal, YT. Liu, B. Messmer, S. Esener, J. Fischer, "Silica Cloaking of Adenovirus Enhances Gene Delivery while Reducing Immunogenicity." in preparation

A. Sapre, E. Novitskaya, V. Vakharia, A. Cota, W. Wrasdilo, S. Hanrahan, S. Derenzo, M. Makale, O. Graeve, "Optimized Scintillator YAG:Pr Nanoparticles for X-ray Inducible Photodynamic Therapy", *Materials Letters*, accepted.

S. Esener, N. Mokhtari, M. Vaidyanathan, Y. Yeh, B. Ahiska, A. Sapre, "Nano-Scale delivery device and applications thereof", provisional patent, 09/07/2017, 15/449, 83.

L. Ruff, A. Sapre, J. Plaut, E. De Maere, C. Mortier, V. Nguyen, K. Separa, S. Vandenbogaerde, L. Vandewalle, S. Esener, B. Messmer, "Selection of DNA nanoparticles with preferential binding to aggregated protein target", *Nucleic Acids Research*, 44, 10, 2016.

ABSTRACT OF THE DISSERTATION

Nanoparticle Cloaking of Viral Vectors for Enhanced Gene Delivery

by

Ajay Ajit Sapre

Doctor of Philosophy in Bioengineering

University of California, San Diego, 2018

Professor Adam J. Engler, Chair
Professor Sadik C. Esener, Co-Chair

Gene therapy has the potential to treat a wide range of diseases and ailments from cancer to blindness by altering or overcoming disease at its genetic roots. This is accomplished by adding or alternating genetic information of diseased tissue or at a distant site for systemic treatment. Genetically modified viruses are the most efficient tools for delivery of genes, but have significant side effects that have limited the success of clinical trials. Adenovirus (Ad) is a DNA virus that has been tested in over

100 clinical trials and is the focus of this dissertation. Innate and adaptive immune responses, hepatic clearance, and cellular tropism are the primary causes of poor Ad clinical translation. Cloaking technologies using synthetic or biologic materials have the potential to overcome these issues. Chapter 2 & 3 describes a method to address clinical barriers by encapsulating Ad in silica as a nanoparticle formulation. Silica is biodegradeable, biocompatible, and used in variety of nanoparticle formulations to enhance drug delivery. Silica encapsulated Ad (SiAd) enhances transduction and expands tropism *in vitro*. In immune-compromised mice, SiAd enhanced tumor transduction while reducing liver uptake and in immune-competent mice, SiAd reduced both the innate and adaptive immune response against Ad. As a model for cancer gene therapy, we used Ad expressing TNF-related apoptosis-inducing ligand (TRAIL) and show inhibited tumor growth with SiAd-TRAIL. In chapter 4, we explore applying the concepts of the previous chapters to Adeno-associated virus (AAV), which is another viral vector gaining traction for gene therapy in the clinic and one that is subject to similar barriers to clinical success as Ad. We explore exosome membrane cloaking and silica cloaking as methods to enhance AAV transduction *in vitro*. Overall, this dissertation covers techniques that seek to merge the efficiency of viral gene expression with the versatility of nanoparticle technology to address clinical challenges in the field of gene therapy.

Chapter 1

Introduction

1.1 Surpassing Evolution

We now live in an age where evolution is no longer a primary constraint on us as humans nor on the life we interact with, grow, eat, and use for our musings. We have gleaned some of the inner workings of biology and discovered tools that allow us to manipulate genes at will. Genetic aberration is really just genetic diversity in disguise. The basis for evolutionary success is this genetic diversity, where certain traits are lost or gained and selected out to pass on to future generations. At present, we possess the tools to act on these traits in individuals, but the future may hold a different story when genetic modifications to the human genome pass on from one generation to the next as permanent, augmented traits. We already do this to other organisms, whether that is genetically modifying a strain of rice to withstand drought or the generation of salmon that grow faster than their wild counterparts. It is only

a matter of time that we are faced with the reality of genetic engineering in humans. First, let us focus on the treatment of disease and meaningful patient outcomes.

1.2 Gene therapy

Gene therapy has conceptually been around for over 40 years, but has resulted in few successful clinical outcomes. In this time the field has tested the boundaries of clinical trials and the public's view of scientific research. At its core, gene therapy seeks to treat diseases derived from aberrant genes: genetic mutations or complete loss of genetic information. This concept came out of the finding that cells are able to express foreign DNA and in the late 1960s the discovery that certain viruses are able to stably integrate their genetic information into cells [1]. Shortly after, the advent of recombinant DNA, where part of the genomic information of one organism is expressed in another organism, generally in the form of a plasmid, allowed researchers to produce any known protein of interest. These findings allowed researchers to develop viruses which could produce any therapeutic protein. Though a genetic disease can only be treated if the cause, the deficient protein or mutated sequence is known. One of the major driving forces that accelerated the gene therapy field, biotechnology in general, and molecular medicine was the sequencing of the human genome which essentially opened up the opportunity to act on the 19,000 or so protein encoding genes in our genome [2]. In the early 1990s the first approved gene therapy clinical trials went underway and produced underwhelming results [3]. Then the field

experienced a major setback with death of 18-year old Jesse Gelsinger in a clinical trial to treat his partial deficiency of the liver enzyme ornithine transcarbamylase [4]. His death was directly attributed to his severe immune response to the viral vector, adenovirus, that was used. This event caused the US Food and Drug Administration (FDA) to create new regulations and review processes for gene therapy trials [5]. It also left a sour taste in the public's opinion of gene therapy and the pharmaceutical industry. Since this incident the field has gone back to understanding viral vector biology, designing vectors with improved safety, increasing oversight in clinical trials and developing non-viral vectors.

Gene therapy is an umbrella term that covers many different methods and technologies. The FDA defines gene therapy as "the administration of genetic material to modify or manipulate the expression of a gene product or to alter the biological properties of living cells for therapeutic use." These methods can be broadly categorized as gene replacement, gene addition, altering gene expression, and gene editing (Figure 1.1)[6]. Gene therapy also includes the field of oncolytic viral therapy where conditionally replicative viruses are used to kill (lyse,-lytic) cancer cells. Current legislation only allows gene therapy to be used on somatic cells, where the new or altered genetic material does not pass on to the next generation. This is in contrast to germ line therapy, where the altered genes do pass on from generation to generation as permanent changes. Manipulation of cells can occur *ex vivo*, cells removed from the source, edited, and re-administered, or *in vivo* where cells are edited directly in

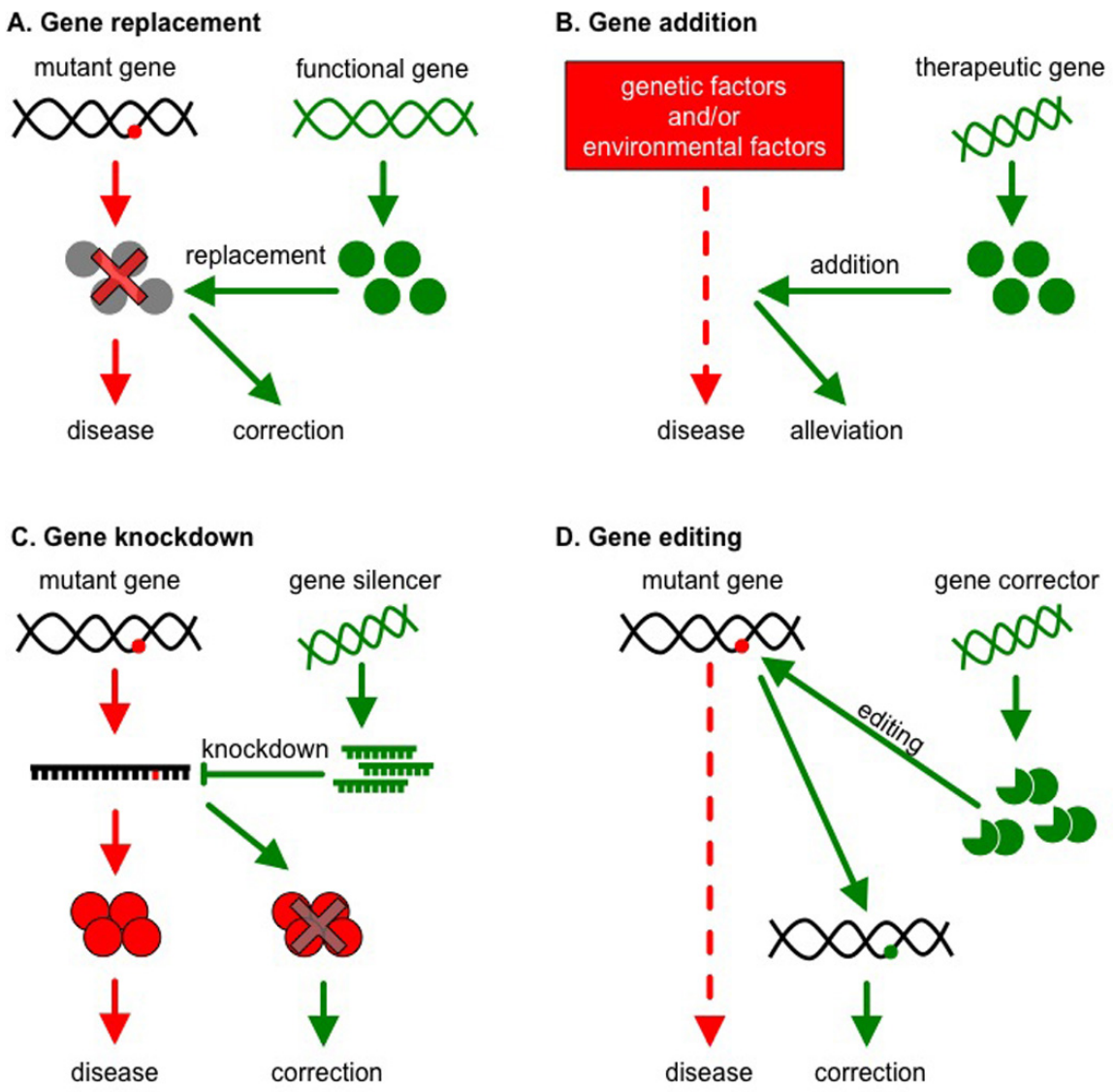

Figure 1.1: (A) Replacement of a mutated protein with a functional one. (B) Addition of gene to alleviate a deficiency. (C) Altering gene expression though RNA analogs. (D) Direct gene editing. Reproduced from [6], copyright Discovery Medicine.

an organism. Gene therapy can be further differentiated into methods that use viral vectors versus ones that use non-viral vectors.

Ideal characteristics of gene therapy vectors include: high gene-transfer efficiency, capacity to carry genes encoding therapeutic proteins, minimal cytotoxicity or selective cytotoxicity, low immunogenicity, ease of production and scale-up, and the potential for selective gene delivery.

1.2.1 Viral Vectors

Viruses have been around since the dawn of life, literally. It is surmised that they may have preceded the emergence of cells [7], [8]. They are everywhere, affecting every organism on our planet. This long evolutionary history has led to complex structures, a daunting variety, and mechanisms that are highly efficient. For the field of gene therapy, this efficiency is the most sought after trait.

Viruses are generally categorized as integrating or non-integrating. Integrating vectors insert their genetic information into the host genome and result in permanent gene expression. Integrating vectors also known as RNA viruses include retroviruses and lentiviruses [9]. Unfortunately, integrating vectors can randomly insert and activate proto-oncogenes, known as insertional mutagenesis [10]. However for permanent gene expression, these are still the vectors of choice. Non-integrating vectors or DNA viruses such as herpes simplex virus (HSV), vaccinia virus, adeno-associated virus (AAV) and adenovirus (Ad) are the most commonly tested. Vector

choice depends on the application or tissue of interest. Each distinct virus family and serotype (subtype) has evolved to transduce a particular cell type, known as tropism. Tropism is mediated by viral coat protein interactions with cell surface proteins/receptors, which are variably expressed across cell types. Thus if a cell does not express a particular receptor then that cell cannot be transduced, infected, by the corresponding virus. Transduction refers to the delivery of foreign genetic information into a cell using a viral vector.

Chapter 2 & 3 of this dissertation will focus on work using Ad and Chapter 4 will focus on AAV. Both of these vectors are well characterized, relatively easy and safe to work with in a lab setting.

1.2.2 Adenovirus

Adenovirus (Ad) is arguably the most well characterized and most clinically tested virus to date. Ad is a large family of viruses which is composed of 51 known human serotypes that contain linear double stranded DNA at 30-40 kb in length. These wild type viruses generally cause mild, self-limiting infections of the respiratory tract and are common causes of "colds" [11]. Though each serotype has distinct tropism, almost all studies and clinical trials use Ad serotype 5 [9], [12], [13]. Ad are non-enveloped virions with a diameter of 90 nm and a characteristic icosahedral capsid structure (20 triangular faces with 12 vertices) comprised of three main proteins: hexon, penton and fiber domains [14]. In contrast, enveloped virions are composed

of a lipid membrane surrounding a protein capsid core. Ad capsid proteins determine cellular tropsim, specifically the 12 fiber domains that protrude from capsid core, which bind the coxsackie-adenovirus receptor (CAR) with high affinity. This triggers subsequent binding of the penton base to α_v integrins via a Arg-Gly-Asp (RGD) motif and leads to clathrin mediated endocytosis (Figure 1.2). Acidification

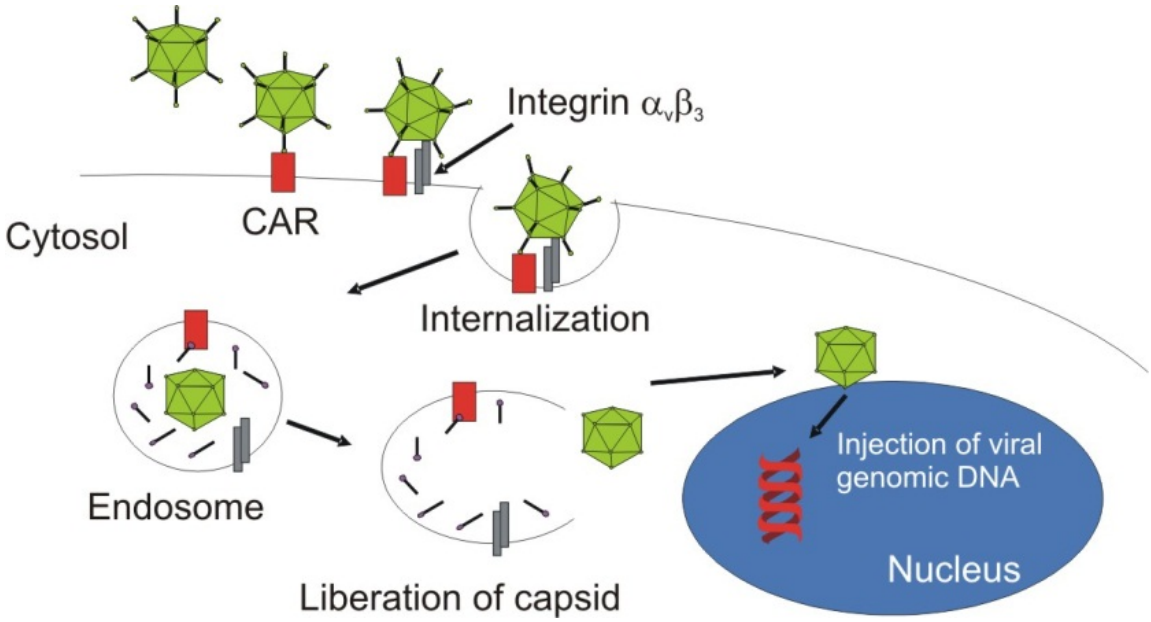

Figure 1.2: Schematic of Ad transduction. Copyright 2013 Stauss et al. Originally published in [13] under CC BY 3.0 license.

of the endosome leads to fiber domains separating from the capsid core and disruption of the endosomal membrane leading to release of the hexon core [14]. Upon release, the capsid is transported to the nuclear membrane and the viral DNA is injected into the nucleus. This viral DNA is not integrated into the host genome, but forms a complex with viral proteins to form an episome. Once viral DNA is delivered, transcription of the viral genome can occur. Ad genomic transcription can

be categorized as early and late phases. The early phase consists of transcription of E1-E4 genes that make the host cellular environment more amenable to viral production and replication. This process includes preventing cellular apoptosis (E1b), inhibiting cellular inflammation (E1a and E1b), and mitigating an immune response (E2). Once DNA replication is activated, the major late promoter (MLP) is turned

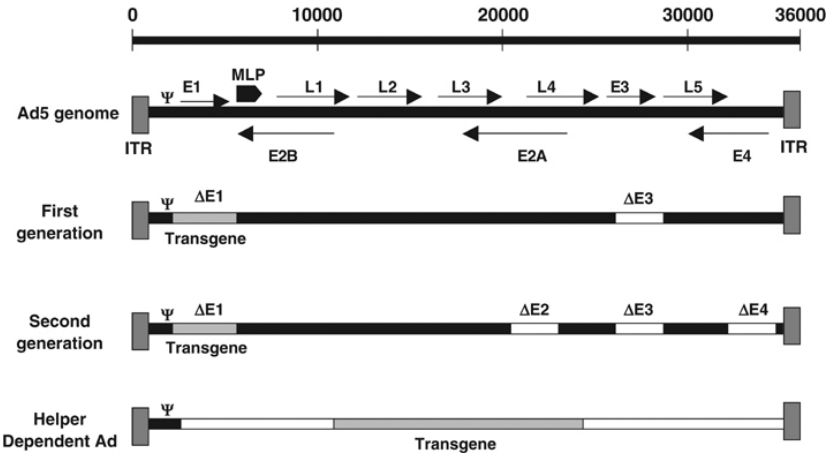

Figure 1.3: Schematic of Ad genome and various modifications for each vector generation. ITR: inverted terminal repeat, Ψ: packaging signal, MLP: major late promoter, Δ: deletion. Reproduced from with permission from [15], copyright Springer Nature.

on to allow late stage genes to be transcribed. These genes produce the structural proteins of the capsid [penton (L2), hexon (L3), and fiber (L5)] and allow for viral replication. The production of viral progeny leads to cell lysis, the release of ∼10,000 progeny virions per cell, and the spread of viral infection. For gene therapy using either non-replicative or conditionally replicative Ad (crAd), not all wild-type (WT) genes are necessary. Deletion of the E1 gene results in a non-replicative virus, one that cannot produce viral progeny. E3 is also non-essential, thus deletions in both

E1 and E3 allow for insertion of approximately 8 kb of foreign DNA. This available cassette is sufficient to produce a variety of proteins. First generation vectors, deletions of E1/E3, have several limitations for use *in vivo*. Specifically they illicit a significant immune response and have associated toxicity due to the large backbone of WT Ad genome. Background levels of E and L genes and the replication of viral DNA leads to cellular inflammation, specifically cytotoxic T lymphocyte (CTL) immune response against transduced cells leading to reduced duration of transgene expression [16]. To overcome some of these problems, a second generation Ad vector was developed with further deletions in E2 and E4 regions (Figure 1.3). With these deletions, second generation vectors can accommodate up to 14kb of foreign DNA, but it was found that these vectors still had associated immunogenicity and did not significantly prolong transgene expression *in vivo* [17]. Most recently, a third generation of Ad vectors was developed. These vectors, known as gutless vectors or helper-dependent Ads, do not contain any of the Ad viral genome outside of the inverted terminal repeats (ITRs) and the packaging signal (Ψ) (Figure 1.3). Gutless vectors can accommodate up to 36 kb of foreign DNA, but require a helper Ad for propagation [15]. Though these circumvent cellular inflammation, these vectors still illicit a humoral immune response *in vivo*. See section "Barriers to Clinical Success" for further discussion of immune response to viral vectors.

Ads are used for gene addition, for vaccination and for lytic activity. All of these methods are dependent on modifications to the Ad genome. Condition-

ally replicative viruses are designed to replicate in and lyse cells of choice. This is achieved by using a tissue or tumor specific promoter to limit replication to cells that are able to activate the promoter, whereas normal or healthy cells are unable to activate replication (see section "Cancer Gene Therapy"). Regardless, for both non-replicative or conditionally replicative Ad, the first barrier to transduction is cellular tropism as transgene expression or replication can only occur once a virion has undergone endocytosis and is physically inside a cell.

1.2.3 Adeno-Associated Virus

Adeno-Associated Virus (AAV) was first discovered in the 1960s as a contaminant of Ad preparations as small 25 nm particles [18]. Interestingly, these viruses were found to be non-autonomous. Thus AAV replication can only occur in the presence of a helper virus such as Ad. To date there have been 12 serotypes identified and none are associated with a human disease; though, approximately 80% of the population are positive for anti-AAV antibodies [19]. AAVs are noneveloped, have an icosahedral structure, and contain linear single stranded DNA at 4.8 kb. The genome is comprised of two genes, rep and cap. The rep gene encodes proteins necessary replication and the cap gene encodes the three capsid proteins. As with Ad, the capsid protein variants play a role in AAV tropsim and most studies focus on AAV2. Table1.1 summarizes the 12 serotypes and associated receptors [18].

The ITR units of the AAV genome contain the elements required for packag-

Table 1.1: AAV serotypes and associated recptors. Adapted from [18].

Serotype	Receptors
AAV1	23/26 N-linked SA
AAV2	HSPG, FGFR1, HGFR, Integrin V5/51, 37/67 kDa LamR
AAV3	HSPG, 37/67 kDa LamR, HGFR
AAV4	23 O-linked SA
AAV5	23 N-linked SA
AAV6	HSPG, 23/ 26 N-linked SA, EGFR
AAV7	Undetermined
AAV8	37/67 kDa LamR
AAV9	Galactose, 37/67 kDa LamR
AAVrh10	Undetermined
AAV11	Undetermined
AAV12	Undetermined

ing, thus the WT genome can be gutted of all viral coding sequences and the genes of choice can be inserted between the ITRs [20]. In the absence of a helper virus, AAVs can induce site-specific integration near AAVS1 on human chromosome 19, though at low efficiency [21]. If integration does not occur then, the viral DNA is expressed in an episomal fashion [18]–[20]. Though, through cellular division episomal expression is diluted over time leaving only expression derived from integration.

Since AAVs are naturally replication deficient and have no known pathogenicity, they are attractive candidates for gene therapy. Most clinical studies focus on AAV2, due to its broad tropsim, for gene addition. The field is now moving to use AAVs for clustered regularly interspaced short palindromic repeats (CRISPR)-CAS9 genome editing. As AAVs are small, one drawback is the constrained transgene size. For example, in the context of CRISPR-CAS9 two AAVs are required (co-

transduction). In the same vain as with all viruses, cellular tropism and *in vivo* immune responses are constraints (see section "Barriers to Clinical Success).

1.2.4 Non-Viral Vectors

To circumvent some of the hurdles associated with viral tropism and immunogenicity, non-viral vectors (NVV) are in development. These vectors can be composed of a variety of materials from lipids to polymers and aim to deliver DNA or RNA payloads. Nucleic acids (DNA/RNA) are negatively charged species that can be complexed or encapsulated in a positively charged carrier i.e. liposomes, solid lipid nanoparticles, and polyplexes. Though NVV are in theory low cost, easy to produce at scale, and have low immunogenicity, they are highly inefficient when compared to viral vectors for transfection [22], [23]. This inefficiency *in vivo* stems from numerous barriers: cellular uptake of NVV, endosomal escape, transport to the nucleus (for DNA), circulation half-life, stability in blood, and cytotoxicity at high concentrations [22], [23]. Note that a virus's long evolutionary history have overcome many of these issues associated with inefficiencies at the cellular level.

1.3 Cancer Gene Therapy

Cancer is a disease that will affect us all, whether friends or family. Despite recent advances in the understanding of cancer biology and the development of new therapeutics, it is still a leading cause of morbidity and the second leading

cause of death in the United States [24]. It is a complex disease defined by cells gaining or losing certain characteristics through genetic and epigenetic mutations, which allow them to proliferate uncontrollably [25]. Traditional means of treatment include surgery, radiation therapy, and chemotherapy. Both surgery and radiation therapy can only treat solid tumors that are known and accessible. Chemotherapy relies on drugs that inhibit cell growth and division (taxanes, anthracyclines, alkylating agents), but these agents are indiscriminate and have off-target toxicities. In the last decade the field has focused on using monoclonal antibodies and immune checkpoint inhibitors to use a patients immune system to attack their cancer, known as immunotherapy. Immunotherapy has been very successful in subsets of patients, but can also have serious side effects [26]. In general the field is moving towards combination therapy where multiple types of treatments are given to achieve clinical outcomes. Another method that is gaining traction is cancer gene therapy also known as oncolytic viral therapy is one method to circumvent off-target toxicity and potentially treat unresectable metastatic disease by using conditionally replicative viruses, which specifically replicate in (kill) cancer cells, but not healthy ones (Figure 1.4). Not only can oncolytic viruses kill cells, they also can be armed with immuno-stumiulatory molecules which are produced in conjuction with viral progeny. Cell lysis also leads to release of cancer antigens that can prime the immune system to attack the cancer. This finding has lead researchers to explore the use of oncolytic viruses in combination with immunotherapy.

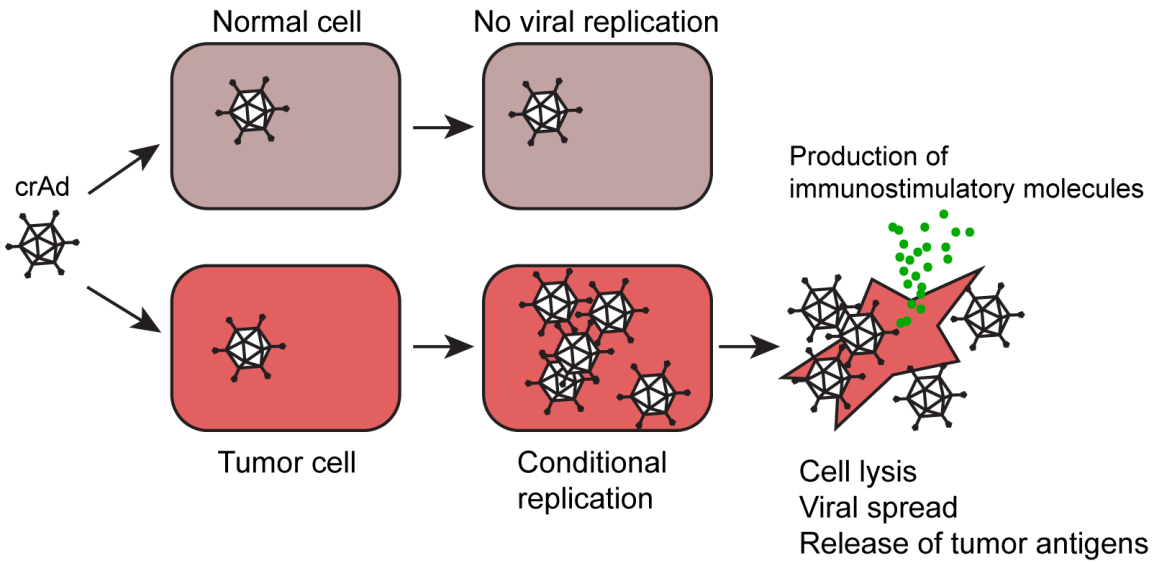

Figure 1.4: Schematic of oncolytic viral therapy using conditionally replicative Ad (crAd).

Conditionally replicative viruses have been tested in the clinic for over 20 years, but have resulted in few clinical outcomes. The first engineered oncolytic agent to enter clinical trials was a condtionally replicative Ad (crAD), known as ONYX-015, with a deletion in the E1b region. It was hypothesized that this deletion rendered the virus replicative in cells deficient in p53, a transcription factor involved in apoptosis, and is a mutation which occurs in the majority of cancers [12], [27]. Initial studies found this to be true, but clinical trial data and further research into the mechanism of action found that replication was independent of p53 and was in fact dependent on the presence of Y-Box Binding Factor 1 (YB-1) [12], [28]. Regardless, ONYX-015 completed phase I and phase II clinical trials in the early 2000s in the US and is an approved therapy in China (known as H101).

Much was learned from these initial trials. The first phase I trial was a

dose escalation study administered intratumorally (IT) to 22 patients with recurrent head and neck cancer (HNSCC) [29]. No dose limiting toxicity was found even at $10^{1}1$plaque-forming units and the main side effect was flu-like symptoms. As expected, 21 of the 22 patients had a increase in neutralizing antibodies to Ad and 13 patients already had detectable levels of anti-Ad pre-treatment, but with no observed treatment response there was no correlation with antibody levels [27], [29]. A phase II study was subsequently conducted to explore multiple dosing regimens as pre-clinical animal studies showed improved efficacy with multiple injections. In this study 40 HNSCC patients were treated either with IT injections for five days or twice a day for two weeks and found that 14% of patients had an objective response [27]. Detectable virus in the blood declined after the first cycle, which was attributed to the striking increase in serum antibody levels. Another trial tested the feasibility of intravenous (IV) injection and had similar, underwhelming findings. This study also found an increase in serum aminotransferase levels, an indicator of liver toxicity [30]. A randomized phase III study was completed in China using an identical virus (H101) and found a significant benefit, more than doubling the response rate, when viral therapy was combined with chemotherapy [31]. These studies showed that Ad administration was well tolerated in patients, that a small set of patients had responses to ONYX-015, and that combination therapy was a viable option. At the time of these trials, p53 status was still the basis for understanding the mechanism of selective replication. Though patients were not compared against or screened for

p53 status. In addition, tumor CAR expression was unexplored.

Since then, numerous crAds have been designed to address viral tropsim and selective replication and have entered early phase testing. Some of these iterations include viruses designed not only with lytic activity, but also the ability to produce immuno-stimulatory molecules such as granulocytemacrophage colonystimulating factor (GMCSF) or CD40L [32]–[34]. GMCSF is a cytokine that stimulates granulocyte and monocyte production leading to antitumor immunity by recruiting natural killer cells and induction of tumor-specific cytotoxic $CD8^+$ T-cells [33], [35]. Koski et al. also used a chimeric Ad with a Ad serotype-3 fiber domain that binds to CD46 (not CAR), which may be more broadly expressed on tumors [33]. They treated 21 patients with Ad3/5-GMCSF and found that 67% had stable disease after one IT injection. Systemic GMCSF has known toxicity, but systemic GMCSF was undetectable suggesting GMSCF production was localized to the site of injection. Again, neutralizing antibodies to Ad increased after treatment. Another group, Pesonen at al., tested a similar chimeric Ad under a hTERT promoter and expressing CD40 ligand (Ad5/3-hTERT-CD40L) [34]. Human telomerase (hTERT) is an enzyme that essentially allows cells to be become immortalized by preventing telomere shortening and is a mutation present in over 90% of cancers [36]. Thus an hTERT promoter restricts Ad replication to cells with this mutation. In addition, the expression of CD40L augments antitumor immunity. This virus was only tested in nine patients, but found the virus was tolerated with no significant adverse events. Both

viral load and serum cytokine levels were found to be low. Overall, these studies suggest that such modifications to Ad may aid cancer specificity and in inducing the immune system to aid treatment. Both Koski et al. and Pesonen et al. suggest that multiple injections are the next step to improving outcomes. Higher viral loads are required due poor delivery efficiency stemming from tropism, pre-existing antibodies, viral loss to systemic circulation and liver clearance.

Another virus that has recently attracted much attention is a modified herpes simplex virus (HSV-1) known as talimogene laherparepvec (T-VEC). HSV is a double stranded DNA virus and has much larger genome than Ad at 152kb. The exact mechanism of action for T-VEC is not completely understood, but it has deletions of $\gamma - 34.5$ and ICP6 genes, which remove its neurovirulence and render replication specific to cells with ribonucleotide reductase expression, respectively [32], [37]. T-VEC also is armed to produce GM-CSF. A randomized phase III trial was completed where 436 melanoma patients either received multiple IT injections of T-VEC or GMCSF alone [38]. This trial found that durable response rate (16.3%) and overall response rate (26.4%) was higher with T-VEC treatment. Adverse events included pain at the injection site, mild flu-like symptoms and cellulitis. Interestingly, in some patients treated with T-VEC it was observed that non-injected lesions responded, suggesting anti-tumor immune response or spread of virions systemically. T-VEC is now the first FDA approved oncolytic virus for "local treatment of unresectable cutaneous, subcutaneous, and nodal lesions in patients with melanoma recurrent after initial

surgery". The field is now moving to test this in combination with immunotherapy and chemotherapy to improve patient outcomes. Though patients are less disposed to having pre-existing neutralizing antibodies to HSV, they will develop them over time thus reducing the efficacy of repeat treatments. The approval of T-VEC has given the field of oncolytic viral therapy and other viral based treatments some hope though there is still progress to be made.

1.4 Clinical Gene Therapy

In contrast to oncolytic viral therapy (cancer gene therapy), therapeutic gene therapy seeks to overcome genetic aberrations through gene replacement, gene addition, gene silencing and gene editing (Figure 1.1). As mentioned previously, viral vectors are the most efficient tool for all four strategies. In the clinic, these methods have been tested both as *ex vivo* manipulation and directly *in vivo*. This section will cover some of the most successful clinical attempts to use viral vectors to achieve these strategies.

Gene replacement is conceptually the simplest form of gene therapy where a single protein is replaced to achieve therapeutic outcome. This is possible because a large number of human diseases are defined by a single mutation, monogenic, that produces a single aberrant protein such as hemophilia. Hemophilia is a monogenic disease characterized by deficiency in blood coagulation factors, either factor VIII for hemophilia A or factor IX (FIX) for hemophilia B [39]. It is treatable though

intravenous (IV) replacement of recombinant FIX or purified plasma throughout the lifespan of the patient. Thus gene replacement is an attractive method to achieve long term endogenous production of a single clotting factor. The field has focused on using AAVs as the vector of choice, either for intramuscular injection (IM) or IV delivery for transduction of the liver. IM delivery seeks to use skeletal muscle as endogenous generator of a protein of interest that releases in the circulation and has a systemic effect. Clinical studies have shown some promise, in one trial bleeding episodes were reduced up to 90% with the replacement of only 5% of the normal clotting factor activity [40]. The efficacy of these trials has been hampered by the finding that AAVs induce a T-cell immune response, which clears transduced cells and leads to loss of protein expression [39]–[41]. In addition, it was found that pre-existing antibodies do reduce efficacy of treatment by reducing viral load [39].

The field of gene replacement has also focused on diseases characterized by enzyme deficiency such as lipoprotein lipase deficiency (LPLD). Patients with this disease are deficient in an enzyme involved in fat metabolism and are prone to pain and inflammation of the pancreas. Glybera, the first gene therapy vector approved in the west, is an non-replicative AAV-1 vector that produces the enzyme lipoprotein lipase. Clinical trials administered a one time IM dose at multiple injection sites. Skeletal muscle is easy to transduce and can act as endogenous source of enzyme. Though Glybera was approved in Europe, its clinical effectiveness is still in question as the clinical efficacy end point was not durable [42]. This is attributed, again,

to the immune response and pre-existing antibodies against AAV [42], [43]. Due to these complications, it is recommended that Glybera be administered along with immuno-suppressants [43].

Treating inherited blindness, Leber's congenital amaurosis, is another focus of the field. This disease is caused by mutations in the RPE65 gene that causes retinal degeneration from birth [44]. Again, AAV has been the vector of choice. Clinical trials using subretinal injection found that patients had improved vision though transient, peaking at 8 months post-injection and then declining [45].

The above examples represent the most successful trials with few ending with real, substantial patient outcomes. These poor results stem from biological barriers innate in our physiology.

1.5 Barriers to Clinical Success

Though there are hundreds of clinical trials in progress using viral vectors, there are still numerous barriers to clinical success and real patient outcomes. These include native viral tropism, liver sequestration, and induction of innate and adaptive immunity against viral particles. These factors are not only important for Ad and AAVs, but apply to all viral vectors. This is especially true for adaptive immunity i.e. the production of antibodies, which will reduce the efficacy of all vectors over repeated treatments.

1.5.1 Tropism

Viral efficacy is essentially a two stage process: the first stage is controlled by viral entry into a cell and the second stage is controlled by promoter driven DNA transcription. Independent on how specific this promoter is, if viral entry cannot occur due to tropism then the virus cannot function. Tropism is defined by the viral structure, capsid proteins, interaction with cell surface receptors, which is evolutionarily derived. Cell or tissue expression of such receptors is variable and thus limits the efficacy of viral vectors in tissues that have low or no receptor expression. For Ad serotype 5 (Ad-5), tropism is primarily mediated coxsackie-adenovirus receptor (CAR) expression. It is well documented that cancer cell lines express CAR at variable levels (Figure 1.5) [46], [47]. This is important to note for *in vitro* studies, but does not tell the full story for *in vivo* models or in human physiology. In humans, CAR is expressed across many tissues, but predominantly in the liver, colon, gall bladder, esophagus, pancreas, and stomach (Figure 1.6) [48]. These tissues may act as off-target tissues that can sequester therapeutic Ads from circulation.

In the context of cancers, CAR expression is highly variable across cancers types, mirroring cell line variability, and across progression of a disease [48]–[51]. In Chinese patients, Ma et al. preformed immunohistochemistry on 251 tissue microarrays comparing normal tissue to coloretal cancer samples and found decreased CAR expression in malignant samples [49]. Similarly, in head and neck squamous cell carcinomas Wunder et al. found the CAR expression correlated with the grade

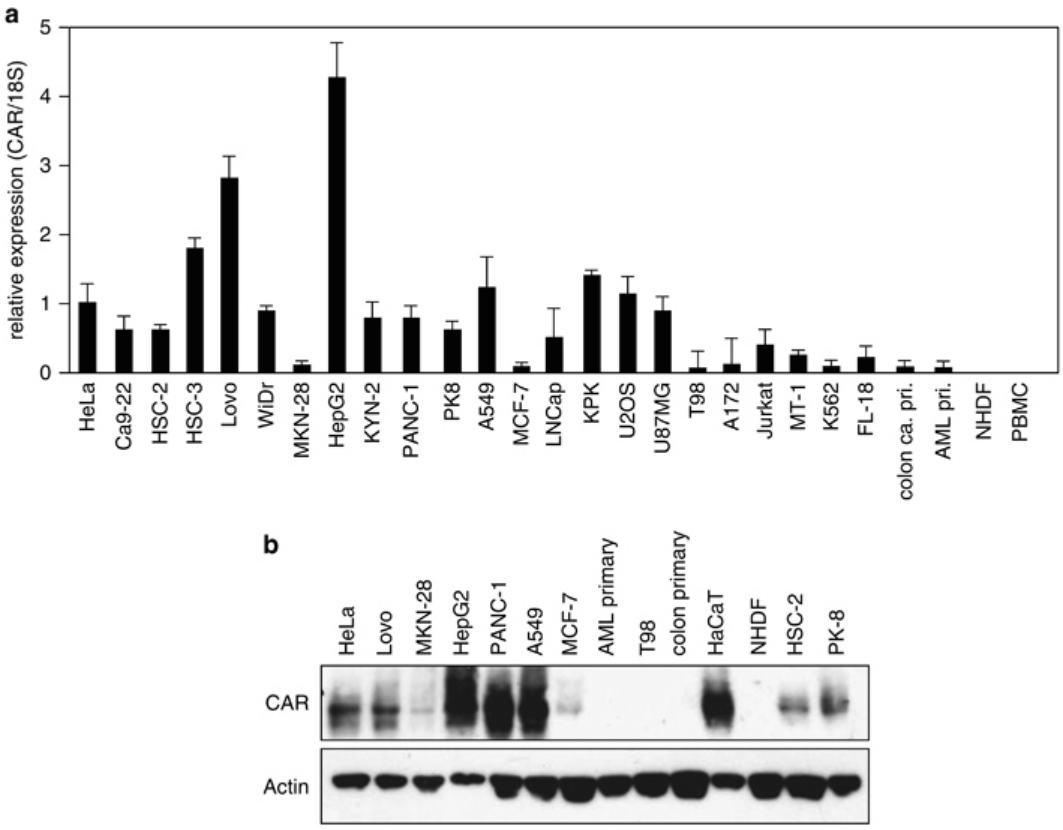

Figure 1.5: (A) CAR expression as measured using RT-PCR. (B) CAR expression as measured by western blotting. Reproduced with permission from [46], copyright Springer Nature.

of tumor, where well differentiated tumors had higher expression than less differentiated ones [51]. In contrast, Martin et al. found that in breast cancer samples CAR expression increased with the grade of tumor and if metastasis were present [50]. Overall, CAR expression is highly variable and cancer type/stage dependent. The authors from the cited work above all recommended that patients be stratified according to CAR expression if Ad based therapy were to be used.

For AAVs, tropism is less defined than for Ad-5, where tropism is primarily defined by cellular glycans. Table1.1 summarizes the 12 serotypes and associated

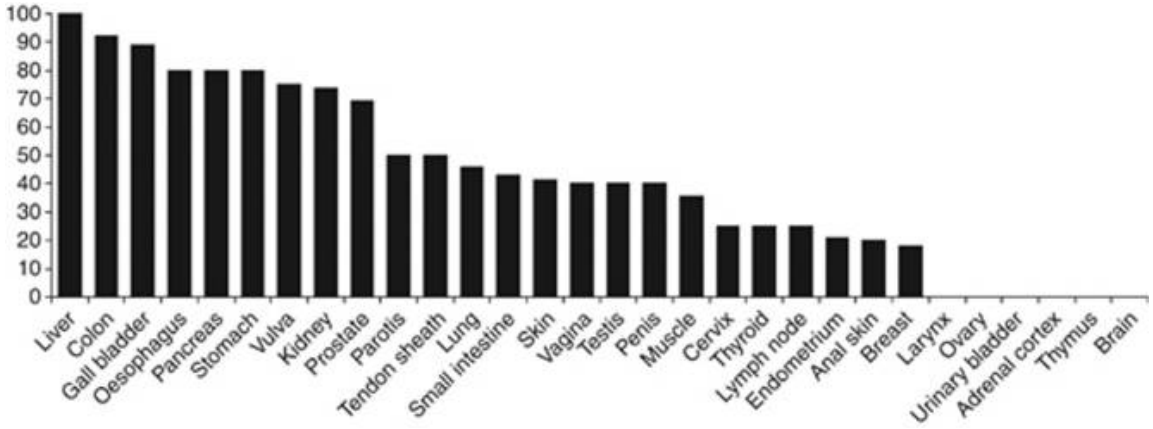

Figure 1.6: Percent CAR positive samples from normal tissues determined by immunohistochemical staining. Reproduced with permission from [48], copyright Springer Nature.

known receptors [18]. As with CAR, these receptors are variably expressed across tissues. Most studies have focused on work *in vivo* in mice models to determine AAV tropism. Zincarelli et al. examined systemic transduction through tail vein injections of serotypes 1-9 in mice and found highly variable transduction across tissues and strong liver transduction for most serotypes [52]. More work needs to be done to better understand AAV tropism in humans and the impact on clinical outcomes.

1.5.2 Liver Sequestration

As suggested above, the liver is ubiquitous destination of Ad and AAVs that end up in the circulation. This is mediated by Kupffer cell uptake and by binding of coagulation factors to the capsid surface resulting in hepatocyte uptake. Liver sequestration of Ad has been well known since the 1990s and was originally thought to be primarily due to Kupffer cells in the liver [53]. These cells are specialized

macrophages that are part of the mononuclear phagocytic system and take part in many roles, but importantly are capable of clearing particles from the circulation [54]. Further research found that the primary pathway for liver uptake of Ad was binding of coagulation factor IX and complement component C4-binding protein to the capsid structure, which results in robust hepatocyte transduction [55]. This binding has an affinity that is almost 40-fold stronger than the affinity for CAR [56]. Thus the majority of virions that end up in the ciculation, whether that be from IV injection or from leakage out of the injection site even when injected IT or IM, are cleared by the liver and result in liver transduction [57]. This transduction results in hepatotoxicity and inflammation [55], [58].

AAV is plagued by the same mechanism. In a clinical trial to treat spinal muscular atrophy with a single high dose of AAV-9 delivered IV, patients had elevated transaminase levels (a measure of liver toxicity) [59]. This was recently supported by a study in non-human primates (NHP) and piglets, where animals were IV injected a high dose of AAV-9 [60]. Again, animals had elevated transaminase levels and one NHP had to be euthanized four days post-injection due to acute liver failure.

1.5.3 Innate and Adaptive Immune Response

The biggest downside to the use of viral vectors for *in vivo* gene therapy is the innate and adaptive (humoral) immune response. Our bodies have evolved to fight and adapt to invading pathogens whether that is novel virus serotypes or

ones that our immune system has seen previously. This was clearly demonstrated as the main factor for Jesse Gelsinger's death the OTC clinical trial where a high dose of Ad was directly injected into his hepatic artery. Within days his severe immune reaction induced a coma and eventual death. This result was from both innate and adaptive immune components. Innate responses are non-specific and act on all foreign objects. It is comprised of anatomical barriers (i.e. mucus), the complement cascade, and variety of leukocytes: natural killer (NK) cells, mast cells, eosinophils, basophils, macrophages, neutrophils, and dendritic cells. Whereas the adaptive immune system is specific and long-lasting with memory. It is comprised of lymphocytes (a variety of T cells and B cells) and antibody production/recognition. Both these systems compliment each other though a complex web of interactions. This section will review the relevant components related to Ad and AAV induced response.

Table 1.2: Innate Immune Cytokines. Adapted from [61].

Cytokine	Function/Pathway
IL-1	Proinflammatory, endogenous pyrogen
TNF-α	Induces apoptosis
IL-6	Secreted by macrophages, induces fever
IFN-γ	Activates macrophages, induces MHC expression
IL-12	Stimulates T cells and NK cells
IP-10	Chemoattractant for neutrophils
RANTES	Chemoattractant, recruits leukocytes
MIP-1	Chemoattractant for NK cells
MCP-1	Chemoattractant for monocytes

The method of injection does influence the overall immune response as the

viral load in the blood correlates to the amount of virus that can be initially acted on. Even with direct tumoral injections viruses are released to the circulation though at a lower load. Thus, the innate immune reaction is considered dose dependent and is triggered upon cellular transduction at the site of interest or in the liver. The primary cytokines and chemokines involved include: tumor necrosis factor α (TNF-α), IL-6, IL-1, interferon γ (IFN-γ), IL-12, macrophage inflammatory protein (MIP)-2, IFN-γ-inducible protein 10 (IP-10), RANTES (regulated on activation, normal T cell expressed and secreted), MIP-1α, MIP-1β, and monocyte chemo-attractant protein 1 (MCP-1) [61]. See Table1.2 for overview. At a cellular level, a cell initiates the innate immune response upon viral binding and endocytosis of a virion. Recognition of foreign DNA by toll-like receptors induces interferon pathways and IL-1 production [62]. It was found that the capsid proteins alone, without viral replication or viral gene expression, can induce a similar innate response suggesting that capsid proteins themselves play an important role [61]. This complex milieu of molecules can be measured within hours of Ad transduction.

Once the innate cascade is triggered, activation of CD4+ and CD8+ T cells, and B cells (of the adaptive immune system) can occur. This takes places through a helper T cell I (Th-1) response that is proinflammatory and occurs in response to most pathogens. CD8+ cytotoxic T lymphocytes (CTL) play a role in clearing transduced cells which limits transgene expression [64]. Dendritic cells (DCs) are critical to the adaptive response and act as a antigen presenting cell (APC) through MHC

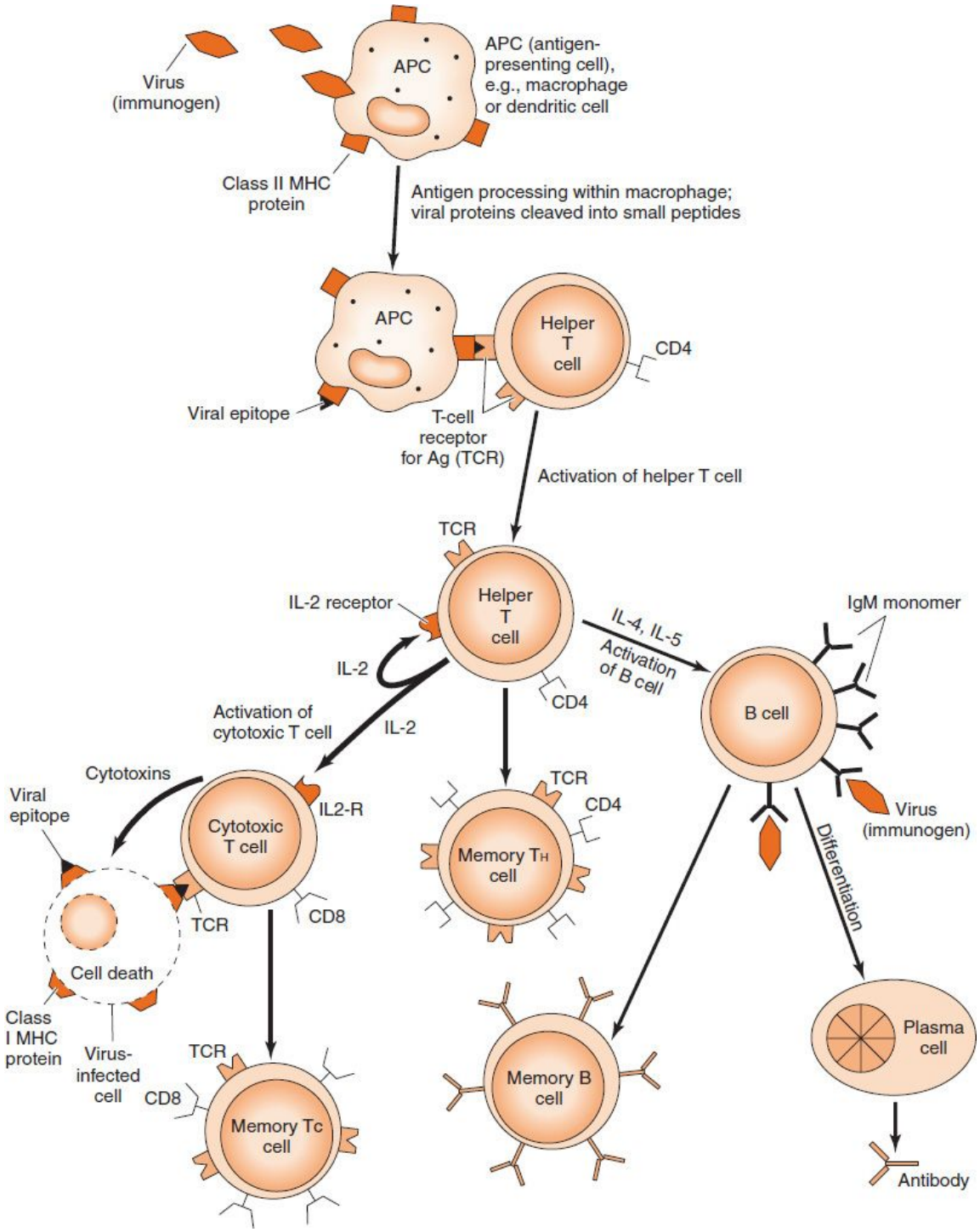

Figure 1.7: Overview of immune response to viruses. Reproduced with permission from [63], copyright 2014 McGraw-Hill Education.

class II upregulation [65]. APCs digest pathogens and present fragments as antigens on their surface to interact with helper T cells. These cells release interleukins that activate B cells. Once B cells are activated they can proliferate and mature into plasma cells, which secrete antibodies against the antigen. See Figure 1.7 for review.

Neutralizing antibodies play an important role in clearing viral particles against a second and subsequent infections. For Ad, antibodies are generated against the fiber and hexon proteins. It is believed that fiber antibodies cause viral aggregation and block CAR receptor binding. Ad infections are believed to be quite common and is reflected by the presence of neutralizing antibodies in the majority of patients. Bauer et al. found that 98.8% of the 667 human patient samples tested, not selected for viral infection, had antibodies to Ad-5 hexon proteins [66]. They also found that these samples had varying degrees of antibodies to other Ad serotypes. Similarly, Yu et al. found that 90% of samples tested positive for anti-fiber antibodies [67]. The prevalence of antibodies is an important consideration especially for IV injections, but also for IT and IM injections. Multiple injections are now the standard procedure tested in clinical trials, which only augments antibody production and the potential for inflammation.

Immune responses to AAV follow a similar fashion. AAV2 antibodies are prevalent in humans and AAVs have a high degree of conservation between serotypes leading to cross reactivity of antibodies [68]. Studies have found that in both humans and animal models that low levels of antibodies are able to neutralize large doses or,

in clinical trials, prevent transgene expression [69], [70]. Thus for all vectors, patients with pre-existing antibodies are less likely to have successful outcomes.

1.6 Overcoming Clinical Barriers

1.6.1 Capsid Modification

Natural viral vectors all have evolutionary constrained tropism and can initiate an immune response. To overcome some of the issues related to tropism, chimeric viral capsids or directed viral evolution have been tested. Chimeric capsids are composed of multiple serotype components, in general, the field has focused on fiber domain replacement or modification. For example, in a clinical trial (mentioned above) researchers used a chimeric Ad with an Ad-5 backbone and a Ad-3 fiber domain to transduce cells through the CD46 receptor [33]. Others have modified the fiber domain with lysine motifs, RGD peptides, or with a Sigma knob [71]. Modification of the fiber can in theory allow a variety of receptors to be targeted, but is balanced against downstream structure-function relationships between capsid proteins. To take chimeric capsids one step further, Grimm et al. used DNA family shuffling technology to create a library of AAV capsids derived from five different serotypes [72]. Selection against human hepatocytes revealed a type 2/type 8/type 9 chimera called AAV-DJ, which enhanced transduction across cell lines. Directed evolution has also been tested to create new Ads. This approach uses selective pressure to generate mutations in Ads that enhance transduction, lytic activity, or even

ones resistant to antibody neutralization [73]–[75]. These approaches may expand viral tropism, but they do not overcome liver clearance and activation of an immune response.

A common technique to increase the circulation half-life of proteins, enzymes, and nanoparticles is to covalently modify the surface of such with poly(ethylene glycol) (PEG). PEG is a hydrophilic polymer that creates a hydration layer on the surface of particles and inhibits adsorption of proteins. This polymer can be congujated to surface amine groups through N-hydroxysuccinimide chemistry. For Ad, surface amines occur in both the hexon and fiber domains. Though chemical conjugation to capsid proteins disrupts efficient binding to CAR and reduces tansduction efficiency, in some cases completely ablating it [76]. Studies have shown that PEGylated Ad also has reduced liver uptake, due to both reduced overall tansduction and from the PEG hydration layer [77].

1.6.2 Nanoparticle Formulations

Methods to overcome an immune response, outside of using purely non-viral vectors, include shielding or encapsulation of virions in nanoparticles. Nanoparticles can be composed of a variety of organic and inorganic materials such as lipids (liposomes), metals, polymers, and silica. Most studies have focused on the use of polymers to shield Ad. This shielding is accomplished through the use of electrostatic interactions where positively charged polymers are complexed with negatively

charged Ad [78], [79]. Poly(ethylenimine) (PEI) and poly(l-lysine) (PLL) are positively charged polymers that have been tested in this context. Molecular weight and degree of branching are important parameters to consider as both influence the degree of toxicity [80]. These polymer complexes work well *in vitro* to enhance transduction, but are quickly cleared *in vivo* from adsorption of plasma proteins to the positively charged surface. Enhanced transduction is believed to be caused by the cationic polymer interacting with the anionic cell membrane inducing non-specific uptake [81]. PEGylation of the polymer surface can increase circulation half-life, but again hampers transduction. Using electrostatic interactions to "coat" Ad is a simple approach, but produces particles with surfaces that are brush-like and capable of adsorbing unwanted proteins.

1.6.3 Silica Nanoparticles

Silica is another material that has been explored for numerous nanoparticle formulations for drug delivery and imaging, but not for encapsulation of Ad [82]. In this context, specifically for drug delivery, mesoporous silica nanoparticles (MSNs) have many advantages such as large surface area, adjustable pore size and volume, easy modification of surface properties through silanol chemistry, and acceptable *in vivo* biocompatibility and biodegredation [82], [83]. Traditional synthesis methods of MSNs use a template driven approach where templates consist of cationic surfactants or of solid cationic polymeric nanoparticles. Silicate precursors, commonly tetraethyl

orthosilicate (TEOS) or tetramethyl orthosilicate (TMOS), are hydrolyzed in solution and produce anionic species or silanol groups (Si-OH). Silanol groups react with each other known (Si-OH + OH-Si) as water condensation or react with methoxy groups (Si-OH + Si-OCH3) known as alcohol condensation. Reaction using TMOS shown below.

$$\mathrm{Si(OCH_3)_4 + H_2O \xrightarrow{hydrolysis} Si(OCH_3)_3OH + CH_3OH}$$

$$\mathrm{Si-O-H + H-O-Si \xrightarrow{water\ condensation} Si-O-Si + H_2O}$$

$$\mathrm{Si-O-H + H_3C-O-Si \xrightarrow{alcohol\ condensation} Si-O-Si + CH_3OH}$$

Both TEOS and TMOS are tetra-valent, with four reactive groups where initial condensation reactions produce nucleation sites which then enter a growth phase. At a pH above the isoelectric point (pH = 2) of silanol groups, these silicate precursors are negatively charged [84]. If a cationic substrate is present then these precursors will condense via electrostatic interactions. Cationic surfactants can form a variety of structures in solution, as emulsions, from micelles to rods and act as a soft template whereas cationic polymeric nanoparticles act as a hard template. Once condensation of silica has completed the templates may be removed using an etching process with the use of solvents or high temperatures to produce hollow porous nanoparticles [85]. These hollow porous particles can act as drug delivery vehicles or successfully shield enzymes from immune recognition [86].

The use of viruses, specifically the plant viruses: tobacco mosaic virus (TMV) and cowpea mosaic virus (CPMV), have been used as silica nanoparticle templates,

but for applications outside of medicine [87], [88]. To template silica onto the surface of TMV, pH has been used as driving force [88]. In the case of CPMV, surface modification directly to the capsid proteins has been used to create a charge difference [87]. In both cases the capsid surface acts as template for silica deposition. The use of other viruses has not been reported.

In the context of Ad, only large silica sol-gel implants have been tested as viral depots [89]. These implants were reported to be very large (7 - 11mm) and required surgical implantation. These implants were formed by pre-making a silica gel and then mixing in viral stock solutions. This mixture was then put into a mold and cooled to form a gel made of 90% water. This delivery system did improve viral kinetics by extending the duration of virus present at the surgical location, but this system does not address the issue of Ad viral tropism and it was found that significant liver transduction still occurred.

1.7 Scope of Dissertation

The work presented in this dissertation covers methods which seek to overcome some of the clinical barriers associated with viral vector gene therapy. Chapter 2 and Chapter 3 of this dissertation will cover a technique to encapsulate Ad in silica as a nanoparticle formulation. Chapter 2 focuses on optimization of silica coated Ad (SiAd), characterization using techniques designed for nanoparticles and viruses, and covers experiments performed *in vitro* to elucidate SiAd's characteristics. Chapter

3 covers experiments performed *in vivo* in both immune compromised and immune competent mouse models to evaluate the bio-distribution of and the immune response to SiAd. Chapter 4 focuses translating the knowledge gained from Chapter 2 to develop methods to encapsulate AAVs in silica or in exosomal derived membranes as way to enhance transduction *in vitro*.

1.8 References: Chapter 1

[1] T. Friedmann, "A brief history of gene therapy," *Nat Genet*, vol. 2, no. 2, pp. 93–8, 1992.

[2] I. Ezkurdia, D. Juan, J. M. Rodriguez, A. Frankish, M. Diekhans, J. Harrow, J. Vazquez, A. Valencia, and M. L. Tress, "Multiple evidence strands suggest that there may be as few as 19 000 human protein-coding genes," *Human Molecular Genetics*, vol. 23, no. 22, pp. 5866–5878, 2014.

[3] T. Wirth, N. Parker, and S. Ylä Herttuala, "History of gene therapy," *Gene*, vol. 525, no. 2, pp. 162–169, 2013.

[4] S. G. Stolberg, "The biotech death of jesse gelsinger," *N Y Times Mag*, pp. 136–140, 149–150, 1999.

[5] B. Sibbald, "Death but one unintended consequence of gene-therapy trial," *CMAJ: Canadian Medical Association Journal*, vol. 164, no. 11, pp. 1612–1612, 2001.

[6] D. Wang and G. Gao, "State-of-the-art human gene therapy: Part ii. gene therapy strategies and applications," *Discovery medicine*, vol. 18, no. 98, pp. 151–161, 2014.

[7] C. Zimmer, "Did dna come from viruses?" *Science*, vol. 312, no. 5775, pp. 870–2, 2006.

[8] K. Moelling, "Are viruses our oldest ancestors?" *EMBO Reports*, vol. 13, no. 12, pp. 1033–1033, 2012.

[9] J. L. Howarth, Y. B. Lee, and J. B. Uney, "Using viral vectors as gene transfer tools (cell biology and toxicology special issue: Etcs-uk 1 day meeting on genetic manipulation of cells)," *Cell Biology and Toxicology*, vol. 26, no. 1, pp. 1–20, 2010.

[10] U. Modlich and C. Baum, "Preventing and exploiting the oncogenic potential of integrating gene vectors," *The Journal of Clinical Investigation*, vol. 119, no. 4, pp. 755–758, 2009.

[11] T. Lion, "Adenovirus infections in immunocompetent and immunocompromised patients," *Clin Microbiol Rev*, vol. 27, no. 3, pp. 441–62, 2014.

[12] C. Larson, B. Oronsky, J. Scicinski, G. R. Fanger, M. Stirn, A. Oronsky, and T. R. Reid, "Going viral: A review of replication-selective oncolytic adenoviruses.," *Oncotarget*, vol. 6, no. 24, 2015.

[13] B. E. Strauss and E. Costanzi-Strauss, "Gene therapy for melanoma: Progress and perspectives," in *Recent Advances in the Biology, Therapy and Management of Melanoma*, L. M. Davids, Ed. InTech, 2013, Ch. 12. DOI: 10.5772/54936. [Online]. Available: http://dx.doi.org/10.5772/54936.

[14] W. C. Russell, "Adenoviruses: Update on structure and function," *J Gen Virol*, vol. 90, no. Pt 1, pp. 1–20, 2009.

[15] R. Alba, A. Bosch, and M. Chillon, *Gutless adenovirus: Last-generation adenovirus for gene therapy.* 2005, vol. 12 Suppl 1, S18–27. DOI: 10.1038/sj.gt.3302612.

[16] Y. Yang, F. A. Nunes, K. Berencsi, E. E. Furth, E. Gonczol, and J. M. Wilson, "Cellular immunity to viral antigens limits e1-deleted adenoviruses for gene therapy," *Proceedings of the National Academy of Sciences of the United States of America*, vol. 91, no. 10, pp. 4407–4411, 1994.

[17] S. Wen, D. B. Schneider, R. M. Driscoll, G. Vassalli, A. B. Sassani, and D. A. Dichek, "Second-generation adenoviral vectors do not prevent rapid loss of transgene expression and vector dna from the arterial wall," *Arterioscler Thromb Vasc Biol*, vol. 20, no. 6, pp. 1452–8, 2000.

[18] M. Salganik, M. L. Hirsch, and R. J. Samulski, "Adeno-associated virus as a mammalian dna vector," *Microbiol Spectr*, vol. 3, no. 4, 2015, ISSN: 2165-0497. DOI: 10.1128/microbiolspec.MDNA3-0052-2014.

[19] M. D. Weitzman and R. M. Linden, "Adeno-associated virus biology," *Methods Mol Biol*, vol. 807, pp. 1–23, 2011.

[20] L. Lisowski, S. S. Tay, and I. E. Alexander, "Adeno-associated virus serotypes for gene therapeutics," *Current Opinion in Pharmacology*, vol. 24, pp. 59–67, 2015, ISSN: 1471-4892. DOI: https://doi.org/10.1016/j.coph.2015.07.006. [Online]. Available: http://www.sciencedirect.com/science/article/pii/S1471489215000934.

[21] D. M. McCarty, J. Young S. M., and R. J. Samulski, "Integration of adeno-associated virus (aav) and recombinant aav vectors," *Annu Rev Genet*, vol. 38, pp. 819–45, 2004.

[22] M. Ramamoorth and A. Narvekar, "Non viral vectors in gene therapy- an overview," *Journal of Clinical and Diagnostic Research : JCDR*, vol. 9, no. 1, GE01–GE06, 2015. DOI: 10.7860/JCDR/2015/10443.5394. [Online]. Available: http://www.ncbi.nlm.nih.gov/pmc/articles/PMC4347098/.

[23] H. Yin, R. L. Kanasty, A. A. Eltoukhy, A. J. Vegas, J. R. Dorkin, and D. G. Anderson, "Non-viral vectors for gene-based therapy," *Nature Reviews Genetics*, vol. 15, p. 541, 2014. DOI: 10.1038/nrg3763. [Online]. Available: http://dx.doi.org/10.1038/nrg3763.

[24] R. L. Siegel, K. D. Miller, and A. Jemal, "Cancer statistics, 2017," *CA: A Cancer Journal for Clinicians*, vol. 67, no. 1, pp. 7–30, 2017, ISSN: 1542-4863. DOI: 10.3322/caac.21387. [Online]. Available: http://dx.doi.org/10.3322/caac.21387.

[25] D. Hanahan and R. A. Weinberg, "Hallmarks of cancer: The next generation," *Cell*, vol. 144, no. 5, pp. 646–674, ISSN: 0092-8674. DOI: 10.1016/j.cell.2011.02.013. [Online]. Available: http://dx.doi.org/10.1016/j.cell.2011.02.013.

[26] Y. Yang, "Cancer immunotherapy: Harnessing the immune system to battle cancer," *J Clin Invest*, vol. 125, no. 9, pp. 3335–7, 2015, ISSN: 0021-9738. DOI: 10.1172/jci83871.

[27] S. Ries and W. M. Korn, "Onyx-015: Mechanisms of action and clinical potential of a replication-selective adenovirus," *British Journal Of Cancer*, vol. 86, p. 5, 2002. DOI: 10.1038/sj.bjc.6600006. [Online]. Available: http://dx.doi.org/10.1038/sj.bjc.6600006.

[28] C. C. O'Shea, L. Johnson, B. Bagus, S. Choi, C. Nicholas, A. Shen, L. Boyle, K. Pandey, C. Soria, J. Kunich, Y. Shen, G. Habets, D. Ginzinger, and F. McCormick, "Late viral rna export, rather than p53 inactivation, determines onyx-015 tumor selectivity," *Cancer Cell*, vol. 6, no. 6, pp. 611–23, 2004. DOI: 10.1016/j.ccr.2004.11.012.

[29] I. Ganly, D. Kirn, S. G. Eckhardt, G. I. Rodriguez, D. S. Soutar, R. Otto, A. G. Robertson, O. Park, M. L. Gulley, C. Heise, D. D. Von Hoff, and S. B. Kaye, "A phase i study of onyx-015, an e1b attenuated adenovirus, administered intratumorally to patients with recurrent head and neck cancer," *Clinical Cancer Research*, vol. 6, no. 3, pp. 798–806, 2000.

[30] J. Nemunaitis, C. Cunningham, A. Buchanan, A. Blackburn, G. Edelman, P. Maples, G. Netto, A. Tong, B. Randlev, S. Olson, and D. Kirn, "Intravenous infusion of a replication-selective adenovirus (onyx-015) in cancer patients: Safety, feasibility and biological activity," *Gene Ther*, vol. 8, no. 10, pp. 746–59, 2001.

[31] Z. J. Xia, J. H. Chang, L. Zhang, W. Q. Jiang, Z. Z. Guan, J. W. Liu, Y. Zhang, X. H. Hu, G. H. Wu, H. Q. Wang, Z. C. Chen, J. C. Chen, Q. H. Zhou, J. W. Lu, Q. X. Fan, J. J. Huang, and X. Zheng, "Phase iii randomized clinical trial of intratumoral injection of e1b gene-deleted adenovirus (h101) combined with cisplatin-based chemotherapy in treating squamous cell cancer of head and neck or esophagus.," *Ai zheng = Aizheng = Chinese journal of cancer*, vol. 23, no. 12, pp. 1666–1670, 2004.

[32] M. R. Patel and R. A. Kratzke, "Oncolytic virus therapy for cancer: The first wave of translational clinical trials," *Translational Research*, vol. 161, no. 4, pp. 355–364, 2013, ISSN: 1931-5244. DOI: https://doi.org/10.1016/j.trsl.2012.12.010. [Online]. Available: http://www.sciencedirect.com/science/article/pii/S193152441200446X.

[33] A. Koski, L. Kangasniemi, S. Escutenaire, S. Pesonen, V. Cerullo, I. Diaconu, P. Nokisalmi, M. Raki, M. Rajecki, K. Guse, T. Ranki, M. Oksanen, S.-L. Holm, E. Haavisto, A. Karioja-Kallio, L. Laasonen, K. Partanen, M. Ugolini, A. Helminen, E. Karli, P. Hannuksela, S. Pesonen, T. Joensuu, A. Kanerva, and A. Hemminki, "Treatment of cancer patients with a serotype 5/3 chimeric oncolytic adenovirus expressing gmcsf," *Molecular Therapy*, vol. 18, no. 10, pp. 1874–1884, 2010, ISSN: 1525-0016. DOI: https://doi.org/10.1038/mt.2010.161. [Online]. Available: http://www.sciencedirect.com/science/article/pii/S1525001616308723.

[34] S. Pesonen, I. Diaconu, L. Kangasniemi, T. Ranki, A. Kanerva, S. K. Pesonen, U. Gerdemann, A. M. Leen, K. Kairemo, M. Oksanen, E. Haavisto, S.-L. Holm, A. Karioja-Kallio, S. Kauppinen, K. P. L. Partanen, L. Laasonen, T. Joensuu, T. Alanko, V. Cerullo, and A. Hemminki, "Oncolytic immunotherapy of advanced solid tumors with a cd40l-expressing replicating adenovirus: Assessment of safety and immunologic responses in patients," *Cancer Research*, vol. 72, no. 7, pp. 1621–1631, 2012.

[35] V. Cerullo, S. Pesonen, I. Diaconu, S. Escutenaire, P. T. Arstila, M. Ugolini, P. Nokisalmi, M. Raki, L. Laasonen, M. Sarkioja, M. Rajecki, L. Kangasniemi, K. Guse, A. Helminen, L. Ahtiainen, A. Ristimaki, A. Raisanen-Sokolowski, E. Haavisto, M. Oksanen, E. Karli, A. Karioja-Kallio, S. L. Holm, M. Kouri, T. Joensuu, A. Kanerva, and A. Hemminki, "Oncolytic adenovirus coding for granulocyte macrophage colony-stimulating factor induces antitumoral immunity in cancer patients," *Cancer Res*, vol. 70, no. 11, pp. 4297–309, 2010.

[36] T. Liu, X. Yuan, and D. Xu, "Cancer-specific telomerase reverse transcriptase (tert) promoter mutations: Biological and clinical implications," *Genes*, vol. 7, no. 7, p. 38, 2016.

[37] F. J. Kohlhapp and H. L. Kaufman, "Molecular pathways: Mechanism of action for talimogene laherparepvec, a new oncolytic virus immunotherapy," *Clinical Cancer Research*, vol. 22, no. 5, pp. 1048–1054, 2016.

[38] H. I. A. Robert, L. K. Howard, C. Frances, A. Thomas, S. Neil, C. Jason, A. D. Keith, E. S. Lynn, P. Igor, S. A. Sanjiv, M. Mohammed, C. Lee, C. Brendan, L. Karl, R. Merrick, G. Troy, P. L. Gerald, A. D. Gregory, H. Kevin, R. M. Mark, J. Wilson H. Miller, S. Z. Jonathan, Y. Yining, Y. Bin, L. Ai, D. Susan, V. Ari, G. Jennifer, and S. C. Robert, "Talimogene laherparepvec improves durable response rate in patients with advanced melanoma," *Journal of Clinical Oncology*, vol. 33, no. 25, pp. 2780–2788, 2015. DOI: 10.1200/jco.2014.58.3377. [Online]. Available: http://ascopubs.org/doi/abs/10.1200/JCO.2014.58.3377.

[39] G. L. Rogers and R. W. Herzog, "Gene therapy for hemophilia," *Frontiers in bioscience (Landmark edition)*, vol. 20, pp. 556–603, 2015.

[40] A. C. Nathwani, U. M. Reiss, E. G. Tuddenham, C. Rosales, P. Chowdary, J. McIntosh, M. Della Peruta, E. Lheriteau, N. Patel, D. Raj, A. Riddell, J. Pie, S. Rangarajan, D. Bevan, M. Recht, Y. M. Shen, K. G. Halka, E. Basner-Tschakarjan, F. Mingozzi, K. A. High, J. Allay, M. A. Kay, C. Y. Ng, J. Zhou, M. Cancio, C. L. Morton, J. T. Gray, D. Srivastava, A. W. Nienhuis, and

A. M. Davidoff, "Long-term safety and efficacy of factor ix gene therapy in hemophilia b," *N Engl J Med*, vol. 371, no. 21, pp. 1994–2004, 2014.

[41] W. Miesbach, K. Meijer, M. Coppens, P. Kampmann, R. Klamroth, R. Schutgens, M. Tangelder, G. Castaman, J. Schwable, H. Bonig, E. Seifried, F. Cattaneo, C. Meyer, and F. W. G. Leebeek, "Gene therapy with adeno-associated virus vector 5 human factor ix in adults with hemophilia b," *Blood*, vol. 131, no. 9, pp. 1022–1031, 2018.

[42] L. M. Bryant, D. M. Christopher, A. R. Giles, C. Hinderer, J. L. Rodriguez, J. B. Smith, E. A. Traxler, J. Tycko, A. P. Wojno, and J. M. Wilson, "Lessons learned from the clinical development and market authorization of glybera," *Human Gene Therapy Clinical Development*, vol. 24, no. 2, pp. 55–64, 2013.

[43] V. Ferreira, H. Petry, and F. Salmon, "Immune responses to aav-vectors, the glybera example from bench to bedside," *Frontiers in Immunology*, vol. 5, p. 82, 2014.

[44] E. A. Pierce and J. Bennett, "The status of rpe65 gene therapy trials: Safety and efficacy," *Cold Spring Harbor Perspectives in Medicine*, vol. 5, no. 9, a017285, 2015.

[45] J. W. Bainbridge, M. S. Mehat, V. Sundaram, S. J. Robbie, S. E. Barker, C. Ripamonti, A. Georgiadis, F. M. Mowat, S. G. Beattie, P. J. Gardner, K. L. Feathers, V. A. Luong, S. Yzer, K. Balaggan, A. Viswanathan, T. J. de Ravel, I. Casteels, G. E. Holder, N. Tyler, F. W. Fitzke, R. G. Weleber, M. Nardini, A. T. Moore, D. A. Thompson, S. M. Petersen-Jones, M. Michaelides, L. I. van den Born, A. Stockman, A. J. Smith, G. Rubin, and R. R. Ali, "Long-term effect of gene therapy on leber's congenital amaurosis," *N Engl J Med*, vol. 372, no. 20, pp. 1887–97, 2015.

[46] K. Saito, M. Sakaguchi, H. Iioka, M. Matsui, H. Nakanishi, N. H. Huh, and E. Kondo, "Coxsackie and adenovirus receptor is a critical regulator for the survival and growth of oral squamous carcinoma cells," *Oncogene*, vol. 33, no. 10, pp. 1274–86, 2014, ISSN: 0950-9232. DOI: 10.1038/onc.2013.66.

[47] Z. You, D. C. Fischer, X. Tong, A. Hasenburg, E. Aguilar-Cordova, and D. G. Kieback, "Coxsackievirus-adenovirus receptor expression in ovarian cancer cell lines is associated with increased adenovirus transduction efficiency and transgene expression," *Cancer Gene Ther*, vol. 8, no. 3, pp. 168–75, 2001, ISSN: 0929-1903. DOI: 10.1038/sj.cgt.7700284.

[48] M. Reeh, M. Bockhorn, D. Gorgens, M. Vieth, T. Hoffmann, R. Simon, J. R. Izbicki, G. Sauter, U. Schumacher, and M. Anders, "Presence of the coxsackievirus and adenovirus receptor (car) in human neoplasms: A multitumour array analysis," *British Journal of Cancer*, vol. 109, no. 7, pp. 1848–1858, 2013, ISSN: 0007-0920 1532-1827. DOI: 10.1038/bjc.2013.509. [Online]. Available: http://www.ncbi.nlm.nih.gov/pmc/articles/PMC3790165/.

[49] Y.-Y. Ma, X.-J. Wang, Y. Han, G. Li, H.-J. Wang, S.-B. Wang, X.-Y. Chen, F.-L. Liu, X.-L. He, X.-M. Tong, and X.-Z. Mou, "Loss of coxsackie and adenovirus receptor expression in human colorectal cancer: A potential impact on the efficacy of adenovirus-mediated gene therapy in chinese han population," *Molecular Medicine Reports*, vol. 14, no. 3, pp. 2541–2547, 2016, ISSN: 1791-2997 1791-3004. DOI: 10.3892/mmr.2016.5536. [Online]. Available: http://www.ncbi.nlm.nih.gov/pmc/articles/PMC4991754/.

[50] T. A. Martin, G. Watkins, and W. G. Jiang, "The coxsackie-adenovirus receptor has elevated expression in human breast cancer," *Clin Exp Med*, vol. 5, no. 3, pp. 122–8, 2005. DOI: 10.1007/s10238.005.0076.1.

[51] T. Wunder, U. Schumacher, and R. Friedrich, "Coxsackie adenovirus receptor expression in carcinomas of the head and neck," *Anticancer Reseach*, 2012.

[52] C. Zincarelli, S. Soltys, G. Rengo, and J. E. Rabinowitz, "Analysis of aav serotypes 1-9 mediated gene expression and tropism in mice after systemic injection," *Mol Ther*, vol. 16, no. 6, pp. 1073–80, 2008, ISSN: 1525-0016. DOI: 10.1038/mt.2008.76.

[53] N. Tao, G.-P. Gao, M. Parr, J. Johnston, T. Baradet, J. M. Wilson, J. Barsoum, and S. E. Fawell, "Sequestration of adenoviral vector by kupffer cells leads to a nonlinear dose response of transduction in liver," *Molecular Therapy*, vol. 3, no. 1, pp. 28–35, 2001, ISSN: 1525-0016. DOI: https://doi.org/10.1006/mthe.2000.0227. [Online]. Available: http://www.sciencedirect.com/science/article/pii/S1525001600902272.

[54] L. J. Dixon, M. Barnes, H. Tang, M. T. Pritchard, and L. E. Nagy, "Kupffer cells in the liver," *Comprehensive Physiology*, vol. 3, no. 2, pp. 785–797, 2013, ISSN: 2040-4603. DOI: 10.1002/cphy.c120026. [Online]. Available: http://www.ncbi.nlm.nih.gov/pmc/articles/PMC4748178/.

[55] D. M. Shayakhmetov, A. Gaggar, S. Ni, Z. Y. Li, and A. Lieber, "Adenovirus binding to blood factors results in liver cell infection and hepatotoxicity," *J Virol*, vol. 79, no. 12, pp. 7478–91, 2005. DOI: 10.1128/JVI.79.12.7478-

7491.2005. [Online]. Available: http://www.ncbi.nlm.nih.gov/pubmed/15919903.

[56] O. Kalyuzhniy, N. C. Di Paolo, M. Silvestry, S. E. Hofherr, M. A. Barry, P. L. Stewart, and D. M. Shayakhmetov, "Adenovirus serotype 5 hexon is critical for virus infection of hepatocytes in vivo," *Proceedings of the National Academy of Sciences of the United States of America*, vol. 105, no. 14, pp. 5483–5488, 2008, ISSN: 0027-8424 1091-6490. DOI: 10.1073/pnas.0711757105. [Online]. Available: http://www.ncbi.nlm.nih.gov/pmc/articles/PMC2291105/.

[57] A. Koski, S. Bramante, A. Kipar, M. Oksanen, J. Juhila, L. Vassilev, T. Joensuu, A. Kanerva, and A. Hemminki, "Biodistribution analysis of oncolytic adenoviruses in patient autopsy samples reveals vascular transduction of noninjected tumors and tissues," *Mol Ther*, vol. 23, no. 10, pp. 1641–52, 2015, ISSN: 1525-0016. DOI: 10.1038/mt.2015.125.

[58] M. Machitani, F. Sakurai, K. Wakabayashi, K. Nakatani, M. Tachibana, N. Kato, T. Fujiwara, and H. Mizuguchi, "Suppression of oncolytic adenovirus-mediated hepatotoxicity by liver-specific inhibition of nf-kb," *Molecular Therapy - Oncolytics*, vol. 7, pp. 76–85, ISSN: 2372-7705. DOI: 10.1016/j.omto.2017.10.003. [Online]. Available: http://dx.doi.org/10.1016/j.omto.2017.10.003.

[59] J. R. Mendell, S. Al-Zaidy, R. Shell, W. D. Arnold, L. R. Rodino-Klapac, T. W. Prior, L. Lowes, L. Alfano, K. Berry, K. Church, J. T. Kissel, S. Nagendran, J. L Italien, D. M. Sproule, C. Wells, J. A. Cardenas, M. D. Heitzer, A. Kaspar, S. Corcoran, L. Braun, S. Likhite, C. Miranda, K. Meyer, K. Foust, A. H. Burghes, and B. K. Kaspar, "Single-dose gene-replacement therapy for spinal muscular atrophy," *New England Journal of Medicine*, vol. 377, no. 18, pp. 1713–1722, 2017. DOI: 10.1056/NEJMoa1706198. [Online]. Available: http://www.nejm.org/doi/full/10.1056/NEJMoa1706198.

[60] C. Hinderer, N. Katz, E. L. Buza, C. Dyer, T. Goode, P. Bell, L. K. Richman, and J. M. Wilson, "Severe toxicity in nonhuman primates and piglets following high-dose intravenous administration of an adeno-associated virus vector expressing human smn," *Hum Gene Ther*, 2018, ISSN: 1043-0342. DOI: 10.1089/hum.2018.015.

[61] D. D. A. Muruve, "The innate immune response to adenovirus vectors," *Human Gene Therapy*, vol. 15, no. 12, pp. 1157–1166, 2004. DOI: 10.1089/hum.2004.15.1157. [Online]. Available: https://www.liebertpub.com/doi/abs/10.1089/hum.2004.15.1157.

[62] B. Thaci, I. V. Ulasov, D. A. Wainwright, and M. S. Lesniak, "The challenge for gene therapy: Innate immune response to adenoviruses," *Oncotarget*, vol. 2, no. 3, pp. 113–121, 2011, ISSN: 1949-2553. [Online]. Available: http://www.ncbi.nlm.nih.gov/pmc/articles/PMC3092742/.

[63] W. Levinson, "Immunity," in *Review of Medical Microbiology and Immunology, 13e*. New York, NY: McGraw-Hill Education, 2014. [Online]. Available: accessmedicine.mhmedical.com/content.aspx?aid=1104263108.

[64] J. Chen, A. J. Zajac, S. A. McPherson, H. C. Hsu, P. Yang, Q. Wu, X. Xu, X. Wang, K. Fujihashi, D. T. Curiel, and J. D. Mountz, "Primary adenovirus-specific cytotoxic t lymphocyte response occurs after viral clearance and liver enzyme elevation," *Gene Therapy*, vol. 12, p. 1079, 2005. DOI: 10.1038/sj.gt.3302494. [Online]. Available: http://dx.doi.org/10.1038/sj.gt.3302494.

[65] J. M. Trevejo, M. W. Marino, N. Philpott, R. Josien, E. C. Richards, K. B. Elkon, and E. Falck-Pedersen, "Tnf-a-dependent maturation of local dendritic cells is critical for activating the adaptive immune response to virus infection," *Proceedings of the National Academy of Sciences*, vol. 98, no. 21, pp. 12 162–12 167, 2001. DOI: 10.1073/pnas.211423598. [Online]. Available: http://www.pnas.org/content/pnas/98/21/12162.full.pdf.

[66] U. Bauer, G. Flunker, K. Bruss, K. Kallwellis, H. Liebermann, T. Luettich, M. Motz, and W. Seidel, "Detection of antibodies against adenovirus protein ix, fiber, and hexon in human sera by immunoblot assay," *Journal of Clinical Microbiology*, vol. 43, no. 9, pp. 4426–4433, 2005, ISSN: 0095-1137 1098-660X. DOI: 10.1128/JCM.43.9.4426-4433.2005. [Online]. Available: http://www.ncbi.nlm.nih.gov/pmc/articles/PMC1234141/.

[67] B. Yu, J. Dong, C. Wang, Y. Zhan, H. Zhang, J. Wu, W. Kong, and X. Yu, "Characteristics of neutralizing antibodies to adenovirus capsid proteins in human and animal sera," *Virology*, vol. 437, no. 2, pp. 118–123, 2013, ISSN: 0042-6822. DOI: https://doi.org/10.1016/j.virol.2012.12.014. [Online]. Available: http://www.sciencedirect.com/science/article/pii/S0042682212006423.

[68] F. Mingozzi and K. A. High, "Immune responses to aav vectors: Overcoming barriers to successful gene therapy," *Blood*, vol. 122, no. 1, pp. 23–36, 2013. DOI: 10.1182/blood-2013-01-306647. [Online]. Available: http://www.bloodjournal.org/content/bloodjournal/122/1/23.full.pdf.

[69] C. S. Manno, G. F. Pierce, V. R. Arruda, B. Glader, M. Ragni, J. J. Rasko, M. C. Ozelo, K. Hoots, P. Blatt, B. Konkle, M. Dake, R. Kaye, M. Razavi, A. Zajko, J. Zehnder, P. K. Rustagi, H. Nakai, A. Chew, D. Leonard, J. F. Wright, R. R. Lessard, J. M. Sommer, M. Tigges, D. Sabatino, A. Luk, H. Jiang, F. Mingozzi, L. Couto, H. C. Ertl, K. A. High, and M. A. Kay, "Successful transduction of liver in hemophilia by aav-factor ix and limitations imposed by the host immune response," *Nat Med*, vol. 12, no. 3, pp. 342–7, 2006, ISSN: 1078-8956 (Print) 1078-8956. DOI: 10.1038/nm1358.

[70] S. L. Murphy, H. Li, S. Zhou, A. Schlachterman, and K. A. High, "Prolonged susceptibility to antibody-mediated neutralization for adeno-associated vectors targeted to the liver," *Mol Ther*, vol. 16, no. 1, pp. 138–45, 2008, ISSN: 1525-0016. DOI: 10.1038/sj.mt.6300334.

[71] S. Zheng, I. V. Ulasov, Y. Han, M. A. Tyler, Z. B. Zhu, and M. S. Lesniak, "Fiber-knob modifications enhance adenoviral tropism and gene transfer in malignant glioma," *The Journal of Gene Medicine*, vol. 9, no. 3, pp. 151–160, 2007, ISSN: 1521-2254. DOI: 10.1002/jgm.1008. [Online]. Available: http://dx.doi.org/10.1002/jgm.1008.

[72] D. Grimm, J. S. Lee, L. Wang, T. Desai, B. Akache, T. A. Storm, and M. A. Kay, "In vitro and in vivo gene therapy vector evolution via multispecies interbreeding and retargeting of adeno-associated viruses," *J Virol*, vol. 82, no. 12, pp. 5887–911, 2008, ISSN: 1098-5514 (Electronic) 0022-538X (Linking). DOI: 10.1128/JVI.00254-08. [Online]. Available: http://www.ncbi.nlm.nih.gov/pubmed/18400866.

[73] T. G. Uil, J. Vellinga, J. de Vrij, S. K. van den Hengel, M. J. W. E. Rabelink, S. J. Cramer, J. J. M. Eekels, Y. Ariyurek, M. van Galen, and R. C. Hoeben, "Directed adenovirus evolution using engineered mutator viral polymerases," *Nucleic Acids Research*, vol. 39, no. 5, e30–e30, 2011, ISSN: 0305-1048 1362-4962. DOI: 10.1093/nar/gkq1258. [Online]. Available: http://www.ncbi.nlm.nih.gov/pmc/articles/PMC3061072/.

[74] N. D. Myers, K. V. Skorohodova, A. P. Gounder, and J. G. Smith, "Directed evolution of mutator adenoviruses resistant to antibody neutralization," *Journal of Virology*, vol. 87, no. 10, pp. 6047–6050, 2013. DOI: 10.1128/jvi.00473-13. [Online]. Available: http://jvi.asm.org/content/87/10/6047.abstract.

[75] I. Kuhn, P. Harden, M. Bauzon, C. Chartier, J. Nye, S. Thorne, T. Reid, S. Ni, A. Lieber, K. Fisher, L. Seymour, G. M. Rubanyi, R. N. Harkins, and

T. W. Hermiston, "Directed evolution generates a novel oncolytic virus for the treatment of colon cancer," *PLOS ONE*, vol. 3, no. 6, e2409, 2008. DOI: 10.1371/journal.pone.0002409. [Online]. Available: https://doi.org/10.1371/journal.pone.0002409.

[76] A. Wortmann, S. Vohringer, T. Engler, S. Corjon, R. Schirmbeck, J. Reimann, S. Kochanek, and F. Kreppel, "Fully detargeted polyethylene glycol-coated adenovirus vectors are potent genetic vaccines and escape from pre-existing anti-adenovirus antibodies," *Molecular Therapy*, vol. 16, no. 1, pp. 154–162, 2008, ISSN: 1525-0016. DOI: https://doi.org/10.1038/sj.mt.6300306. [Online]. Available: http://www.sciencedirect.com/science/article/pii/S1525001616313752.

[77] S. E. Hofherr, E. V. Shashkova, E. A. Weaver, R. Khare, and M. A. Barry, "Modification of adenoviral vectors with polyethylene glycol modulates in vivo tissue tropism and gene expression," *Molecular Therapy*, vol. 16, no. 7, pp. 1276–1282, 2008, ISSN: 1525-0016. DOI: https://doi.org/10.1038/mt.2008.86.

[78] J. Kim, P. H. Kim, S. W. Kim, and C. O. Yun, "Enhancing the therapeutic efficacy of adenovirus in combination with biomaterials," *Biomaterials*, vol. 33, no. 6, pp. 1838–50, 2012, ISSN: 1878-5905 (Electronic) 0142-9612 (Linking). DOI: 10.1016/j.biomaterials.2011.11.020. [Online]. Available: https://www.ncbi.nlm.nih.gov/pubmed/22142769.

[79] F. Kreppel and S. Kochanek, "Modification of adenovirus gene transfer vectors with synthetic polymers: A scientific review and technical guide," *Mol Ther*, vol. 16, no. 1, pp. 16–29, 2008, ISSN: 1525-0024 (Electronic) 1525-0016 (Linking). DOI: 10.1038/sj.mt.6300321. [Online]. Available: http://www.ncbi.nlm.nih.gov/pubmed/17912234.

[80] K. Kunath, A. von Harpe, D. Fischer, H. Petersen, U. Bickel, K. Voigt, and T. Kissel, "Low-molecular-weight polyethylenimine as a non-viral vector for dna delivery: Comparison of physicochemical properties, transfection efficiency and in vivo distribution with high-molecular-weight polyethylenimine," *Journal of Controlled Release*, vol. 89, no. 1, pp. 113–125, 2003, ISSN: 0168-3659. DOI: https://doi.org/10.1016/S0168-3659(03)00076-2. [Online]. Available: http://www.sciencedirect.com/science/article/pii/S0168365903000762.

[81] T. Ishii, Y. Okahata, and T. Sato, "Mechanism of cell transfection with plasmid/chitosan complexes," *Biochimica et Biophysica Acta (BBA) - Biomembranes*, vol. 1514, no. 1, pp. 51–64, 2001, ISSN: 0005-2736. DOI: https://

doi.org/10.1016/S0005-2736(01)00362-5. [Online]. Available: http://www.sciencedirect.com/science/article/pii/S0005273601003625.

[82] Y. Wang, Q. Zhao, N. Han, L. Bai, J. Li, J. Liu, E. Che, L. Hu, Q. Zhang, T. Jiang, and S. Wang, "Mesoporous silica nanoparticles in drug delivery and biomedical applications," *Nanomedicine*, vol. 11, no. 2, pp. 313–27, 2015, ISSN: 1549-9642 (Electronic) 1549-9634 (Linking). DOI: 10.1016/j.nano.2014.09.014. [Online]. Available: http://www.ncbi.nlm.nih.gov/pubmed/25461284.

[83] Y. Yang and C. Yu, "Advances in silica based nanoparticles for targeted cancer therapy," *Nanomedicine*, 2015, ISSN: 1549-9642 (Electronic) 1549-9634 (Linking). DOI: 10.1016/j.nano.2015.10.018. [Online]. Available: http://www.ncbi.nlm.nih.gov/pubmed/26706409.

[84] S. H. Wu, C. Y. Mou, and H. P. Lin, "Synthesis of mesoporous silica nanoparticles," *Chem Soc Rev*, vol. 42, no. 9, pp. 3862–75, 2013, ISSN: 1460-4744 (Electronic) 0306-0012 (Linking). DOI: 10.1039/c3cs35405a. [Online]. Available: http://www.ncbi.nlm.nih.gov/pubmed/23403864.

[85] F. Tang, L. Li, and D. Chen, "Mesoporous silica nanoparticles: Synthesis, biocompatibility and drug delivery," *Adv Mater*, vol. 24, no. 12, pp. 1504–34, 2012, ISSN: 1521-4095 (Electronic) 0935-9648 (Linking). DOI: 10.1002/adma.201104763. [Online]. Available: http://www.ncbi.nlm.nih.gov/pubmed/22378538.

[86] I. Ortac, D. Simberg, Y. S. Yeh, J. Yang, B. Messmer, W. C. Trogler, R. Y. Tsien, and S. C. Esener, "Dual-porosity hollow nanoparticles for the immunoprotection and delivery of non-human enzymes," *Nano Lett*, 2014, ISSN: 1530-6992 (Electronic) 1530-6984 (Linking). DOI: 10.1021/nl404360k. [Online]. Available: http://www.ncbi.nlm.nih.gov/pubmed/24471767.

[87] N. F. Steinmetz, S. N. Shah, J. E. Barclay, G. Rallapalli, G. P. Lomonossoff, and D. J. Evans, "Virus-templated silica nanoparticles," *Small*, vol. 5, no. 7, pp. 813–816, 2009, ISSN: 1613-6829. DOI: 10.1002/smll.200801348. [Online]. Available: http://dx.doi.org/10.1002/smll.200801348.

[88] E. Royston, S.-Y. Lee, J. N. Culver, and M. T. Harris, "Characterization of silica-coated tobacco mosaic virus," *Journal of Colloid and Interface Science*, vol. 298, no. 2, pp. 706–712, 2006, ISSN: 0021-9797. DOI: https://doi.org/10.1016/j.jcis.2005.12.068. [Online]. Available: http://www.sciencedirect.com/science/article/pii/S002197970600004X.

[89] L. Kangasniemi, M. Koskinen, M. Jokinen, M. Toriseva, R. Ala-Aho, V. M. Kahari, H. Jalonen, S. Yla-Herttuala, H. Moilanen, U. H. Stenman, I. Diaconu, A. Kanerva, S. Pesonen, T. Hakkarainen, and A. Hemminki, "Extended release of adenovirus from silica implants in vitro and in vivo," *Gene Ther*, vol. 16, no. 1, pp. 103–10, 2009, ISSN: 1476-5462 (Electronic) 0969-7128 (Linking). DOI: 10.1038/gt.2008.142. [Online]. Available: http://www.ncbi.nlm.nih.gov/pubmed/18754041.

Chapter 2

Synthesis, Characterization, and *In Vitro* Study of Silica Cloaked Adenovirus

2.1 Synthesis of SiAd Nanoparticles

The first experiments performed on synthesizing silica coated Adenovirus (SiAd) were done by Gen Yong, PhD. His thesis (Nanoparticle Formulations for Cancer Therapy, UCSD, 12-Dec-2013) outlined a basic method of synthesis which was expanded upon and explored more here [1]. The core concept behind SiAd formulation is to control silica deposition using surface charge in a template driven manner. This idea was explored in depth by Inanc Ortac, PhD and Ya-San Yeh, PhD for sealing of hollow mesoporous silica nanoparticles [2], [3]. As traditional methods of silica nanoparticle (Stöber method) involve solvents and are incompatible with biological entities, we employed a method that is completely aqueous based

and compatible with enzymes and viruses.

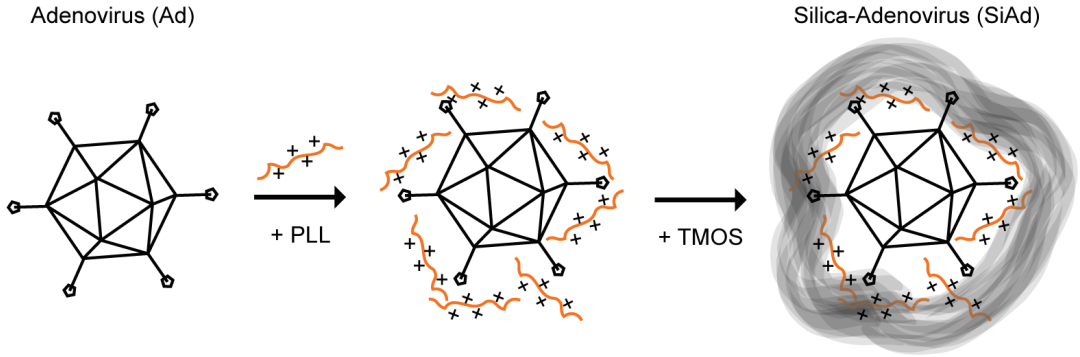

Figure 2.1: Using the native negative charge of Ad, we first complex it with the positively charged polymer, poly-L-lysine (PLL). Next, we add silicic acid (activated TMOS) to induce silica deposition onto the Ad/PLL surface.

The silica reaction we employed is a bulk solution reaction where hydrolyzed tetramethyl orthosilicate (TMOS) condenses in solution. In general, TMOS is acid hydrolyzed in 1 mM hydrochloric acid (HCl) to form highly reactive silicic acid. Nucleation and condensation of silicic acid form precursors to pure silica particles which are negatively charged. If cationic species are present then these precursor particles will condense near such species via electrostatic attraction. If no cationic species are present then these precursor particles will continue to grow and form free silica nanoparticles. Thus there is a competition between directing silica deposition on a desired surface and free silica condensation. Minimizing free silica formation is an important parameter, but not at the expense of incomplete silica deposition or sealing. Thus the surface charge or zeta potential of the template is a defining design parameter.

In the case of Ad, the viral capsid can only act as a template for silica once the surface has been converted to cationic (Figure 2.1). Technically any positively charged polymer such as poly(L-lysine) (PLL), poly(ethylenimine) (PEI), or chitosan can be used in this context. Here we used PLL to mask the negatively charged Ad surface. PLL is a polymer of repeating lysine residues that can be purchased at various molecular weights (MW) or chain lengths. Traditionally PLL (300,000+ MW) was purchased from Sigma-Aldrich Co. LLC. (St. Louis, MO) as a lyophilized powder that was reconstituted in sterile water to make a 1% w/v solution. This solution was further diluted to make a 0.1% w/v solution in sterile filtered water.

Ad expressing green fluorescent protein under a CMV promoter (Ad-GFP) was purchased from Vector Biolabs (Malvern, PA). This stock was supplied at $1x10^10$ PFU/ml and upon arrival dispensed in 10μl aliquots and stored at -80C. Unless noted, for each experiment 10μl was split equally where 5μL was used to make SiAd and the other 5μl used as Ad control. For all tansduction experiments, cells were plated the previous day and subsequently transduced for 48 hours. In general, cells were plated at 90% confluence in 12 well plates. At the time of Ad or SiAd addition the media was replaced. The multiplicity of infection (MOI), the number of viral particles per cell, was based off the number of cells plated, e.g., to achieve a MOI of 1 for 100,000 cells then 1μl of Ad/SiAd (5μl stock diluted to 50μl gave $1x10^6$ PFU/μl) was used. Cells were then visualized using confocal microscopy (Nikon A1R Confocal STORM) and measured using flow cytometry (BD FACSCalibur) for fluorescence. For each

parameter a minimum of 75,000 cells were analyzed in duplicate. Geometric mean fluorescence of all the cells measured is reported due to the finding that some cells transduced with SiAd had fluorescence values greater than 10^4. Unless stated, A549 (lung adenocarcinoma) cell was used as this cell line is easily transduced by Ad. Both neat Ad and cells treated with PBS alone serve as controls for all FACS experiments. Downstream FACS analysis was performed using FlowJo software (Ashland, OR).

Gen Yong, PhD outlined a procedure in "Nanoparticle Formulations for Cancer Therapy" to encapsulate Ad in silica where 10 μl or 1x10^8 PFU Ad stock was incubated with 1.5 uL of 0.1% PLL for five minutes and then a solution of silicic acid was added, 13% v/v TMOS hydrolyzed in HCl. This mixture was diluted to a total of 60 μl and vortexed at room temperature for one hour. Then the solution was spin purified at 14,000 rpm, 4°C for 5 minutes and resuspended to 50 μl in PBS. Attempts to produce SiAd, using the outlined method, with enhanced transduction were unsuccessful. As expanded tropism and enhanced transduction were some of the primary findings from preliminary testing of SiAd, optimization of reaction conditions was explored.

2.2 Optimization of SiAd Reaction Conditions

First, the individual chemical constitutes were tested on Ad to see how each affect transduction. As expected, Ad easily transduces A549 cells (Figure 2.2A blue line). Ad treated with 1 mM HCl or vortexed at room temperature (RT) for two

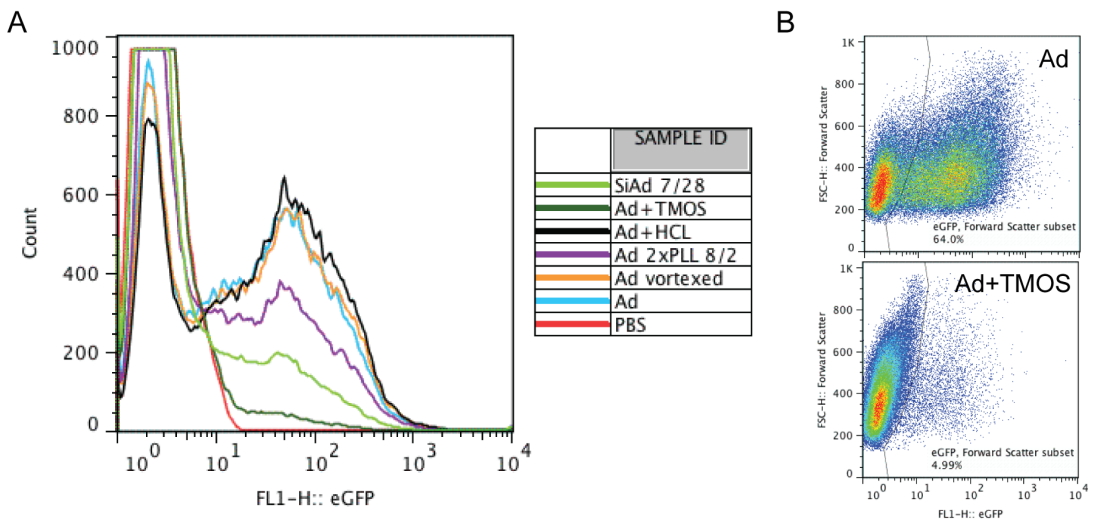

Figure 2.2: (A) FACS histogram, GFP fluorescence, of various conditions. (B) FACS scatter plot of Ad control and Ad treated with TMOS.

hours had no effect on overall transduction (Figure 2.2A, black line and orange line, respectively). When neat TMOS (not prehydrolyzed in HCl) was added to Ad at the same concentration used for SiAd, transduction was essentially ablated suggesting that PLL is necessary and provides a protective layer to the viral capsid (Figure 2.2B). It is possible that TMOS methoxy groups, once hydrolyzed in water, can react with any free hydroxl groups present on the capsid surface such as serine or threonine, which subsequently disrupt viral function. Some groups have shown the PEI complexed with Ad via electrostatic interaction enhances transduction [4]. As a proxy, concentrations of PLL were mixed with stock Ad for 15 minutes and transduction was tested on A549 (Figure 2.3). Surprisingly, no amount of PLL enhanced transduction. Just as PEI is toxic at some level, likely the higher PLL concentrations tested were also toxic. The samples with the lowest PLL concentrations performed

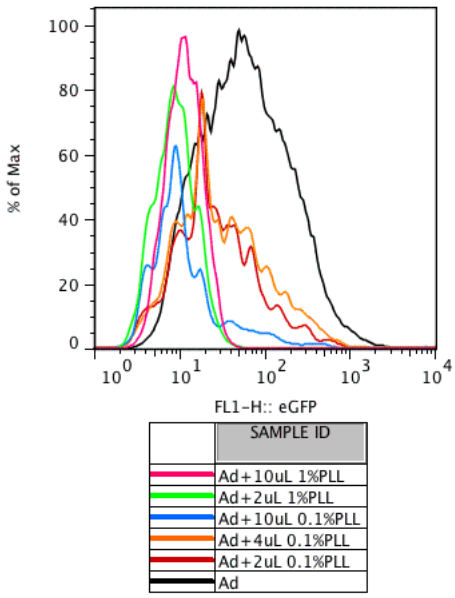

Figure 2.3: Transduction of Ad complexed with various concentrations of PLL. None of which enhanced transduction.

the best, 2 μl and 4 μl of 0.1% PLL. Suggesting that high PLL concentrations were not suitable for silica coating if toxicity was induced. PLL alone as a coating was not explored further.

2.2.1 Trypsin Treatment Test

To develop an easy and quick method of testing silica encapsulation and silica's protective qualities, we employed the use of trypsin as suggested by Yu-Tsueng Liu, PhD. Trypsin is an ubiquitous enzyme used in standard cell culture procedures to detach cells and is easily inactivated by the addition of cell culture media. This proteolytic enzyme is a serine protease that cleaves peptides after arginine and lysine

residues. [5]. We hypothesized that if silica does deposit on the capsid surface then

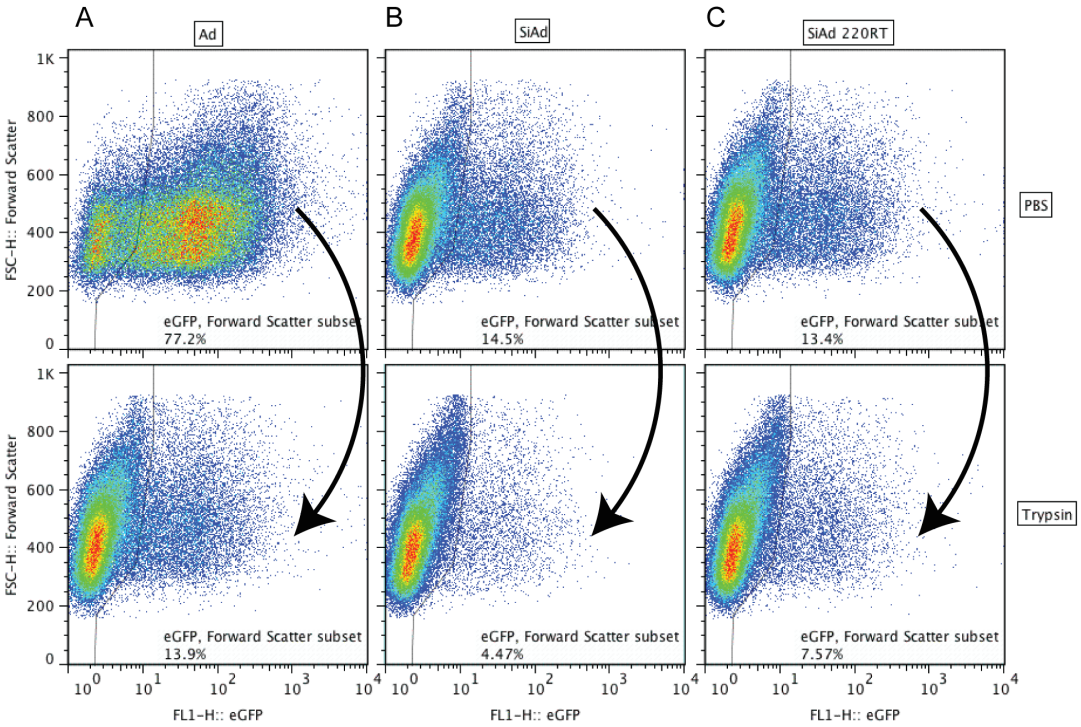

Figure 2.4: Transduction measured before and after 0.25% trypsin treatment for 1 hour (A) Ad (B) SiAd vortexed for 90 minutes (C) SiAd vortexed for 140 minutes.

the capsid proteins would be protected from proteolysis by trypsin. When Ad was incubated with 0.25% trypsin for one hour at 37°C there was a 5.55 fold change in transduction as measured by the difference in geometric mean fluorescence without and with treatment on A549 cells at a MOI of 50 (Figure 2.4A). All geometric mean fluorescence measurements were measured using FlowJo software. The influence of the silica reaction time was tested to see if longer reaction times deposited more silica. Standard SiAd was made for 90 minutes and for 140 minutes. Transduction was compared with and without trypsin treatment (Figure 2.4B & C). Though there

was less overall transduction as compared to Ad, there was a decrease in the loss of transduction post trypsin treatment. This was further enhanced with a longer reaction time where the fold change for standard SiAd (90min) versus SiAd220 (140min) was 3.77 and 1.64, respectively. This suggested that silica does provide a protective mechanism against trypsin treatment. This was further explored as tool for testing encapsulation.

2.2.2 Reduction of Silicic Acid

It was hypothesized that the original formulation tested by Gen Yong had excess silica leading to large particles and free silica formation. Traditionally nanoparticle size is quickly and easily measured using dynamic light scattering (DLS). This measurement uses a cuvette where the smallest cuvette takes a minimum of 70 μl. To achieve sufficient signal and correlation, a full 5 μL of Ad stock must be used or the full sample of one SiAd condition. To save viral stocks, polystyrene beads were tested to determine if the reagents, TMOS and PLL, were in good condition and the amount of free silica formation. Ya-san Yeh, PhD provided hollow mesoporous silica particles (HMSP) to test sealing conditions on. HMSPs were diluted to a similar concentration as Ad viral stock and resuspended in DMEM containing 2 % BSA, 2.5% glycerol in order to mimic Ad conditions. SEM revealed a film coating HMSPs from just the media alone (Figure 2.5A). Using Malvern Zetasizer, the size was 400 nm and the zeta potential was -9.8 mV. Two reactions conditions were tested for

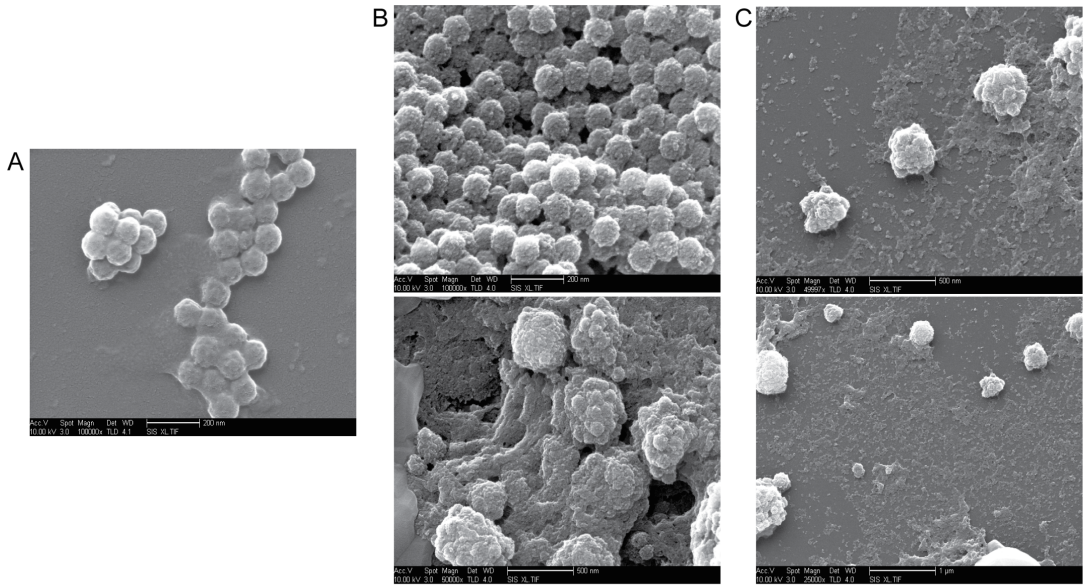

Figure 2.5: (A) SEM of HMSP diluted in DMEM with 2 % BSA, 2.5% glycerol. (B) SEM of HMSPs sealed with less silicic acid, 7.4% v/v. (C) SEM of HMSPs sealed with Yong's formulation, 13% v/v.

sealing with silicic acid. Gen Yong's SiAd formulation used 1.5 μl of 13 % v/v silicic acid (14.8 μl TMOS in 100 μl 1mM HCl or 3.7 μl TMOS in 25 μl 1mM HCl) for 10 μl Ad stock (10^8 PFU). When tested on HMSPs this concentration of silica did seal the HMSPs, but produced excess free silica formation as seen in Figure 2.5C as the "popcorn" like background. A lower concentration of TMOS was tested at 7.4% v/v (2 μl TMOS in 25 μl 1mM HCl). This also sealed HMSPs, but with less excess silica and with a zeta potential of -7.5 mV (Figure 2.5B). Sealing of HMSPs serves as a proxy for coating of virions.

This finding was then translated to coating of Ad. The silica reaction procedure was carried out keeping all parameters constant except for the concentration of

silica used. The particles were test on A549 cells at a MOI of 50 and transduction measured at 48 hours using FACS. When 7.4% v/v silicic acid was used transduction was significantly enhanced as compared to SiAd made with 13% silicic acid (Figure 2.6). Though overall transduction was not enhanced over Ad. Interestingly, there appears to be a population of cells that are super transduced with SiAd, these cells appear with fluorescence greater than 10^4. These cells are likely transduced by particles that contain more than single virions. In addition to reducing the silicic

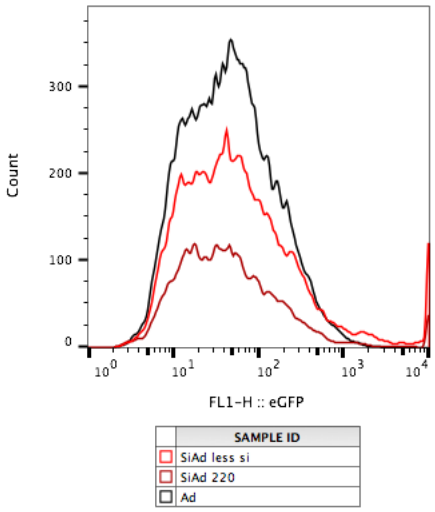

Figure 2.6: Comparing transduction of Ad, SiAd original formulation and SiAd made with less silica.

acid concentration, the length of PLL incubation was increased from 5 minutes to 15 minutes to insure sufficient interaction between negatively charged Ad and positively charged PLL. This new formulation with reduced silica (SiAdv2) was tested against trypsin to determine silica encapsulation. Surprisingly with trypsin treatment on SiAd formulations with longer PLL incubation time resulted in an increase

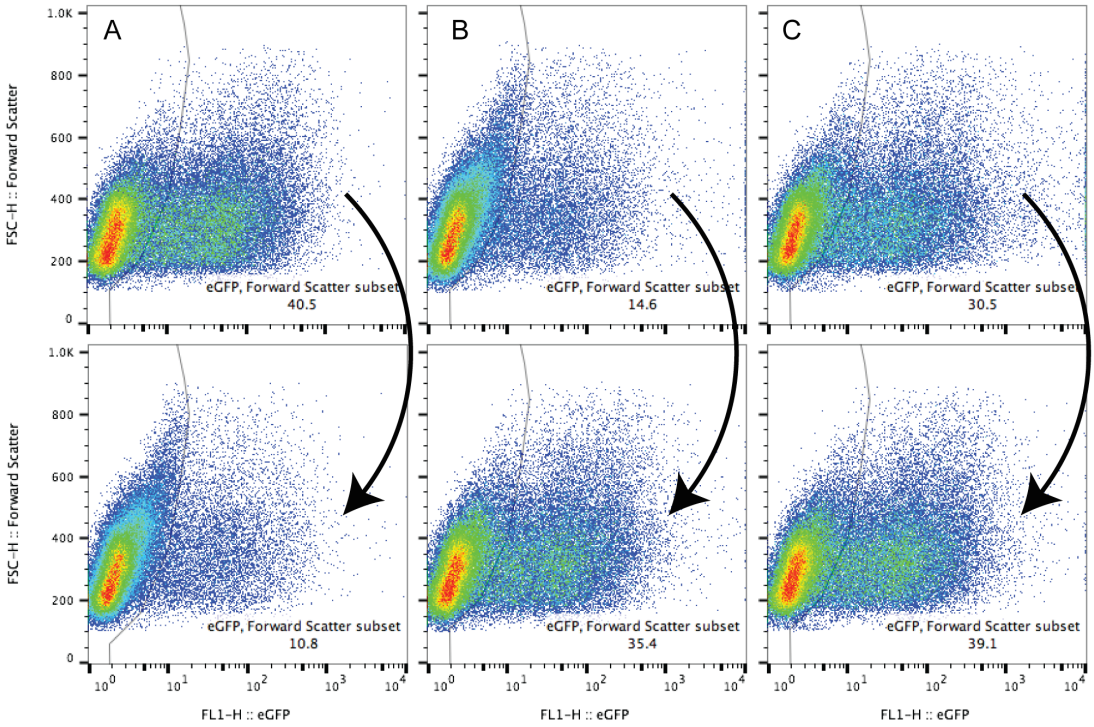

Figure 2.7: Transduction measured before and after 0.25% trypsin treatment for 1 hour (A) Ad (B) SiAd220 (13% silicic acid) (C) SiAd74 (7.4% silicic acid).

in transduction. The fold change in transduction, without treatment/treatment, for SiAd220 and SiAd74 was 0.4 and 0.7, respectively (Figure 2.7A, 2.7B). Considering trypsin can cleave PLL, this suggests that trypsin may actually be breaking up aggregates of SiAd particles that are joined by PLL strands. This is also supported by the reduction in super bright cells, fluorescence greater than 10^4, after trypsin treatment. Again, this population of cells are ones likely transduced by multiple virions, which are likely aggregates of SiAd particles. Less silica and longer PLL incubation improved SiAd transduction with overall transduction efficiency approaching that of Ad (5.5±1.3 vs. 8.7±1.2 geometric mean fluorescence of total cell population).

Dynamic light scattering (DLS) was used to test the effect of the amount of silicic acid (SA) at this reduced concentration, 7.4%, had on particle size. At the amounts tested, particle size was comparable (Figure 2.8).

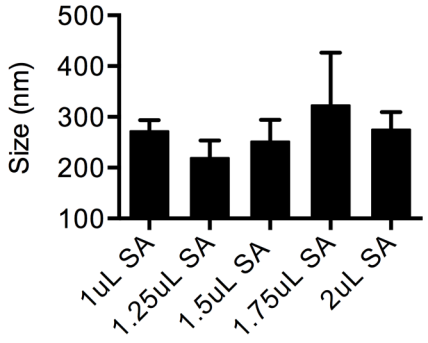

Figure 2.8: Particle size is independent of silicic acid amount. Measured by DLS.

2.2.3 PLL Chain Length

We hypothesized that the PLL chain length could have an effect on the coating process. PLL was purchased at three different chain lengths: 30-70k MW, 70-150k MW and 300k+ MW. Each was reconstituted in sterile water at 1% w/v. Traditionally 300k+ PLL was used for synthesis of hollow mesoporous silica nanoparticles. PLL is known to form nanoparticles in solution. Hydrodynamic radius, measured with DLS, revealed that both 30-70k PLL and 70-150k had aggregates of PLL and large distribution of particles (Figure 2.9 and 2.10). Interestingly, DLS of 300k+ PLL revealed a population of particles that was around 1nm and a small population of aggregates (Figure 2.11). To minimize the downstream particle distribution, 300k+ PLL was used for all experiments.

		Size (d.nm):	% Intensity:	St Dev (d.nm):
Z-Average (d.nm): 319.8	Peak 1:	502.1	71.0	286.7
PdI: 0.460	Peak 2:	4413	11.7	914.8
Intercept: 0.380	Peak 3:	39.05	10.8	22.00

Result quality : Refer to quality report

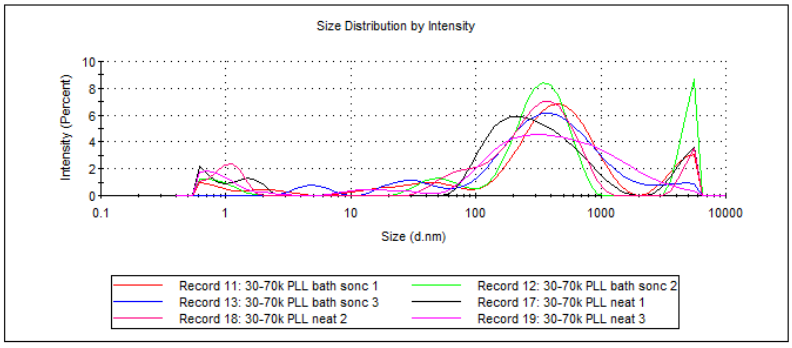

Figure 2.9: Hydrodynamic radius of 30-70k PLL in water.

		Size (d.nm):	% Intensity:	St Dev (d.nm):
Z-Average (d.nm): 230.7	Peak 1:	1652	70.0	1079
PdI: 1.000	Peak 2:	115.6	30.0	55.47
Intercept: 0.409	Peak 3:	0.000	0.0	0.000

Result quality : Refer to quality report

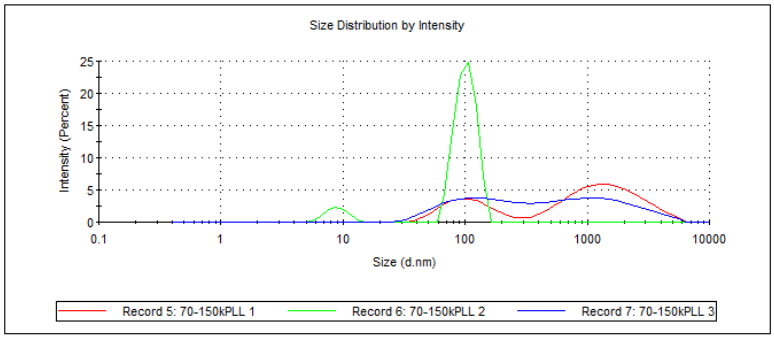

Figure 2.10: Hydrodynamic radius of 70-150k PLL in water.

We tested both the 30-70k and 70-150k PLL to see the effect of PLL chain length on SiAd transduction. Stock solutions were made at 1mg/ml in sterile water. Assuming 300k+ PLL had a molecular weight of 300,000 g/mol, that 70-150k PLL had a molecular weight of 110,000 g/mol, and that 30-70k had a molecular weight of 50,000 g/mol, we normalized all PLL concentrations to the standard formulation

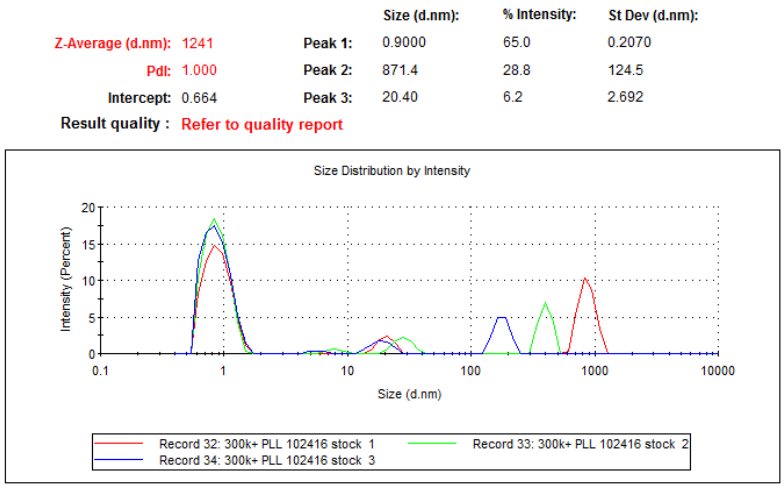

Figure 2.11: Hydrodynamic radius of 300k+ PLL in water.

using $5x10^{-}12$ mol of each. We tested transduction on A549 cells as a measure of efficiency and found only particles made with 300k+ improved transduction over neat Ad (Figure 2.12).

2.2.4 PBS Concentration and Optimized SiAd

Improved transduction with less silicic acid suggested that free silica formation and/or a thick layer of silica is inhibitory to Ad transduction. Yasan Yeh, PhD found that reducing the ionic strength of the solution during the sealing process produced less free silica in solution [3]. Though, performing the reaction in pure water did not seal HMSPs suggesting that dissolved salts act as silica precursor nucleation sites. Thus, SiAd made in 0.05x PBS (5% PBS in sterile water) was tested. To maximize the number of experiments derived from Ad stock, all future experiments used 5 μl Ad stock or $5x10^{7}$ PFU. Subsequently, TMOS was hydrolyzed at 3.6% v/v (1.8 μl

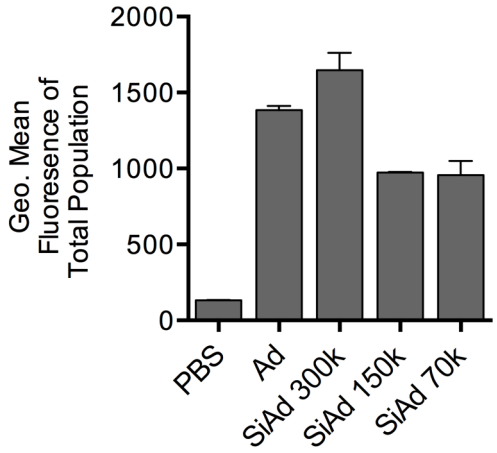

Figure 2.12: SiAd was made with three different PLL chain lengths: 300k+ PLL (300k), 70-150k PLL (150k) and 30-70k PLL (70k). Lysine amount was normalized to the concentration used for 300k formulation. Transduction was tested on A549.

in 48.2 μl 1mM HCl for 1 minute) and the total reaction volume was reduced to 30 μl. First, Ad was incubated with 1.5 μl of 0.1% PLL for 15 minutes and bath sonicated (QSonica, Newton, CT) on low power for 3 minutes. Then 1.5 μl of 3.6% v/v silicic acid was added. This mixture was then diluted to 30 μl in total in 0.05x PBS and vortexed for 140 minutes. Post-vortexing the solution was centrifuged

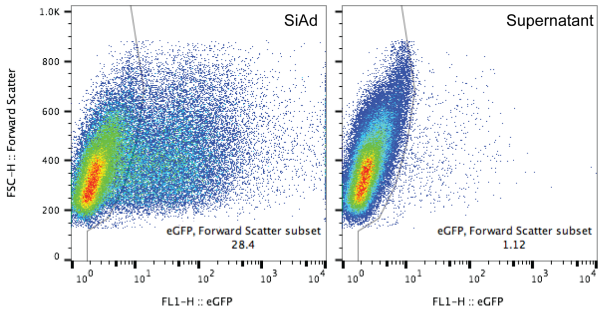

Figure 2.13: Supernatant was collected after centrifuging SiAd and tested on A549 cells.

at 14,000 rpm for 30 minutes at 4°C. Post-centrifugation, 27 μl of supernatant was

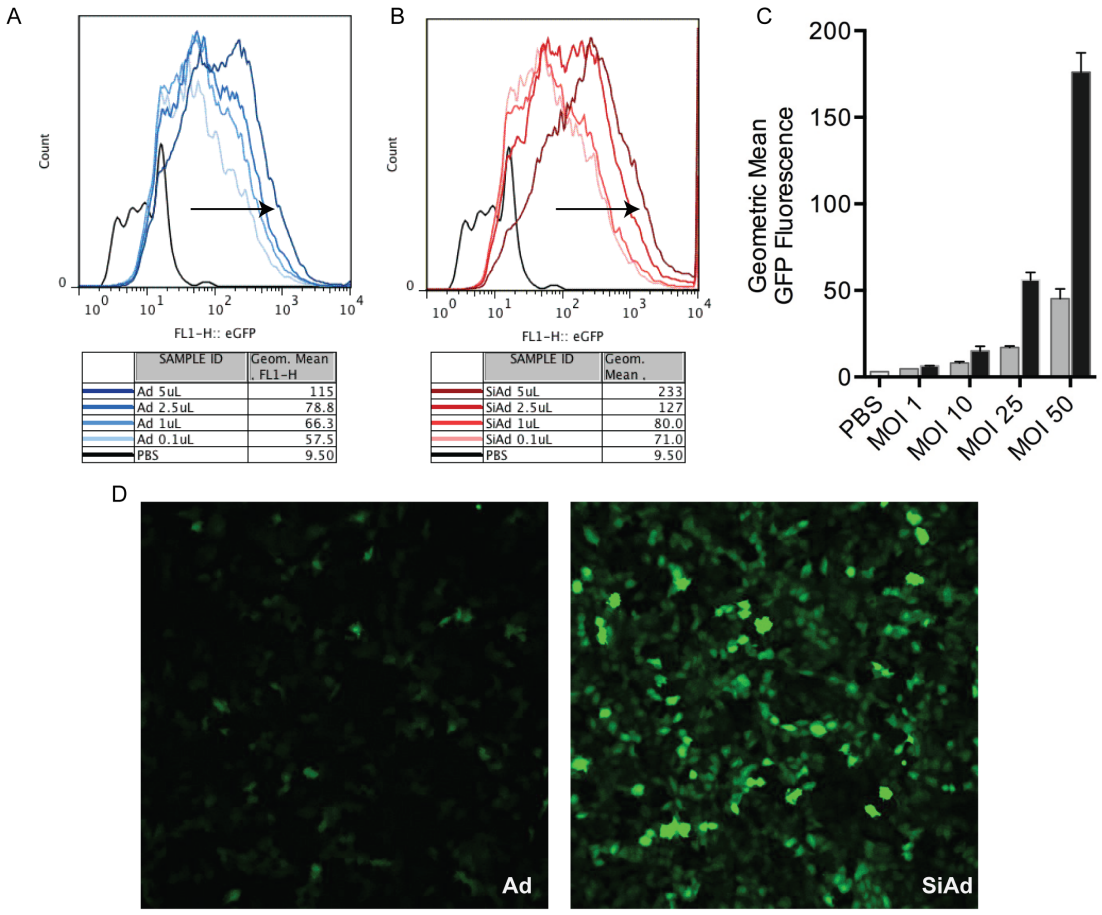

Figure 2.14: Optimized synthesis of SiAd produced particles that enhanced transduction on A549 cells. Histograms of GFP positive cell population at various MOIs (A) Ad and (B) SiAd. (C) Geometric mean fluorescence of total cell population at same MOIs for Ad, grey bars, and SiAd, black bars. (D) Confocal images of Ad and SiAd at MOI 50.

removed and replaced with 47 μl of PBS. To ensure maximum collection of SiAd particles during spin purification the spin time was increased from 5 to 30 minutes. It was suggested that SiAd would not "pellet" at 14,000 rpm, but the supernatant was collected from SiAd and tested for transduction. No significant transduction was found (Figure 2.13). Changing the reaction media to 0.05x PBS significantly improved the transduction of SiAd (Figure 2.14B). This optimized formulation also had enhanced transduction vs. Ad for all MOIs on A549 cells and confirmed with confocal microscopy (Figure 2.14C & D).

2.3 Characterization of SiAd

2.3.1 Transmission Electron Microscopy

Transmission electron microscopy (TEM) is a standard method for visualization of viruses and nanoparticles that cannot be resolved using light. Image contrast is dependent on electron density of the sample. Biological entities i.e. proteins, provide poor contrast and the use of a negative stain such as uranyl acetate is the standard method to stain proteins. Images were taken on a FEI Sphera (UCSD) operating at 200 kV or FEI Technai (OHSU) operating at 120 kV. Copper grids (formvar/carbon-coated, 400 mesh copper, Ted Pella) were prepared by glow discharging the surface at 20 mA for 1.5 minutes. Then 3.5 μl of sample was placed on the grid and allowed to sit for 30 seconds. The solutions were wicked away and washed with water. For imaging of naked Ad, grids were treated with three drops of

1% w/w uranyl acetate to provide negative staining. Ad has a distinct icosahedral

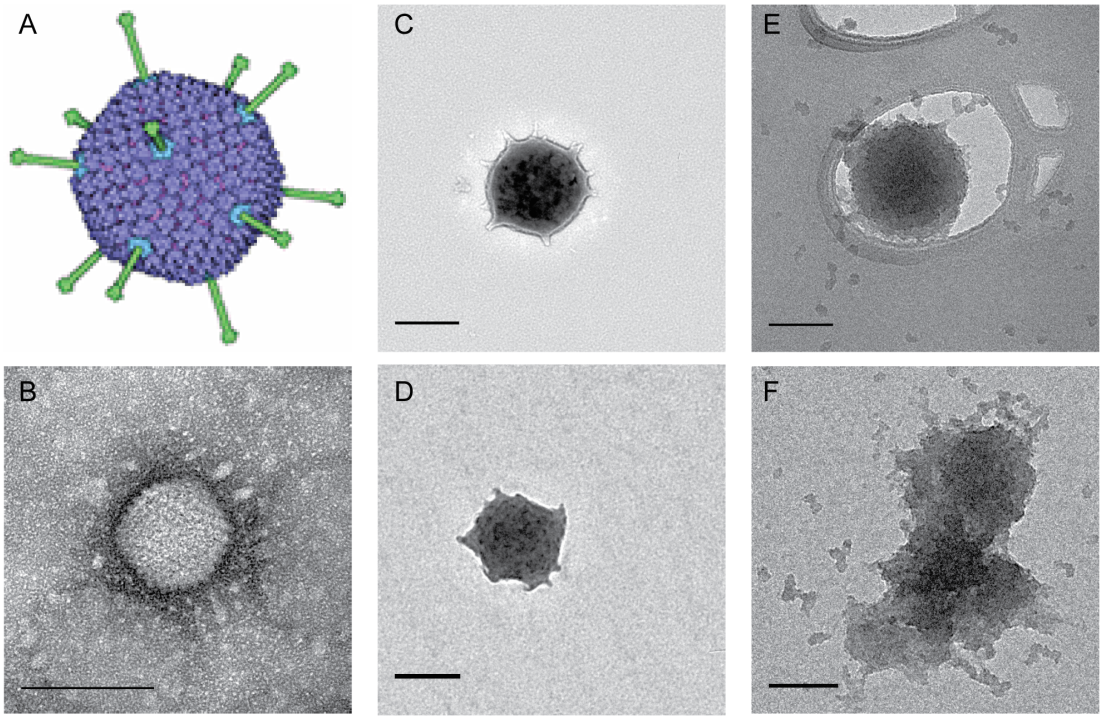

Figure 2.15: (A) Crystal structure of Ad. TEM of Ad stained with uranyl acetate (B) and of SiAd unstained (C, D, E, F). Representative images of particles likely containing a single virion (C, D, E) and a representative image of a SiAd particle likely containing multiple virions (F). All scale bars represent 100 nm.

shape consisting of hexon proteins with fibers at each vertex. The crystal structure of Ad (10.2210/rcsb_pdb/mom_2010_12) is known (Figure 2.15A). TEM of Ad stained with uranyl acetate revealed the classic icosahedral shape though without the resolution of the fiber domains (Figure 2.15B). As silica is electron dense enough to provide contrast in the context of silica nanoparticles, SiAd particles were imaged neat without the use of negative stain. TEM revealed particles that retain similar shape and size as Ad. In Figure 2.14C and Figure 2.15D, spikes protruding from particles appear to be fiber domains coated in silica. The preservation of capsid

proteins is important to retain further downstream function of Ad. In both Figure 2.15D and 2.15F, small 10 nm sized particles are seen littering the background. These small particles are free silica. In Figure 2.15F a particle which likely contains multiple virions can been seen. It is expected to have a distribution of particle sizes considering the silica reaction is a stochastic process which is directed by electrostatic interactions and the because reaction is performed in bulk.

2.3.2 Particle Size and Charge

TEM is an effective technique for qualitatively evaluating particle morphology, but a large number of images need to be taken in order to calculate average particle size. One standard technique to measure particle size is dynamic light scattering (DLS) which measures hyrodynamic radius of particles in solution based on Brownian motion. For DLS measurements on a Malvern Zetasizer ZSP instrument a sufficient concentration of particles is required to get a viable correlation function. Unfortunately the total SiAd sample was required (5 μl of Ad stock) to achieve sufficient concentration even when using a small volume cuvette (70 μl). A significant limitation of DLS is that resolution is limited to particles that are more than three times larger than other particles in solution. Thus, polydisperse samples that contain particles in a range less than a factor of three are not represented properly in DLS measurement.

To get a better representation of the particle size distribution of SiAd, the use

of nanoparticle tracking analysis (NTA) was explored. NTA uses a laser to illuminate the sample, a microscope to visualize particles in solution and a camera to record videos of the particle's Brownian motion. Knowing the temperature and viscosity of the solution allows NTA to calculate particle diameter using the StokesEinstein equation and is not limited to monodisperse samples. In addition, NTA calculates particle concentration. Both Ad and SiAd were measured using Malvern Nanosight (Figure 2.16A & 2.16B). Samples were diluted to 1 mL and five acquisitions at 30 seconds each were taken. The average size of Ad was 205.4 ± 5.7 nm, the mode size was 122.3 ± 1.3 nm, and the estimated concentration was 2.09×10^9 particles/ml. The stock Ad solution itself contains aggregates of viruses even after vortexing and bath sonication. The bimodal distribution in Figure 2.15A revealed a majority of particles were around 100 nm (i.e. single virions) and another minor peak closer to 200nm that are likley aggregates of two virions. For SiAd, the average size was 215.2 ± 7.0 nm,

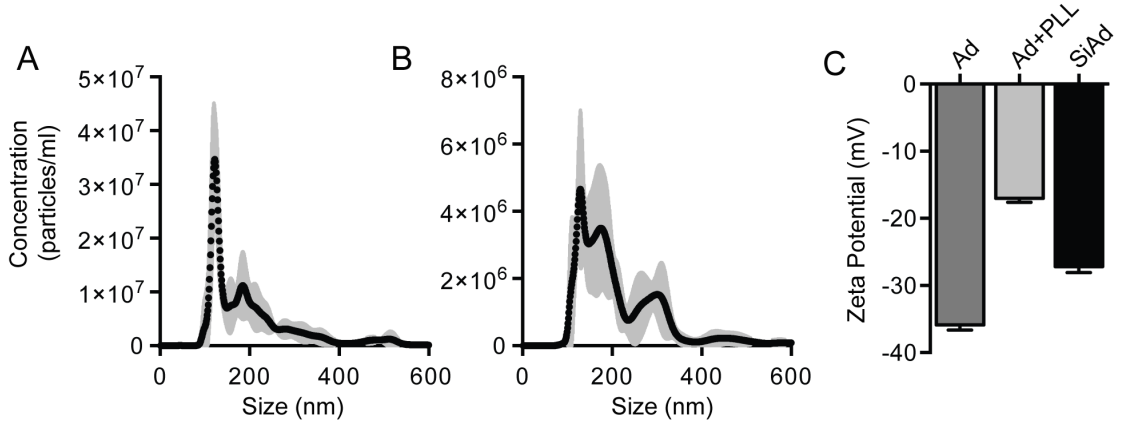

Figure 2.16: (A) NTA of Ad stock. (B) NTA of SiAd. (C) Zeta potential of Ad, Ad+PLL, and SiAd.

the mode size was 141.3 ± 12.1 nm and the estimated concentration was 5.24 x 10^8 particles/ml. As expected the size of Ad increases post encapsulation (Figure 2.16B). Since the stock solution of Ad serves as a template for silica condensation, aggregates of virions will lead to larger silica particles (Figure 2.16B). This is corroborated by the reduction in particle concentration with the assumption that there is minimal loss of virions during the encapsulation process. As previously mentioned, the supernatant from SiAd was tested for viral transduction and no significant transduction was found though not completely negative at 1% of cells being GFP positive (Figure 2.13). Under the assumption that a GFP positive cell was transduced by a single virion then 1% of 100,000 cells results in only 1000 viral particles lost in the supernatant. If the MOI factor is accounted for then there was potentially 50,000 viral particles lost in the supernatant. Ultracentrifugation is one method to ensure complete collection of the sample, but was not tested here. Overall, the NTA data revealed SiAd particles that were slightly larger than Ad alone.

Another method used to characterize nanoparticles is measure the charge as zeta potential. Zeta potential is a bulk measurement that takes into account all charged species in solution and their interaction with the stern double layer of charged particles. This measurement is performed in deionized water as buffered saline or any ionic solution will corrode the electrodes of the device. Attempted zeta measurements of Ad in PBS resulted in burnt electrodes and erroneous measurements. As reported in the literature Ad has a native negative overall charge. Ad purchased from Vector

Biolabs (Malvern, PA) is stored in DMEM with 2% bovine serum albumin (BSA) & 2.5% glycerol. Glycerol is added to impart stability through freeze thaw cycles and is a common additive to viral stock solutions. The zeta potential of Ad stock solution diluted 100 fold in DI water was $-35.9 \pm 0.8mV$ as measured using Malvern's Zetasizer instrument (Figure 2.16C). The presence of BSA and glycerol likely effect both the surface charge and subsequent silica deposition. BSA has an overall negative charge at pH 7 and thus can act as a silica deposition site. The zeta potential of just Ad incubated with PLL before silica deposition was measured at $-17 \pm 0.6mV$ (Figure 2.16C). As expected PLL makes the Ad surface more positive relative to the native Ad capsid. This also suggests that the surface could be made more positive. The zeta potential of SiAd was measured at $-27 \pm 0.9mV$ (Figure 2.16C). As expected the surface becomes more negative post silica encapsulation. The terminal hydroxyl groups of silica contribute to its overall negative charge. In general, the negative charge of silica templated nanoparticles confirms silica deposition onto the positively charged template. In addition, anionic particles reduce the formation of a protein corona associated with serum proteins depositing on cationic surfaces.

2.3.3 qPCR to Detect SiAd

Quantitative polymerase chain reaction (qPCR) is a standard analytical technique for detecting and measuring viral DNA in samples. This is based off of amplification of known target DNA using a designed primer sequence. We tested the use

of qPCR to determine encapsulation efficiency of Ad. The target gene was 3'- GCA CTC CAT TTT CGT CAA ATC TTA TAA TAA GAT GAG CAC TTT GAA CTG TTC CAG ATA TTG GAG CCA AAC TGC CTT TAA CAG CCA -5', which is the fiber region of the Ad genome. A plasmid was selected and amplified against this sequence and used to make a standard curve. Primers were designed using Primer-BLAST (NCBI). All calculations were based of a standard curve derived from serial dilutions of Ad plasmid and measured for each experiment. The cycle threshold (Ct) value is a measure of how much DNA is present. Higher Ct values equate to less DNA amplified and here translated to less virus present. All samples were run in duplicate. qPCR was used to test the robustness of silica encapsulation and if

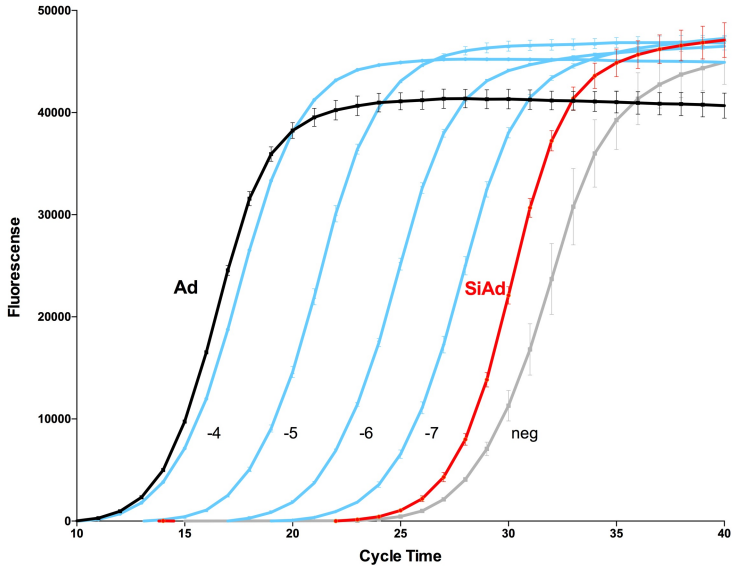

Figure 2.17: As expected qPCR of Ad (black) and plasmid dilutions (light blue) amplified. Interestingly, SiAd (red) did not amplify.

Ad could be quantified post encapsulation. First, Ad and SiAd were tested and we found that Ad amplified as expected, but SiAd did not amplify, a Ct value greater

than 27 (Figure 2.17). This suggested that silica does provide a robust coating of Ad. The first step in qPCR is a ramp to 90°C for 2 minutes, which denatures all hydrogen bonds between DNA base pairs to allow for primer annealing. As SiAd did not amplify, this also suggests that the silica coat is robust enough to withstand such heat treatment.

Next, probe sonication was used to further test the properties of silica. Others in our lab have used probe sonication to break open HMSNs thus it was hypothesized that probe sonication of SiAd could break open the silica coat and allow for viral detection. SiAd was diluted in PBS and treated with various pulse sequences and time using a QSonica Q125 sonicator. The instrument calculates a energy output for each run, measured in joules. These samples were then processed with a Qiagen DNA extraction kit and run on qPCR. Similar to previous experiments, SiAd amplified at a average Ct = 27.8. When treated at 600 J the Ct decreased to 23 suggesting that probe sonication was breaking SiAd and allowing DNA extraction. Each Ct represents a two fold increase in DNA. Other energy outputs were tested on SiAd: Ct = 24.6 at 2743 J, Ct = 26.8 at 5688 J, Ct = 26 at 140 J and Ct = 26 at 8037 J. Surprisingly, higher energy outputs resulted in less DNA extracted, likely due to damaged DNA. Overall, probe sonication was not a reproducible and reliable method for detecting SiAd via qPCR.

To test if silica itself was inhibitory to qPCR analysis, SiAd was spiked into plasmid dilutions to see if there would be an affect on Ct value. Plasmid dilutions

-4, -5, -6, and -7 had Ct values of 15.6, 18.5, 21.8, and 25.6, respectively. Plasmid dilutions spiked with SiAd had Ct values of 16, 18.8, 21.6, and 23.1, respectively. The only sample that was significantly affected was the -7 plasmid dilution, which had a lower Ct. This is counter to other qPCR experiments and likely error. Though on average this suggests that SiAd is not inhibitory to qPCR amplification.

Another method was tested to be able to quantify SiAd with qPCR. Previous experiments showed that SiAd contained functional virions (Figure 2.14), which implied that SiAd nanoparticles are endocytosed and follow a similar pathway as Ad. During endosmal uptake, endosomal vesicles acidify. It was hypothesized that this process dissolves the silica coat and release functional viral particles. Lactic acid was tested to mimic this process *ex vivo*. If the silica coating could be removed with acid treatment then qPCR would likely be able to detect Ad DNA. SiAd was treated with

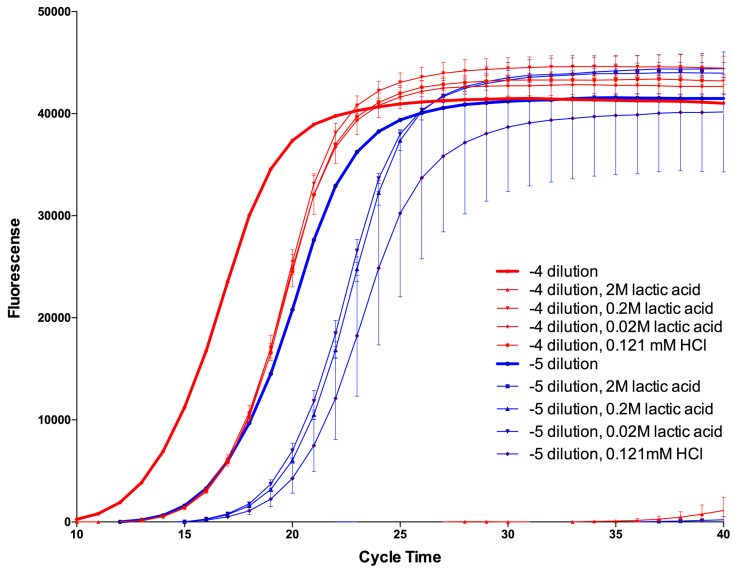

Figure 2.18: Neat plasmid dilutions treated with lactic acid dilutions resulted in variable Cts.

lactic acid or HCl at 37°C for 1.5 hours, subsequently extracted using a Qiagen kit, and run on qPCR. SiAd untreated did not amplify (no Ct), SiAd treated with 0.02M lactic acid had a Ct = 23.3, SiAd treated with 1.21 mM HCl had a Ct = 24.4 and SiAd treated with 0.121 μM HCl had a Ct = 24.7. Lactic acid treatment resulted in detectable DNA from SiAd, but it was suggested that residual acid would affect downstream amplification. Thus plasmid dilutions were tested with acid treatment and it was found that almost all acid concentrations changed the Ct value for plasmid standards (Figure 2.18). Due to this finding, quantification of SiAd via qPCR was abandoned. Overall, SiAd samples with background or non-detectable Ct values were considered samples with particles that were effectively encapsulated in silica.

2.4 *In Vitro* Data

2.4.1 Expanded Tropism and Enhanced Transduction

Viral tropism is parameter defined through evolution where virions transduce specific cells using cellular surface receptors. In the case of Ad, virions interact with the coxsackie-adenovirus receptor (CAR) and cellular integrins for cellular uptake. CAR expression is variable among cell types and within tumors (see section 1.5.1). With optimized SiAd particles (Figure 2.13), characterization and behaviour of such particles was explored *in vitro* using various cell lines. For all experiments, flow cytometry (FACS) was used to quantitatively measure GFP fluorescence and confocal microscopy was used to qualitatively visualize cells 48 hours after seeding Ad

or SiAd at various MOIs. Geometric mean fluorescence is reported to reduce skew associated with super bright cells and is measured on the total cell population not just GFP positive cells. Note that absolute fluorescent protein expression cannot be compared between cell lines due to differences in DNA transcription and DNA translation. Mentioned previously, A549 was used as a positive control cell line since Ad easily transduces these cells and is reported as CAR positive [6]. HeLa (human cervix adenocarcinoma) is another common cell line that is reported as CAR positive [7]. Conversely, T98G (human glioblastoma multiforme), MCF7 (human breast adenocarcinoma), CHO-K1 (Chinese hamster ovary) are inefficiently transduced by Ad are reported as having low CAR expression [8], [9]. CHO-K1 being a non-human cell line is ostensibly CAR negative. As expected both Ad and SiAd transduce in a dose dependent manner. Across all MOIs, SiAd enhanced transduction on A549, T98G, CHO-K1 and MCF7 (Figure 2.19 & Figure 2.20). This is most apparent at MOI 50 where SiAd increased transduction, measured as total GFP fluorescence, by 3.9 fold for A549, 35.6 fold for T98G, 7.6 fold for CHO-K1, 14 fold for MCF-7. On HeLa, only at MOI 50 did SiAd enhance transduction, by 1.6 fold, which suggests that this cell line is strongly CAR positive (Figure 2.19). Clinical MOIs are less the MOI 10 and likely closer to 1 or less depending on tumor volume and dosage. FACS histograms showed a clear shift and increase in GFP positive cells with SiAd treatment even at an MOI 10 (Figure 2.19B). Confocal images confirmed this finding (Figure 2.19C). Enhanced transduction of fluorescent proteins serves as a proxy for

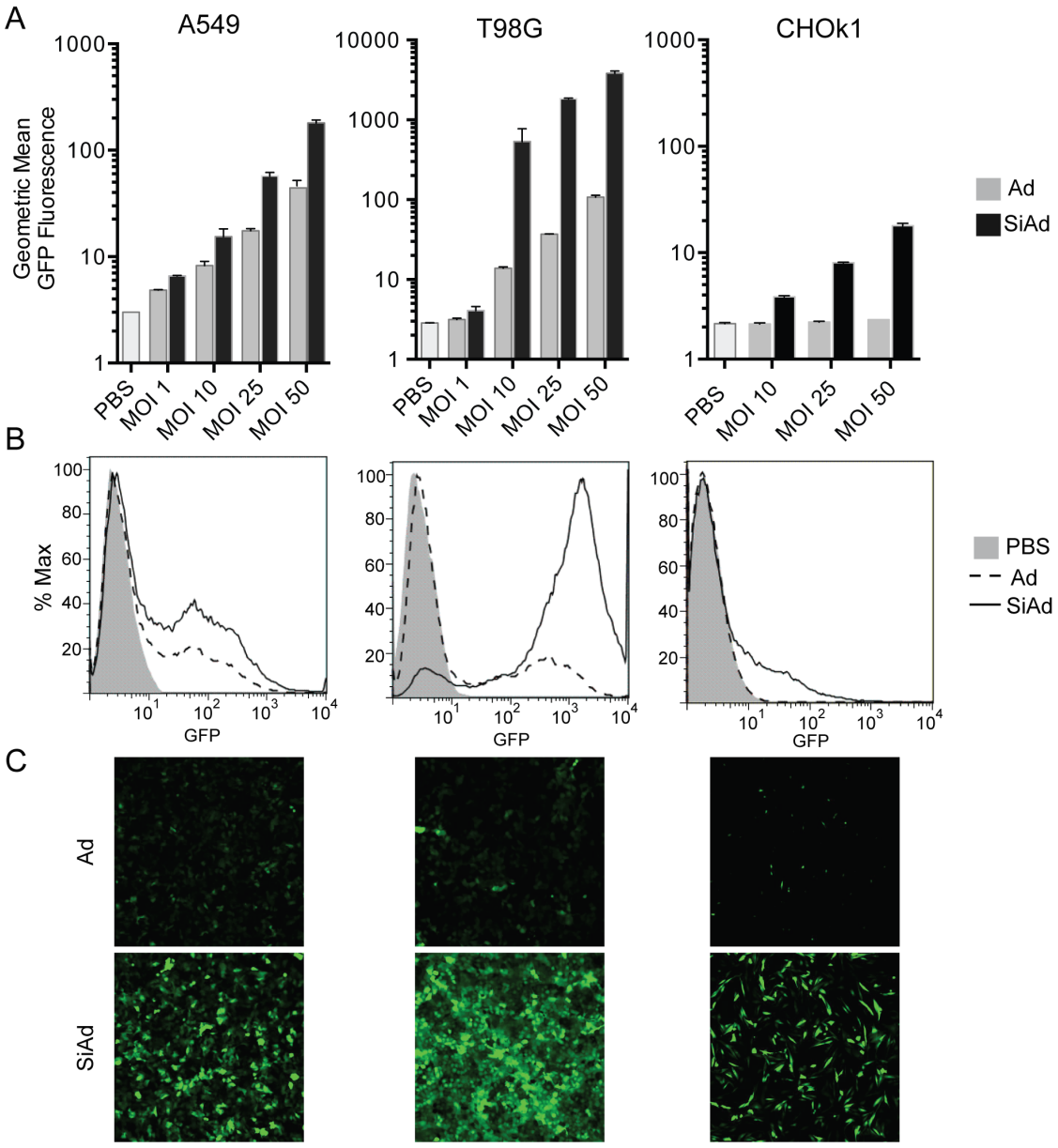

Figure 2.19: (A) Transduction measured by FACS for A549, T98G, and CHO-K1. (B) FACS histograms at MOI 10. (C) Confocal images showing transduction.

enhanced delivery of any protein of interest and even enhanced production of viral progeny.

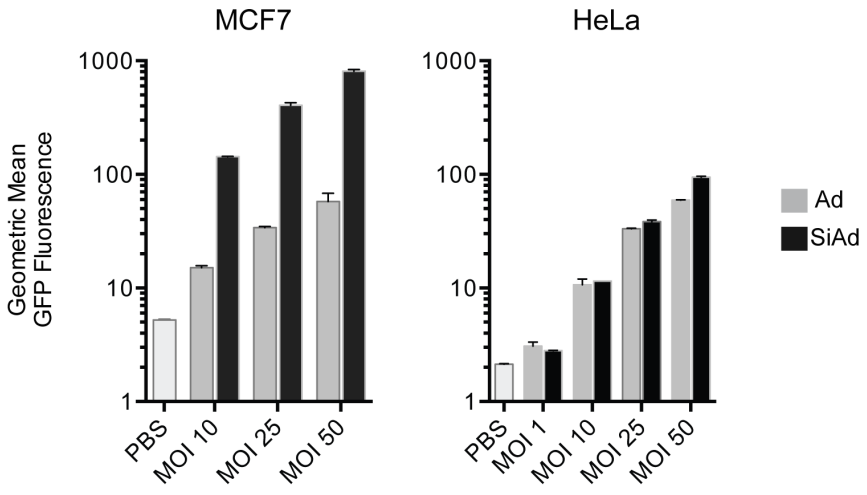

Figure 2.20: Transduction measured by FACS for MCF7 and HeLa.

To test if enhanced transduction in a dish was due to particle settling, transduction was tested on cell lines comparing dishes placed on a orbital shaker versus dishes statically placed in an incubator. Across three cell lines (HeLa, CHO-K1, and SKOV3) transduction was reduced 1.45 fold for Ad and 1.43 fold for SiAd, based off geometric mean fluorescence. This suggests that particle settling is also a factor that enhances transduction for Ad.

2.4.2 Co-tansduction with SiAd

First, to confirm that enhanced transduction with SiAd is not an aberration of GFP, Ad-RFP (cat.#1660) or Ad-mcherry (cat.#1767) was tested. As expected

SiAd enhanced transduction though both red fluorescent proteins tested are not as bright or efficiently produced by cells. For example, at the same MOI there are more GFP positive cells than cells positive for RFP or mCherry. Both NTA and TEM data revealed a population of particles that likely contained multiple virions (size ∼200 - 400 nm). A mixing experiment was devised that used two different virions, Ad-GFP and Ad-RFP, to test if SiAd particles could contain both viruses. Equal parts of Ad-GFP and Ad-RFP were mixed. One aliquot was used for Ad control and another aliquot was used to make Si(Ad-GFP + Ad-RFP). In addition, SiAd made only with Ad-GFP or only with Ad-RFP and then mixed was tested. Confocal microscopy revealed that cells transduced with Si(Ad-GFP + Ad-RFP)

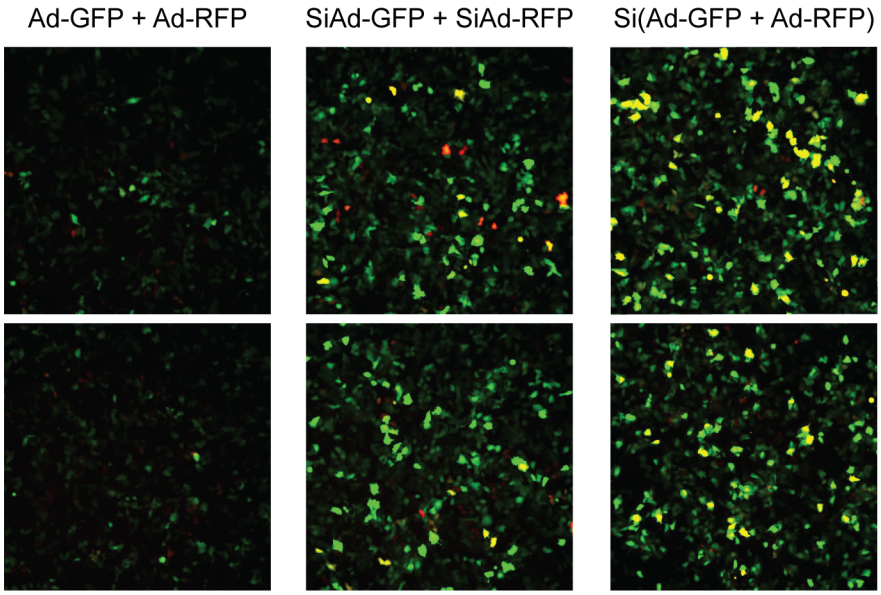

Figure 2.21: Transduction of Ad-RFP + Ad-GFP, SiAd-GFP + SiAd-RFP, and Si(Ad-GFP + Ad-RFP). Cells that expressed both colors (yellow) were transduced with both viruses. Performed in duplicate.

showed significantly more cells expressing both GFP and RFP, cells appear yellow,

as compared to mixing of SiAd-GFP and SiAd-RFP or compared to Ad mixture (Figure 2.21). If SiAd particles only contained one type of virus then there would have been no difference between Si(Ad-GFP + Ad-RFP) and SiAd-GFP + SiAd-RFP transduction.

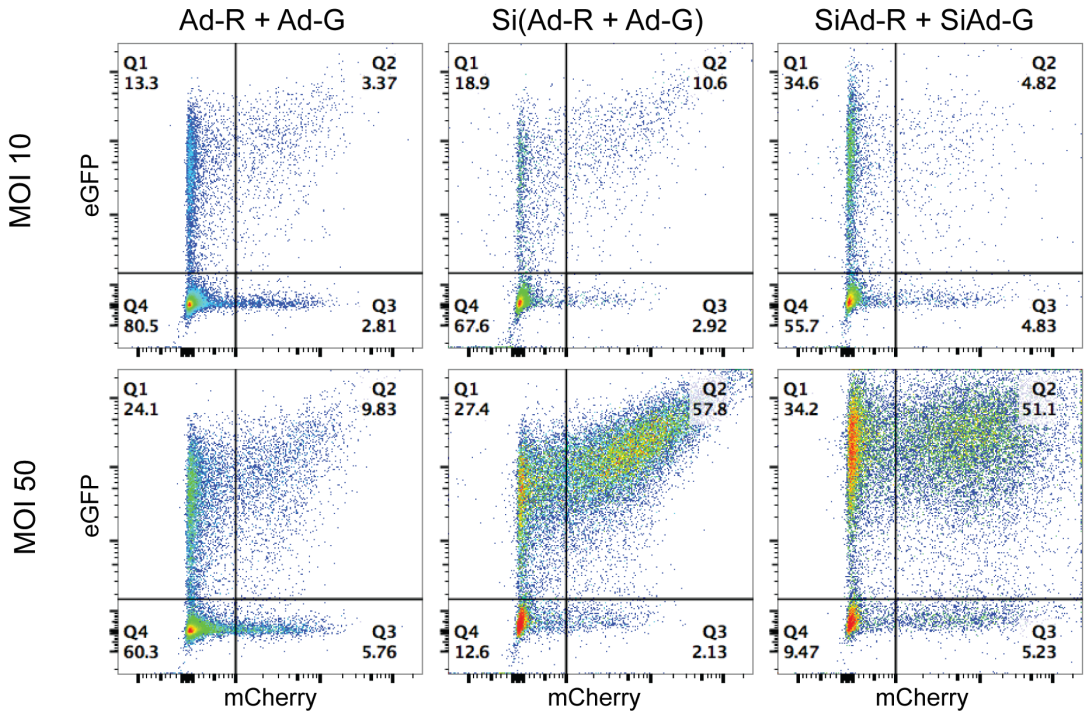

Figure 2.22: Transduction of Ad-RFP + Ad-GFP, SiAd-GFP + SiAd-RFP, and Si(Ad-GFP + Ad-RFP) as measured using flow cytometry on T98G cells.

This was confirmed using T98G cells at both MOI 10 and 50 and measured using flow cytometry (Figure 2.22). Again, we saw enhanced co-transduction of cells with Si(Ad-GFP + Ad-RFP) at both MOIs. At MOI 10, both Ad-R/G and SiAd-R + SiAd-G showed similar levels of co-transduction at 3.3% and 2.8%, respectively, but Si(Ad-R + Ad-G) had 10.6% co-transduction. At MOI 50, Ad-R/G only co-transduced 9.8% of cell but SiAd-R + SiAd-G and Si(Ad-R + Ad-G) showed similar

high levels of co-transduction at 51.1% and 57.8%, respectively. Quadrant 2 (Q2) on the FACS plots corresponds to cells expressing both eGFP (G) and mCherry (R). Enhanced co-transduction of two fluorescent proteins serves as a proxy for any two therapeutic genes of interest.

2.4.3 Live Cell Imaging

Live cell imaging (Nikon A1R STORM) was performed to study kinetics of transduction between Ad and SiAd at MOI 50 over 12 hours. A549 and MCF7 cells were plated in a six well plate that had a coverslip bottom (6-well No. 1.5 coverslip, Mattek Corporation). Confocal images were taken at 15 minute intervals for a 12 hour period. Since protein expression follows transduction, imaging was started four hours (240 minutes) post-addition of particles. As expected and consistent with previous data, SiAd enhanced transduction on both A549 and MCF7 (Figure 2.23A & B). Cutouts show a zoomed in view of the first 300 minutes and revealed that for the first 440 minutes Ad fluorescence is greater than SiAd. For cells treated with SiAd there was a marked increase in fluorescence between 440-540 minutes post-transduction. This delay can be attributed to differences in receptor mediated endocytosis of Ad versus non-specific uptake mechanisms for SiAd. It is surmised that there is also a delay due to dissolution of the silica coat within the cell and subsequent viral release, which is reflected in this initial delay.

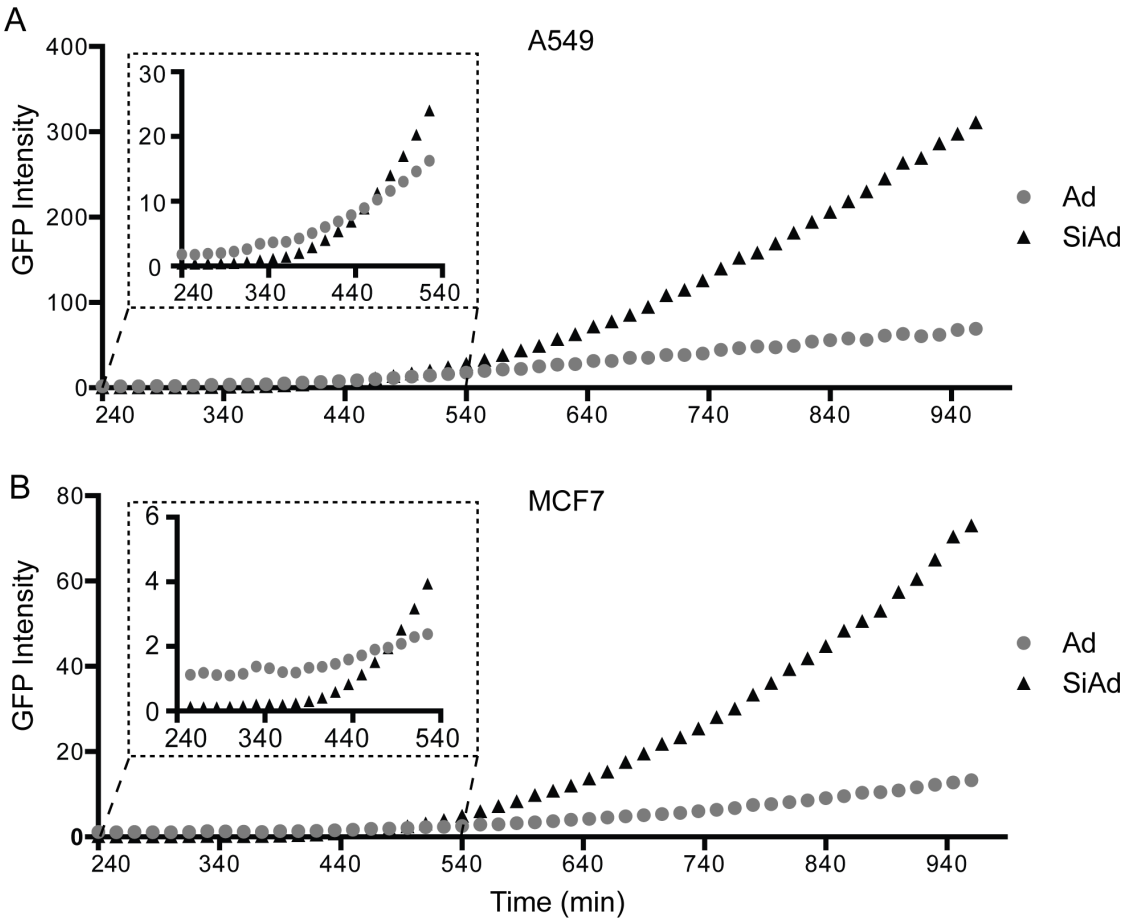

Figure 2.23: GFP intensity over 12 hour period on (A) A549 and (B) MCF7 transduced with Ad or SiAd.

2.4.4 Cell Line CAR Expression

Western blotting was used to measure cellular CAR expression as CAR expression is variable between cell lines. Cell lysates were normalized using a Bradford assay and run on a SDS-Page gel (Bio-Rad). Protein was then transferred and probed with either Anti-CAR (Santa Cruz Biotechnology) or Anti-CAR (Cell Signaling Technology). Bands were visualized using horseradish peroxidase secondary antibody. Actin was used as a positive control for all blots. We found that both antibodies used to probe for CAR resulted in smearing of bands and potential non-specific binding. Interestingly, MCF7 showed the strongest level of CAR expression by western blot (Figure 2.24A), which is in contrast to the relatively lower levels of Ad transduction observed. Chinese Hamster Ovary cells (CHO-K1) are ostensibly human CAR negative and thus should be negative for CAR expression, but showed bands for CAR (Figure 2.24b). From these results, we determined that western blot was a poor technique for determining CAR expression using the antibodies available for purchase. CAR expression can be extrapolated from the efficiency of neat Ad transduction.

2.4.5 Endosome Acidification and Trafficking

Endosomes and their derivatives play an important role in cellular uptake and intracellular release of all types of particles [10]. Viral uptake and release mechanisms are well understood, but synthetic particle trafficking is relatively a black box and

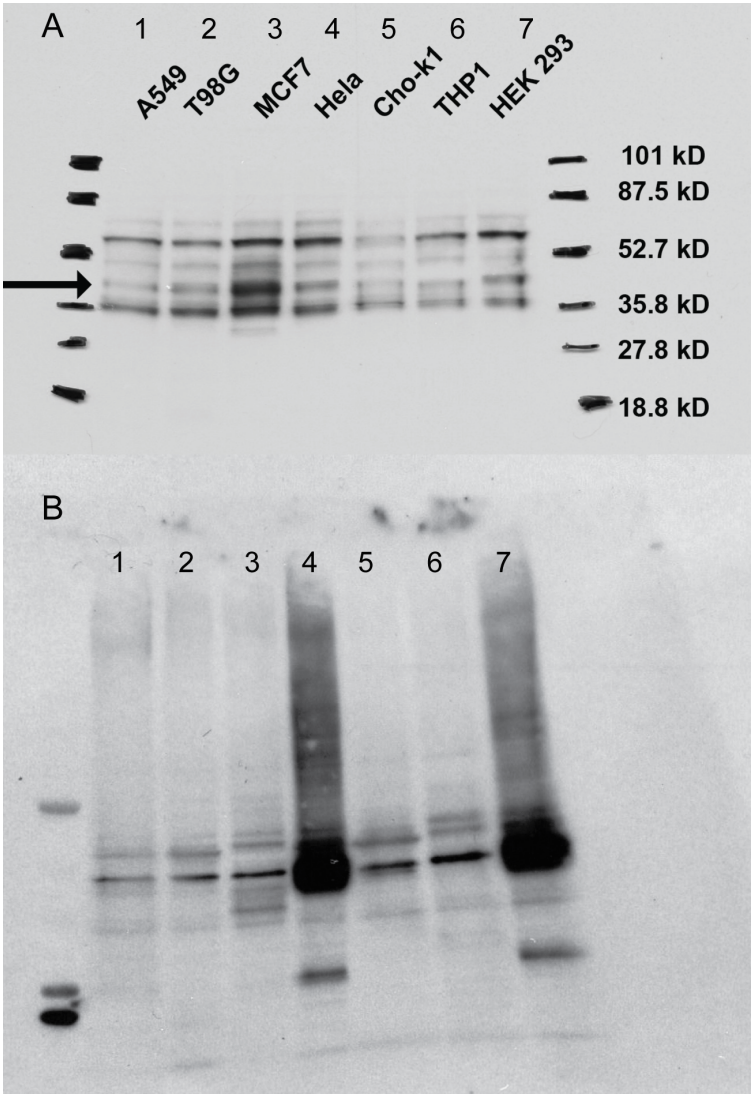

Figure 2.24: (A) Western blot using Santa Cruz Anti-CAR and (B) probed with Cell Signaling Anti-CAR on cancerl cell lines.

dependent on particle surface charge, size, shape, and material of choice. Silica is known to dissolve in both acidic and basic conditions. This is an important attribute for SiAd's function. To investigate this, we used chloroquine phosphate (CP) to inhibit endosome acidification on A549 cells. Deprotonated CP can easily diffuse across cellular membranes and into endosomes where it quickly becomes protonated and trapped; thus, acting as a proton sink [11]. CP is a drug traditionally used to inhibit pH-dependent processes in malarial infections and has also been explored as a anti-HIV treatment [12]. A549 cells were plated overnight. The media was removed and replaced with 2.32M chloroquine phosphate (Sigma Aldrich) made in FBS free media. The cells were incubated for one hour with CP treated media, washed with PBS, and subsequently transduced at MOI 50 in standard media. Geometric mean fluorescence measured by FACS was used to determine the effect of CP. We found that post CP treatment, SiAd transduction reduced by 73.8% while Ad transduction was reduced by 19.3% (Figure 2.25A). We found that endosome acidification was more important for SiAd transduction and a critical step for function. Blocking of endosome acidification likely prevents the dissolution of the silica coat and subsequent viral release leading to reduced transduction. Initially virologists believed that Ad disassembly was also a pH dependent process that occurred in late endosomes, but recently it has been shown that disassembly may take place near the cell membrane and therefore makes Ad less sensitive to inhibition of endosome acidification [13].

To further investigate endosomal trafficking of particles we employed the use

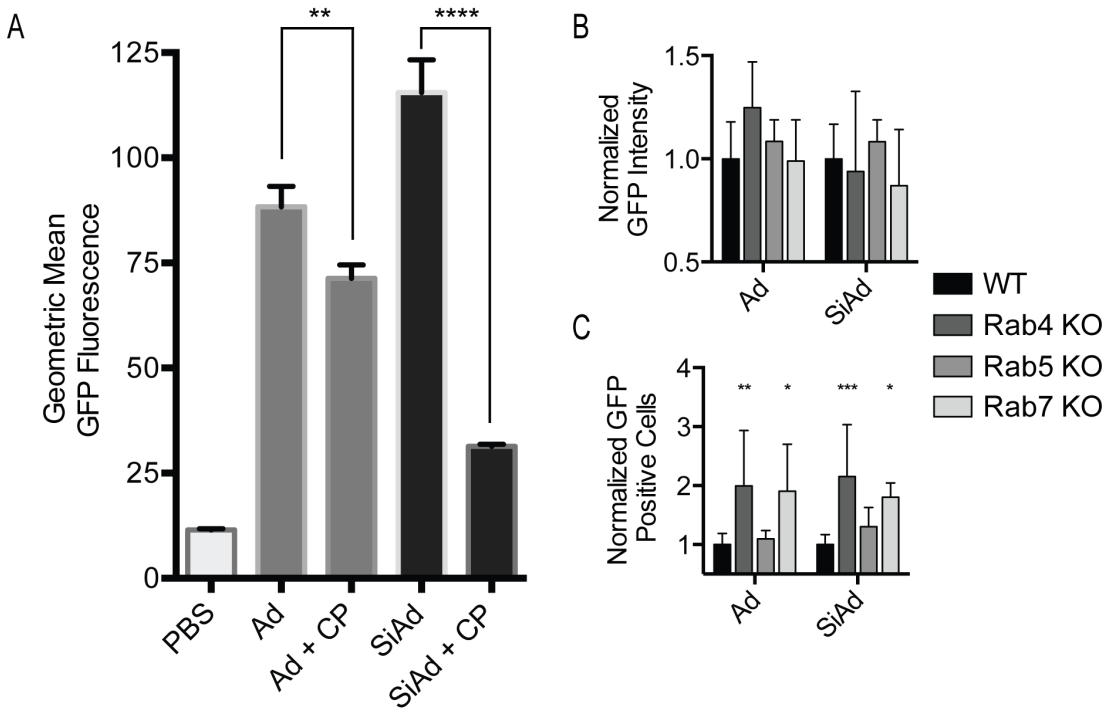

Figure 2.25: (A) Inhibition of endosome acidification on A549 using chloroquine phosphate (CP) significantly reduces SiAd transduction. (B) Transduction of HAP deficient in Rab4A, Rab5A or Rab7a. GFP intensity normalized to wild type (WT) in each group. (C) Number of GFP positive cells normalized to WT in each group. Statistical comparison done with respect to WT. $*P \leq 0.1, **P \leq 0.01, ***P \leq 0.001, ****P \leq 000.1$

of modified haploid cells (HAP) deficient in Rab4A, Rab5A and Rab7A proteins, which are implicated in endosome recycling, early formation, and transition to late endosomes, respectively [14], [15]. There are numerous Rab proteins involved in the complex exchange of intracellular vesicles. These modified cells help elucidate trafficking mechanisms, but biology has redundant mechanisms and generally cells deficient in a single protein are too simplistic a model. HAP cells were generated by Horizon Discovery via CRISPR-Cas9 knockout and maintained in Iscove's Modified Dulbecco's Medium. Cells were transduced at a MOI 10 and the number of GFP positive cells was counted at 48 hours using ImageJ software. As only endocytosis of one virion can lead to GFP production, the number of GFP positive cells was analyzed. Examining the GFP fluorescence did not reveal any significant differences (Figure 2.25B). Experiments are normalized to wild type HAP cells. For both Ad and SiAd, there was an increase in the number transduced cells in the Rab4a and Rab7a knock out cell lines (Figure 2.25C). As expected, endosome recycling and formation of late endosomes are pathways that limit viral release and function. These results suggest that SiAd follows a similar endosomal trafficking pathway as Ad and supports the finding that SiAd particles contain viable, functional virions.

Next, we attempted to determine if CAR had any direct effect on SiAd uptake. It is clear that SiAd can transduce across many cell lines and ones that have low CAR expression (see Figure 2.19), but was not definitive if this property was independent of CAR expression. To determine this, ideally, a cell line that tradi-

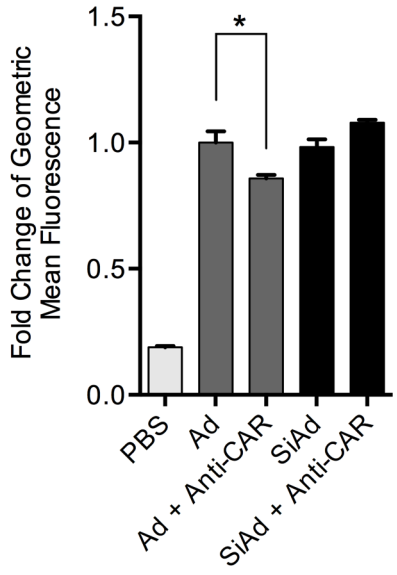

Figure 2.26: Transaction was tested on cells treated with Anti-CAR antibody, $*P \leq 0.1$

tionally expresses CAR could be genetically modified via CRISPR or other gene editing tools to not express CAR, a CAR knock out. An easier and cheaper method of achieving something similar is to use an antibody against the receptor to block it. Anti-CAR was purchased against the extracellular domain (E1-1, Santa Cruz Biotechnology). Serial dilutions of antibody were tested with Ad to determine the effective concentration, which was the concentration of the stock solution. A549 cells were plated overnight and subsequently incubated with 1:10 dilution of Anti-CAR in FBS free media for three hours. Media was then replaced with standard media and cells were transduced at MOI 1. We observed only a slight change in Ad tansduction of Anti-CAR treated cells and no difference in SiAd transduction (Figure 2.26). Antibodies are notoriously variable from company to company and we expected a

larger decrease in Ad tansduction. CAR is the primary receptor used by Ad and aided by cellular integrins, but there are secondary receptors such as heparan sulfate glycosaminoglycans that can also lead to transduction though with lower binding affinity [16].

Experiments were attempted to parse out cellular uptake of Ad or SiAd using the inhibitors: chlorpromazine (clathrin-mediated endocytosis inhibitor), genistein (caveolae-mediated endocytosis inhibitor), or amiloride (macropinocytosis-mediated endocytosis inhibitor), but were unsuccessful.

2.4.6 Silica Bio-compatibility

Silica dioxide, silica, is a FDA approved food additive and has been tested in many biomedical applications [17]. To confirm that SiAd was biocompatible *in vitro*, we used a simple MTT assay to look for cell viability. This assay technically tests cell metabolic activity where the MTT reagent is reduced to formazan in metabolically active cells and is detectable by a colomertric assay. Non-metabolically active cells are assumed to be dead or dying from treatment toxicity. No toxicity was detected for either Ad or SiAd up to a MOI 1000 (Figure 2.27). Triton-x was used as a positive control to ensure the assay was able to detect cell death.

2.4.7 Antibody Neutralization

There are 51 serotypes of Ad that can infect humans which leads to the large population, estimated between 45 to 80%, of people (potential patients of gene

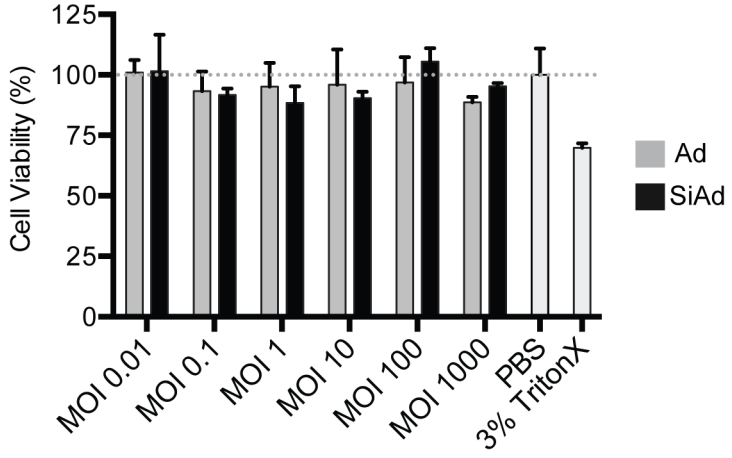

Figure 2.27: MTT assay on serial dilutions of Ad and SiAd. 3% Triton-x was used as a positive control.

therapy) that have neutralizing antibodies already in their system [18]. These neutralizing antibodies reduce the efficacy of Ad based treatments. We hypothesized that coating of Ad could mask antigen recognition in the presence of such neutralizing antibodies. The hexon protein is the major constituent of the capsid and the majority of antibodies are generated against it. Thus we tested transduction of Ad and SiAd with serial dilution of anti-hexon spiked into the culture media. Unfortunately we found that SiAd had reduced transduction in the presence of anti-hexon antibodies (Figure 2.28A). To test if this was due to nonspecific binding, we first tried blocking the surface of SiAd with human albumin. This alone reduced transduction, but not for naked Ad, supporting that surface charge was an important factor (Figure 2.28B). This is surprising since fetal bovine serum (FBS) is used to make cell culture media and a major component of FBS is bovine serum albumin (BSA). Traditionally, polyethylene glycol (PEG) is used to increase circulation half-

life of proteins and nanoparticles by creating a hydration layer that "shields" the particle. This modification improves pharmacokinetics, but changes how these particles engage the cell surface. Cell surface interaction is an important step for Ad transaction to occur thus pegylation reduces transduction [19]. Using PEG-silane to modify SiAd further ablated transduction, as expected (Figure 2.28B). This non-

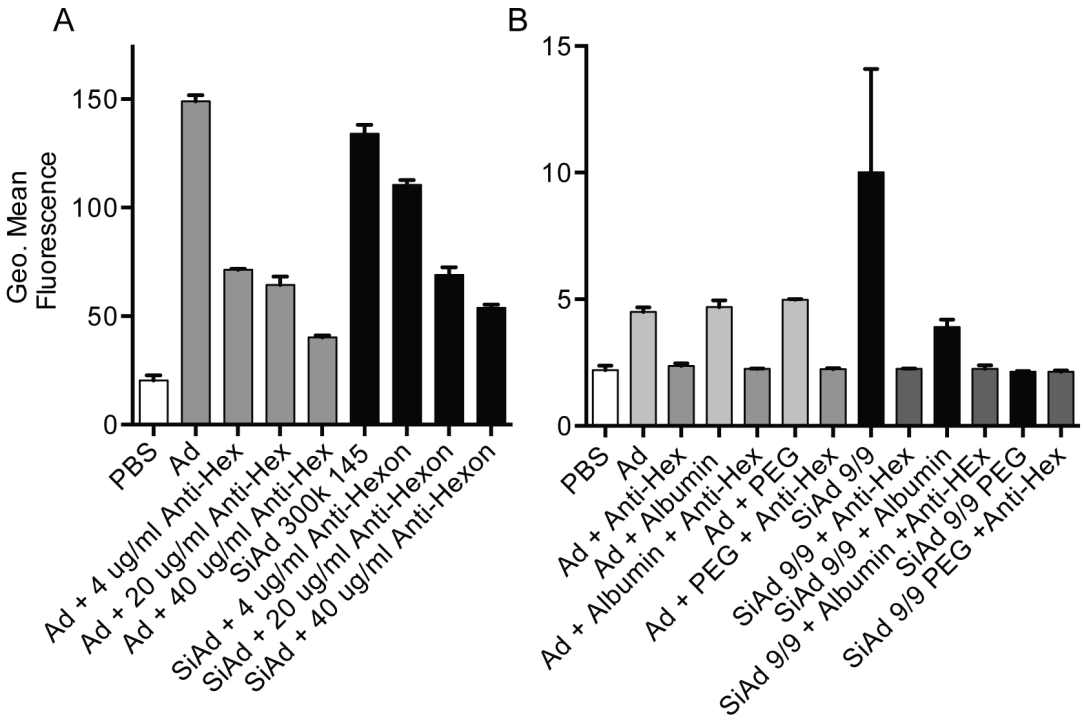

Figure 2.28: (A) Transduction in the presence of anti-hexon. (B) Effect of albumin, PEG, anti-hexon.

specific binding phenomenon was tested with other antibodies such as human IgG and mouse IgG and it was observed that transduction was reduced. One factor that should be considered is that *in vitro* concentrations of antibodies are likely much higher than found in blood. Overall these experiments suggest that the silica layer is sticky and potentially can adsorb serum proteins.

2.4.8 Co-delivery with Cetuximab

This sticky or nonspecific binding nature of the silica layer was at first viewed as serious downfall, but we tested to see if we could use it to our advantage. Antibodies can be used as stand alone drugs or as targeting moieties for nanoparticles. Targeting of nanoparticles using a small molecule or antibody is way to increase specificity and reduce off target effects. These targeting molecules are chosen based off over expression profiles of the cancer of interest [20]. Cetuximab is a FDA approved chimeric antibody to the epidermal growth factor receptor (EGFR) that is over expressed in many epithelial cancers [21]. To test if SiAd's nonspecific uptake of antibodies could be used for targeting, we premixed Cetuximab with SiAd or Ad at multiple concentrations and tested transduction on EGFR positive A549. In addition, these formulations were tested in the presence of anti-Ad antibodies to determine if Cetuximab could act as a blocking agent. We found that addition of Cetuximab only slightly increased transduction, though non-significant, and that pre-mixing with Cetuximab did not prevent neutralization by Ad antibodies (Figure 2.29). Effect of PLL chain length was discussed previously.

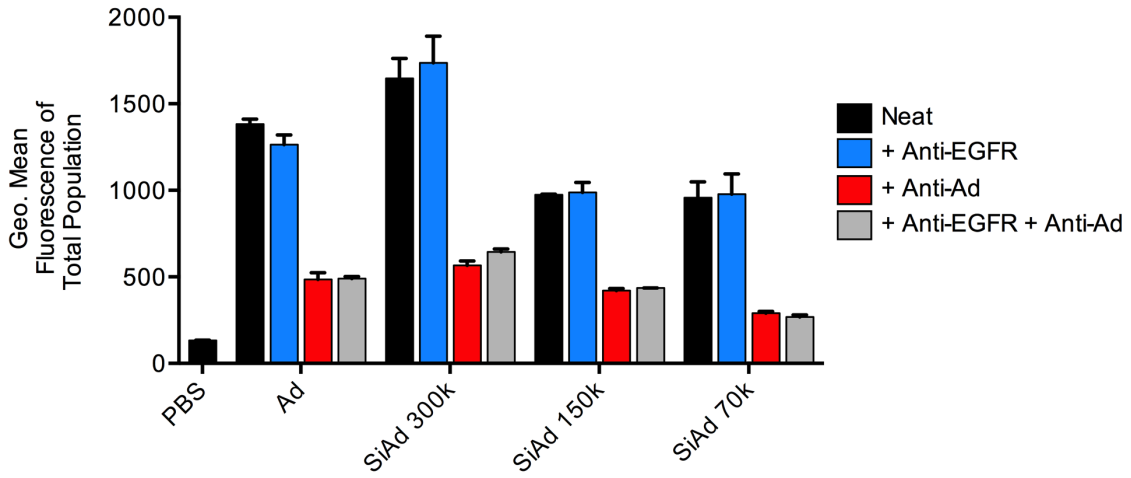

Figure 2.29: Transduction with Anti-EGFR and/or in the presence of Anti-Ad antibodies. Particles were also synthesized with 70-150k PLL (150k) and 30-70k PLL (70k).

2.4.9 Particle Stability

Nanoparticle stability is an important factor to consider for large-scale production and manufacturing. In general, viruses are stable when stored frozen at -80°C and it is well known that viral efficacy decreases after multiple freeze-thaw cycles. We found that viral preparations made with sequential cesium-chloride purification significantly lose activity after a single freeze-thaw cycle (see Figure 3.8). Viral stocks that are stored in buffers containing media and glycerol were found to be stable over multiple freeze-thaw cycles. To test SiAd stability and function, formulations were split and either stored at -80°C or 4°C for seven days. Transduction was tested on A549 cells and compared against fresh preparations (Figure 2.30). We found that for SiAd formulations, transduction was reduced under both storage conditions. This is likely due to unreacted free silicic acid present in solution or from

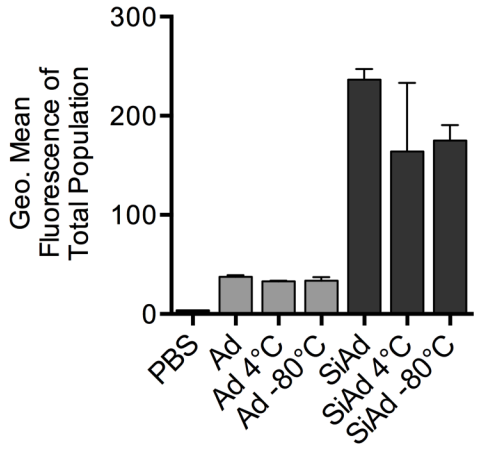

Figure 2.30: Effect of storage conditions on transduction.

freeze-thaw physically breaking SiAd particles. For all experiments both fresh Ad and SiAd were made and used the same day. Further experiments need performed to improve SiAd stability. Dielectrophoresis is one method that could be used to separate unreacted silicic acid from particles in solution.

2.4.10 Enhanced CAS9 Expression

To test delivery of an actual protein of interest, we purchased Ad-eGFP-Cas9 (Vector Biolabs cat.#1901) and tested transduction. This vector is designed to produce the Cas9 protein along with a GFP reporter. Cas9 is a endonuclease used for guide RNA directed cutting of DNA and is the basis for CRISPR-Cas9 gene editing [22]. As expected we saw enhanced transduction of cells with SiAd as measured using the GFP reporter that correlates with Cas9 expression. Future work seeks to use enhanced Cas9 expression to improve the efficiency of gene editing using

this technique.

2.5 Summary and Future Directions

We developed a technique that encapsulates adenovirus in silica as a nanoparticle formulation. Using nanoparticle characterization techniques we showed SiAd nanoparticles that are slightly larger than neat Ad and that can be visualized using TEM. The synthesis reaction was optimized to produce particles that significantly enhance transduction of cancer cell lines, which have varying degrees of Ad transduction efficiency i.e. coxsackie-adenovirus receptor expression. Expanded tropism using SiAd overcomes the long evolutionary history of Ad, which is dependent on CAR binding. Mixing experiments with two viruses (GFP & mCherry) supported both the NTA and TEM data that suggested that SiAd formulations had a population of particles containing more than individual virions. This opens up the potential to combine multiple virions that have synergistic therapeutic genes to be delivered to any cell of interest. The endosome is an important cellular compartment that controls internalization and release of foreign objects i.e. viruses and nanoparticles. We found that endosome acidification is a critical step for silica dissolution and SiAd function. In addition, using cell lines deficient in Rab proteins we found the SiAd and Ad particles follow similar endosomal trafficking pathways supporting hypothesis that SiAd contains functional virions. Overall, these experiments show that SiAd can enhance transduction of many cells *in vitro* and could be applicable

to *ex vivo* therapies that modify cells in a dish. Fluorescent protein expression is a proxy for viral replication and the expression of any protein, shRNA, or cytokine of interest. Thus enhanced delivery of Ad is important not only for oncolytic viral therapy, but also for other gene delivery applications. This technique could also be

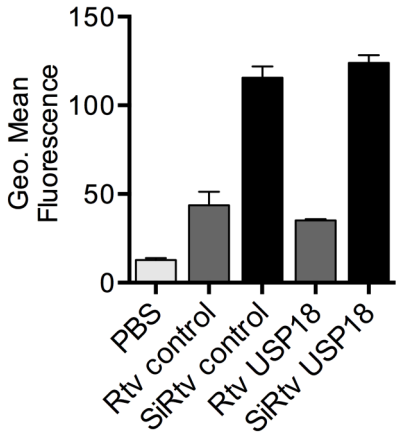

Figure 2.31: Enhanced transduction of retroviruses (Rtv) with SiAd synthesis procedure.

applied to other viruses, specifically the enveloped viruses: retrovirus and lentivirus, which integrate their genomic information resulting in permanent transgene expression. These viruses are commonly used in chimeric antigen receptor T-cell therapy where T-cells are modified *ex vivo* and re-administered to the patient. Preliminary experiments showed enhanced transduction of retroviruses (Rtv) on A549 cells using the same procedure as SiAd synthesis (Figure 2.31). Further characterization and optimization of SiRtv needs to be explored.

2.6 Acknowledgements

Laura Ruff, PhD helped with setting up the qPCR experiments and troubleshooting. Zeynep Sayar helped take TEM images at OHSU. Ya-san Yeh, PhD was an invaluable resource for troubleshooting silica reaction conditions. Kersi Pestonjamasp, PhD assisted with live-cell imaging. Adam Burgoyne, MD, PhD assisted with performing western blots. Guarav Sahay lab provided HAP1 cells to study endosome trafficking. Kei-ichiro Arimoto, PhD provided the retroviruses used in the last experiment described.

The dissertation author was the primary investigator and author of this material. This chapter, in part, is being prepared for submission for publication as Sapre, Ajay; Yong, Gen; Yeh, Ya-san; Ruff, Laura; Sayar, Zeynep; Plaut, Justin; Martinez, Jacqueline; Nguyen, Theresa; Agawal, Anupriya; Liu, Yu-Tsueng; Messmer, Bradley; Esener, Sadik and Fischer, Jared. "Silica Cloaking of Adenovirus Enhances Gene Delivery while Reducing Immunogenicity."

2.7 References: Chapter 2

[1] G. Yong, "Nanoparticle formulations to improve gene therapy," Ph.D. Dissertation, University of California, San Diego, 2014.

[2] I. Ortac, D. Simberg, Y. S. Yeh, J. Yang, B. Messmer, W. C. Trogler, R. Y. Tsien, and S. C. Esener, "Dual-porosity hollow nanoparticles for the immunoprotection and delivery of non-human enzymes," *Nano Lett*, 2014, ISSN: 1530-6992 (Electronic) 1530-6984 (Linking). DOI: 10.1021/nl1404360k. [Online]. Available: http://www.ncbi.nlm.nih.gov/pubmed/24471767.

[3] Y. Yeh, "Engineered silica nanoparticles for enhancing circulation," Ph.D. Dissertation, University of California, San Diego, 2017.

[4] C. Lee, D. Kasala, Y. Na, M. Lee, S. Kim, J. Jeong, and C. Yun, "Enhanced therapeutic efficacy of an adenovirus-pei-bile-acid complex in tumors with low coxsackie and adenovirus receptor expression," *Biomaterials*, vol. 35, pp. 5505–16, 2014.

[5] W. Brown and F. Wold, "Alkyl isocyanates as active-site-specific reagents for serine proteases. identification of the active-site serine as the site of reaction.," *Biochemistry*, vol. 12, pp. 835–40, 1973.

[6] Z. Chen, Q. Wang, J. Sun, A. Gu, M. Jin, Z. Shen, Z. Qiu, J. Wang, X. Wang, Z. Zhan, and J. W. Li, "Expression of the coxsackie and adenovirus receptor in human lung cancers.," *Tumour Biology*, vol. 34, no. 1, pp. 17–24, 2013.

[7] A. Bruning and I. B. Runnebaum, "Car is a cell-cell adhesion protein in human cancer cells and is expressionally modulated by dexamethasone, tnfalpha, and tgfbeta," *Gene Therapy*, vol. 10, no. 3, pp. 198–205, 2003.

[8] C. O. Yun, A. R. Yoon, J. Y. Yoo, H. Kim, M. Kim, T. Ha, G. E. Kim, H. Kim, and J. H. Kim, "Coxsackie and adenovirus receptor binding ablation reduces adenovirus liver tropism and toxicity," *Human Gene Therapy*, vol. 16, no. 2, pp. 246–261, 2005.

[9] M. E. Wohlfahrt, B. C. Beard, A. Lieber, and H. P. Kiem, "A capsid-modified, conditionally replicating oncolytic adenovirus vector expressing trail leads to enhanced cancer cell killing in human glioblastoma models," *Cancer Research*, vol. 67, no. 18, pp. 8783–90, 2007.

[10] L. Y. T. Chou, K. Ming, and W. C. W. Chan, "Strategies for the intracellular delivery of nanoparticles," *Chemical Society Reviews*, vol. 40, pp. 233–245, 2011.

[11] M. A. Al-Bari, "Chloroquine analogues in drug discovery: New directions of uses, mechanisms of actions and toxic manifestations from malaria to multifarious diseases," *J Antimicrob Chemother*, vol. 70, pp. 1608–21, 2015.

[12] A. Savarino, J. R. Boelaert, A. Cassone, G. Majori, and R. Cauda, "Effects of chloroquine on viral infections: An old drug against today's diseases," *The Lancet Infectious Diseases*, vol. 3, pp. 722–727, 2003.

[13] O. Maier, S. A. Marvin, H. Wodrich, E. M. Campbell, and C. M. Wiethoff, "Spatiotemporal dynamics of adenovirus membrane rupture and endosomal escape," *J Virol*, vol. 86, pp. 10 821–8, 2012.

[14] J. Rink, E. Ghigo, Y. Kalaidzidis, and M. Zerial, "Rab conversion as a mechanism of progression from early to late endosomes," *Cell*, vol. 122, no. 5, pp. 735–49, 2005.

[15] M. Zerial and H. McBride, "Rab proteins as membrane organizers," *Nat. Rev. Mol. Cell Biol.*, vol. 2, pp. 107–117, 2001.

[16] Y. Zhang and J. M. Bergelson, "Adenovirus receptors," *J Virol*, vol. 79, no. 19, pp. 12 125–31, 2005.

[17] T. Asefa and Z. Tao, "Biocompatibility of mesoporous silica nanoparticles," *Chemical Research in Toxicology*, vol. 25, no. 11, pp. 2265–2284, 2012.

[18] N. Tatsis and H. C. Ertl, "Adenoviruses as vaccine vectors," *Mol Ther*, vol. 10, no. 4, pp. 616–29, 2004.

[19] S. E. Hofherr, E. V. Shashkova, E. A. Weaver, R. Khare, and M. A. Barry, "Modification of adenoviral vectors with polyethylene glycol modulates in vivo tissue tropism and gene expression," *Molecular Therapy*, vol. 16, no. 7, pp. 1276–1282, 2008, ISSN: 1525-0016. DOI: https://doi.org/10.1038/mt.2008.86.

[20] R. Bazak, M. Houri, S. El Achy, S. Kamel, and T. Refaat, "Cancer active targeting by nanoparticles: A comprehensive review of literature," *J Cancer Res Clin Oncol*, vol. 141, no. 5, pp. 769–84, 2015.

[21] S. H. Tseng, M. Y. Chou, and I. M. Chu, "Cetuximab-conjugated iron oxide nanoparticles for cancer imaging and therapy," *Int J Nanomedicine*, vol. 10, pp. 3663–85, 2015.

[22] J. A. Doudna and E. Charpentier, "The new frontier of genome engineering with crispr-cas9," *Science*, vol. 346, no. 6213, 2014. DOI: 10.1126/science.1258096. [Online]. Available: http://science.sciencemag.org/content/sci/346/6213/1258096.full.pdf.

Chapter 3

Biodistribution and Immune Response to SiAd in Immune-compromised and Immune-competent Mice

It is well known that biomedical technologies from pharmaceuticals to nanoparticles behave differently in an dish than in an animal model. This stems both from the complexity of biological systems and the relatively simplistic *in vitro* experimental setups. A major factor *in vivo* that influences viral and nanoparticle fate is pharmacokinetics, which relates to the distribution, bioavailability, absorption, excretion, and metabolism of drugs/viruses/nanoparticles. This is largely influenced by the method of delivery, particle size, particle charge, and particle shape [1], [2]. This is further complicated by the choice of animal model. Here we tested Ad and SiAd in both immune compromised (NOD scid gamma) and immune competent

(C57BL/6) mice. All animal experiments were approved by the Institutional Animal Care and Use Committee (IACUC) and the Institutional Biosafety Committee (IBC) at Oregon Health and Science University (Portland, OR). In NSG mice, we generated xenografts from the T98G cell line, which showed high levels of SiAd transduction *in vitro*. First, we tested the biodistributiong of SiAd using luciferase (luc) as a reporter gene. Then as a model for cancer gene therapy we used Ad expressing TNF-related apoptosis-inducing ligand (TRAIL) that selectively induces apoptosis in cancer cells. In immune competent mice we tested luc expression in muscle via IM injections and measured plasma cytokine levels as a measure of the innate immune response to Ad or SiAd. In addition, to look for the adaptive immune response we measured plasma neutralizing antibodies. Overall the *in vivo* data makes a strong case for enhanced cancer gene therapy using SiAd.

3.1 Immune Compromised Model

3.1.1 T98G Xenografts

Generation of tumor xenografts, human cells in a animal model, is a common technique to mimic human solid tumors at a basic level. In general, xenografts can only be grown in immune compromised animals of which the easiest to work with are mice. As the T98G cell line showed robust transduction *in vitro*, we generated T98G xenografts in NOD scid gamma (NSG) mice. NSG mice were purchased from the Jackson Laboratory (stock #005557). Mice were housed in high-efficiency particulate

air (HEPA) cages in a specific pathogen-free facility with food and water available ad libitum and a 12-hour light/dark cycle. Both male and female mice were used for the experiments, aged between 8-12 weeks. Xenografts were formed by subcutaneous injection of 200μl into both flanks with 2x10^6 T98G cells (ATCC) in a 1:1 ratio of DMEM:Matrigel HC (Corning) containing 0.5μg/mL recombinant human Vascular Endothelial Growth Factor (VEGF) (R&D Systems) and 1.25μg/mL recombinant human Fibroblast Growth Factor basic (FGF) (R&D Systems). Xenografts were serially passaged by digesting the xenografts with Collagenase/Dispase (Roche) and re-injecting the digested cells subcutaneously in the same solution as performed initially. Xenografts were $\leq$1cm^3 at the time of injection. The first set of tumors took almost three months to grow, but subsequent passages reduced this time to a few weeks.

3.1.2 Intratumoral Injections

We tested Ad expressing luciferase (Ad-luc) purchased from Vector Biolabs (Malvern, PA) at two different concentrations and preparations. The first preparation was one that is commonly used for *in vitro* experiments at 1x10^{1}0 PFU/ml in a crude buffer of DMEM, 2% BSA, 2.5% glycerol. This preparation is similar to the Ad-GFP prep used for all experiments in Chapter 2. A second preparation was also tested, designed for *in vivo* work that was purified with two sequential cesium chloride gradients at 1x10^{1}1 PFU/ml and stored in 5% glycerol in PBS. Note that

luciferase is a common reporter gene derived from fireflies that produces bioluminescense through the enzymatic breakdown of the substrate luciferin. For imaging, 100uL (3mg, 150mg/kg) of VivoGlo Luciferin (Promega) was injected intraperitoneally into mice 9 minutes prior to initial imaging. Mice were anesthetized with isoflurane and then imaged in the IVIS Lumina XRMS Series III (Perkin Elmer). For each mouse both the abdomen and back were imaged with the same settings: 5-minute exposure, medium binning, and F-stop = 1. Mice were imaged a single time per day, but multiple times over the course of an experiment. Unless specified, luciferase expression 5 days post treatment, measured as average radiance (p/s/cm2/sr), is reported. Average radiance was determined using Living Image Software (Perkin-Elmer) at a 25% threshold. When tumors or livers did not show measurable levels of luciferase, a default area was used to calculate signal intensity and was consistent between experiments.

First, we tested low dose Ad-luc (1x10^{1}0 PFU/ml) on T98G xenografts. SiAd was made as outlined in Chapter 2. Tumors were injected with 50μl of Ad or SiAd (5x10^7 PFU). Each mouse received two IT injections of a single treatment and was imaged at day 5. Representative images shown in Figure 3.1A. We found that the average radiance for tumors injected with Ad and SiAd was 9.83x10$^4\pm$ 1.94x10^5 and 2.75x10$^5\pm$ 4.54x10^5, respectfully, though non-significant (Figure 3.1B). On the other hand, we found that liver transduction was significantly reduced in mice treated with SiAd where the majority of mice had background levels of liver luciferase signal

(Figure 3.1B). In line with previous studies, liver transduction in Ad treatment mice was very robust at $4.44x10^5 \pm 1.36x10^5$, which is higher than Ad tumor transduction itself. This is most obvious when comparing the total tumor transduction to liver signal in each mouse where SiAd treated mice had on average significantly reduced off-target transduction by 272 fold (Figure 3.1C). To confirm this finding, we IT injected one tumor with SiAd-GFP and Ad-mCherry and looked for transduction in tumor and liver sections (Figure 3.1D & E). Tumor sections showed comparable levels of SiAd and Ad transduction, however liver sections showed markedly reduced SiAd transduction (green) vs. Ad (red). This data is derived from two separate experiments on passage 2 and passage 3 of tumors.

Considering that 1 cm^3 of tumor tissue contains $1x10^8$ - $1x10^9$ cells and that these initial experiments were done with $5x10^7$ PFU, this resulted in an MOI less than 0.5-0.05 [3]. This is a very low dose of viral particles compared to *in vitro* experiments where typical MOIs range between 5 and 500. To increase the dose, we purchased Ad-luc (Vector Biolabs) at $1x10^11$ PFU/ml. SiAd particles were made under the same conditions as low does particles, though with 10x the concentration of virions [i.e. 5μl of $1x10^11$ PFU/ml was incubated with 1.5μl of 0.1% PLL for 15 minutes then 1μl of silicic acid (1.8μl TMOS + 48.2μl 1mM HCl) was added and the total volume was diluted to 30μl in 0.05x PBS]. Note that the high dose preparation is considered to be more pure than the low dose preparation as viruses are stored in 5% glycerol in PBS.

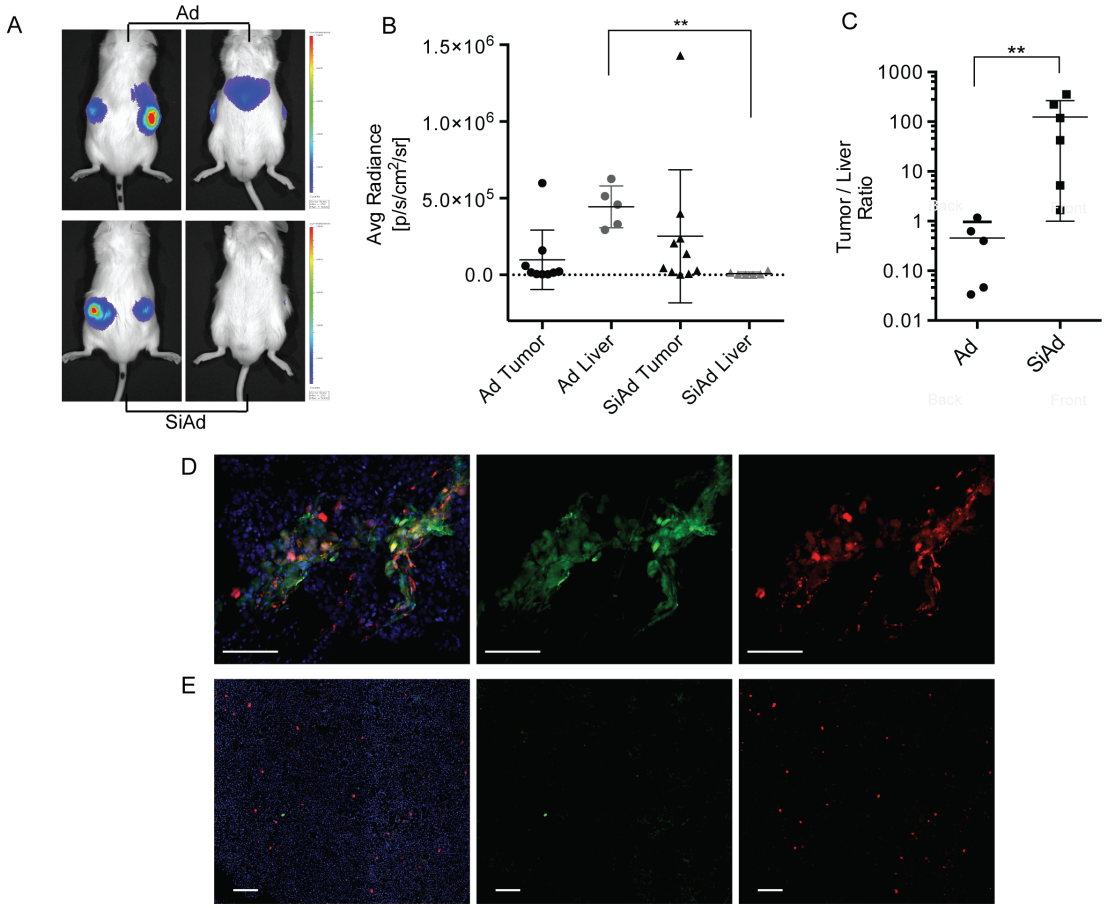

Figure 3.1: T98G xenografts were treated with either Ad (n=5) or SiAd-luc (n=6) at 5x10^7 PFU. (A) Representative IVIS images showing comparable levels of tumor transduction, but reduced liver expression when treated with SiAd. (B) Average radiance of tumors and livers. (C) Comparison of total tumors expression to liver transduction.**p$\leq$0.005, ONE-way ANOVA, Kruskal-Wallis. Data reported as mean $\pm$ STD. (D) Tumor section injected with SiAd-GFP and Ad-mCherry. (E) Liver section from the same mouse as (D). Scale bars represent 200μm.

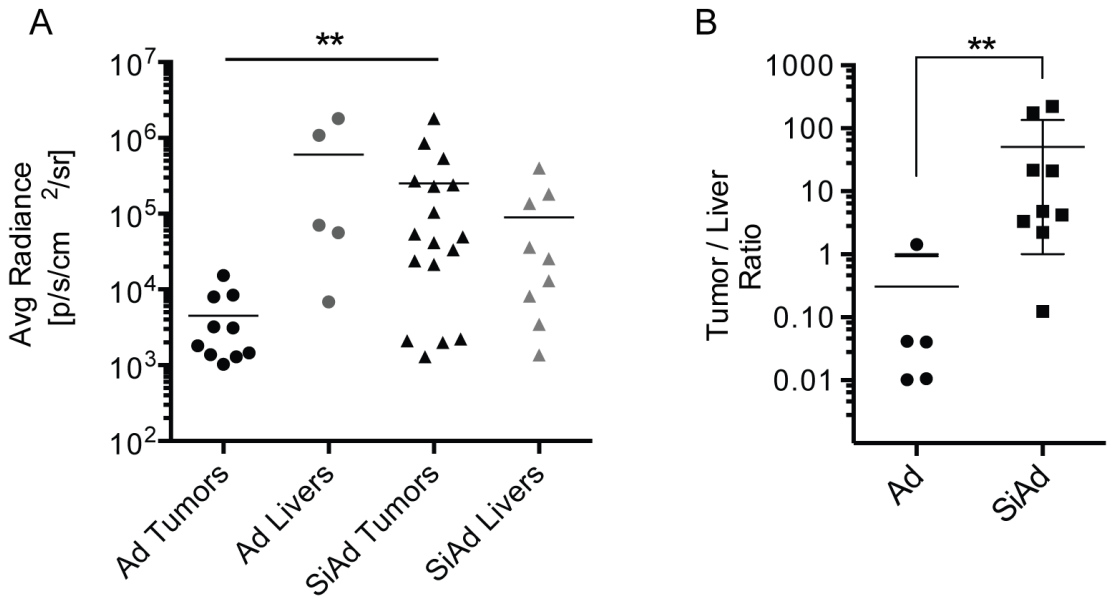

Figure 3.2: T98G xenografts were treated with either Ad (n=5) or SiAd-luc (n=9) at 5x11^8 PFU. (A) Average radiance of tumors and livers. (B) Comparison of total tumor expression to liver transduction.**p$\leq$0.005, ONE-way ANOVA, Kruskal-Wallis. Data reported as mean $\pm$ STD.

We found that tumors treated with Ad had very poor transduction with an average radiance of 4.52x10$^3\pm$ 4.70x10^3 whereas tumors treated with SiAd had 23-fold enhanced transduction with an average radiance of 2.52x10$^5\pm$ 4.65x10^5 (P=0.0094, Kriskal-Wallis) (Figure 3.2A). The liver transduction followed a similar pattern to low dose treatments where livers of Ad treated mice had an average transduction of 6.09x10$^5\pm$ 8.15x10^5 and livers of SiAd treated mice had reduced transduction at 9.02x10$^4\pm$ 1.75x10^5. Again, when comparing the total tumor transduction to liver transduction for each mouse we found SiAd treated mice had on average significantly reduced off-target transduction by 165 fold (Figure 3.2B). This data is derived from three separate experiments on passage 6, passage 7, and passage 10 of tumors. Sur-

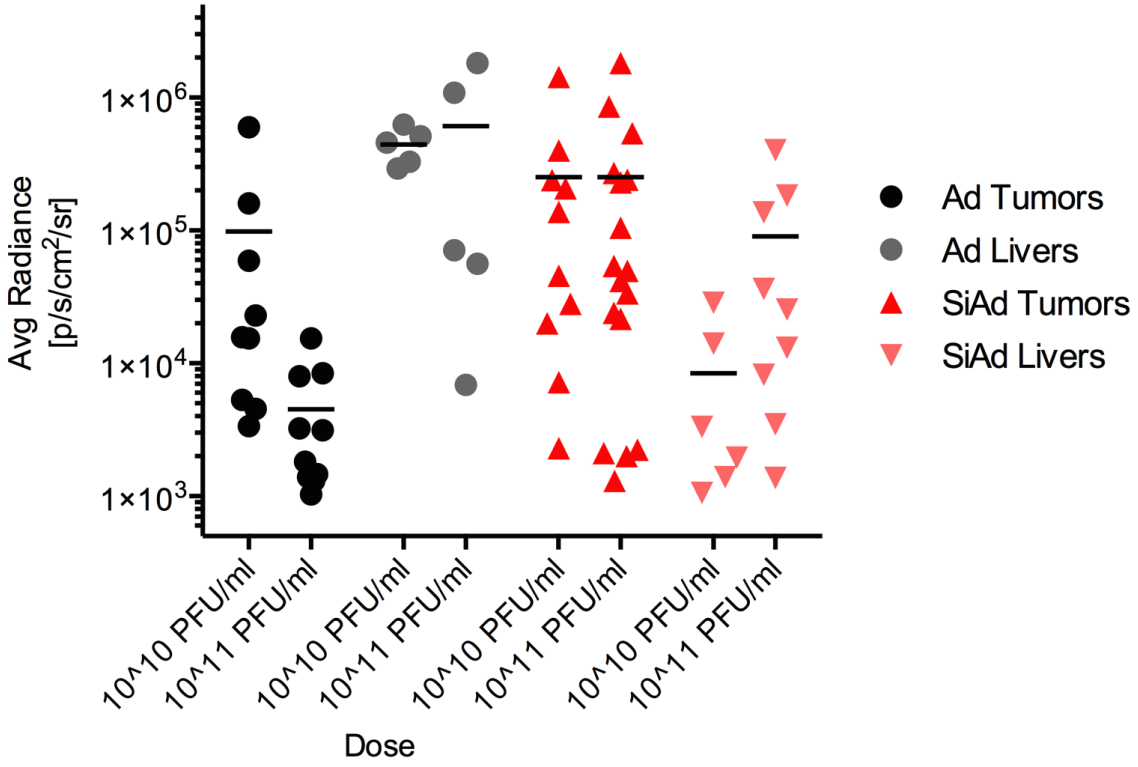

Figure 3.3: Comparison between transduction of tumors and livers with low dose and high dose IT injections.

prisingly on the tenth tumor passage experiment, all five mice that were injected with neat Ad asphyxiated within minutes of IT injections and had to be sacrificed. This response is likely a result of the entire dose entering the circulation and causing an immediate immune reaction. We ruled out the possibility of a toxin in the solution as SiAd particles were made using the same stock and reconstituted in the same PBS.

When comparing the data from low dose and high dose experiments we can find some interesting trends. First, the transduction of Ad tumors was reduced when treated with high dose, but SiAd transduction was comparable between the two doses

(Figure 3.3). This suggests that reduced Ad transduction is due to loss of CAR expression through the serial passaging of tumors *in vivo*. Second, liver transduction was slightly elevated in high dose SiAd treated mice suggesting that encapsulation method may not cover all viral particles since the same coating procedure was used for high dose preps as was used for low dose preparations. qPCR could potentially be used to determine encapsulation efficiency when using high dose preparations since encapsulated particles do not amplify on qPCR (see section 2.3.3).

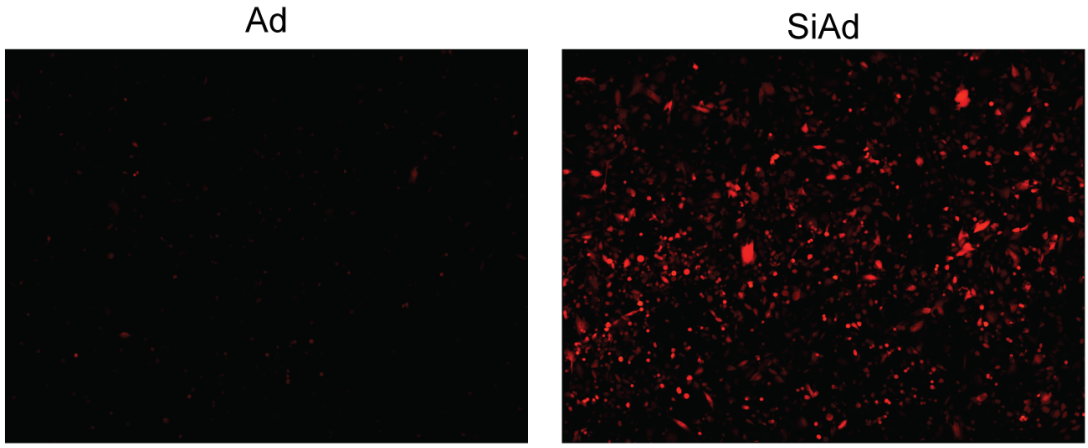

Figure 3.4: Confocal images of Ad and SiAd transduction on passage #3 of T98G xenografts, which was the last viable passage that could grow *in vitro*.

We observed that Ad tumor transduction reduced as we passaged tumors. In addition, in the process of passaging tumors we tried growing an aliquot of cells *in vitro* in a dish. After passage three, cells were no longer able to grow in a dish. This suggested that cells had adapted to grow in NSG mice and possibly were losing CAR expression through differentiation. This is similar to clinical findings that some tumors have variable CAR expression dependent on tumor progression (see section

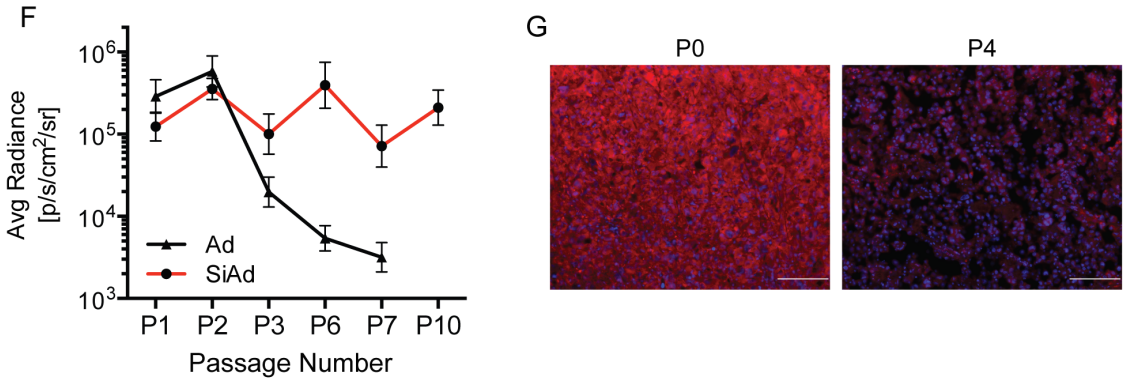

Figure 3.5: (F) Ad tumor transduction reduced over passage number. (G) Tumor CAR expression dramatically reduced from P0 to P4.

1.5.1). We tested the *in vitro* transduction of passage #3 and found that Ad-mCherry had very low transduction even at a MOI 50 (Figure 3.4).

This is further supported by looking at the tumor luciferase expression versus tumor passage number (P#). Passage #3 and on had significantly lower Ad transduction of tumors (P=0.02, ANOVA) whereas SiAd transduction was similar across passage number (Figure 3.5F). To confirm that CAR expression was likely a factor for this finding, we took tumor sections from the first set of xenografts (P0) and from P4 and looked for CAR expression by immunofluorescence. Tumors sections were stained primary CAR antibody (Bioss #bs-2389R, 1:100 dilution) and visualized with alexa fluor 647 secondary antibody (1:400). We observed a clear difference in CAR expression between P0 and P4 tumor sections (Figure 3.5G). This finding supports the *in vitro* data showing expanded tropism across cell lines where CAR expression is also variable and suggests that SiAd can transduce tumors independent of tumor differentiation or progression and CAR expression.

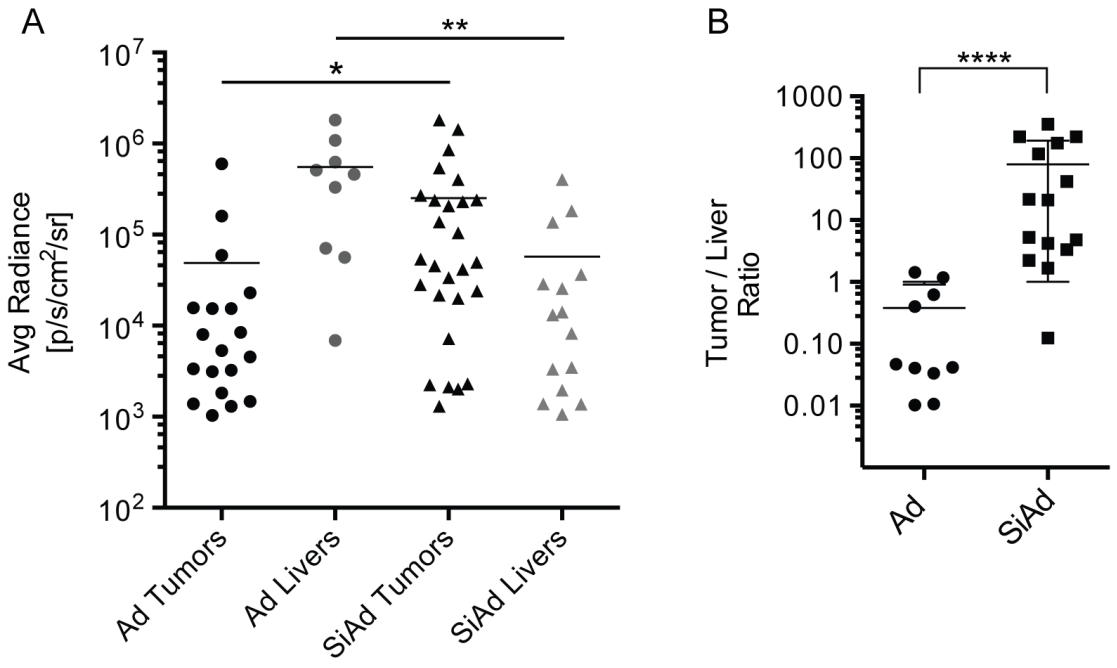

Figure 3.6: T98G xenografts were treated with either Ad or SiAd-luc at $5x11^7$ PFU or $5x11^8$ PFU. (A) Average radiance of tumors and livers. (B) Comparison of total tumor expression to liver transduction. *p≤0.05 **p≤0.005, ****p≤0.0001 ANOVA, Kruskal-Wallis. Data reported as mean ± STD.

Compiling all the data from all experiments performed on T98G xenografts using luciferase expression revealed that SiAd enhanced tumor transduction by 23-fold (P=0.02, Kruskal-Wallis) and reduced off-target liver transduction by 210-fold (p≤0.0001, Mann-Whitney t-test) (Figure 3.6A & 6B). Reduced liver transduction is important to minimize hepatotoxicity assocaited with Kupffer cell uptake of virions and downstream immune response. For oncolytic viral therapy or any gene therapy method that does not seek to treat the liver, liver sequestration is considered a sink for viral load. We found that SiAd improves the retention of particles at the site of injection leading to both enhanced tumor transduction and reduced liver

transduction.

3.1.3 Intramuscular Injections

To further study the biodistribution properties of SiAd, we tested intramuscular injections in NSG mice using a luciferase reporter. Mice were injected into both hind limbs with 50μl of Ad or SiAd and luciferase expression was measured as previously described. Surprisingly, SiAd muscle transduction was low compared

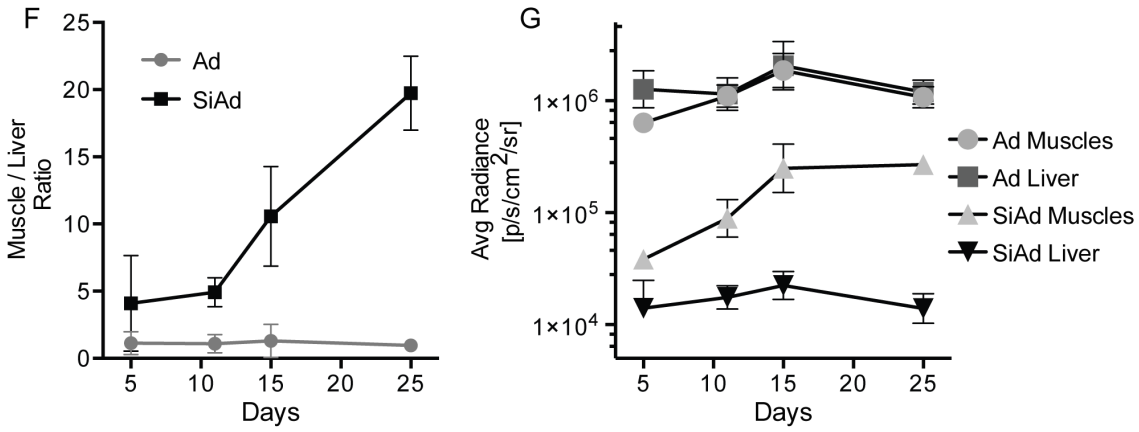

Figure 3.7: IM injections of 5x10^7 PFU of Ad or SiAd in NSG mice. (F) Ratio of total muscle transduction to liver transduction for each mouse. (G) Average radiance of muscles and livers over 25 days.

to Ad, which robustly transduced muscle. When looking at the ratio of muscle to liver transduction (M/L), we found that SiAd had greater M/L for all time points measured and that this ratio increased over time (Figure 3.7F). This is in contrast to the M/L for Ad which remained, around 1, for all time points: days 5, 11, 15 and 25. This is clear when looking at the average radiance of muscles and livers over the time course study. The luciferase signal of muscles injected with SiAd had a 10 fold

increase between days 5 and 15 whereas the liver signals from these mice remained constant (Figure 3.7G). Linear regression analysis showed that only the SiAd muscle signal had significantly non-zero slope suggesting that in muscle, SiAd particles are being slowly released at the site of injection, but not released into the bloodstream which would result in liver transduction.

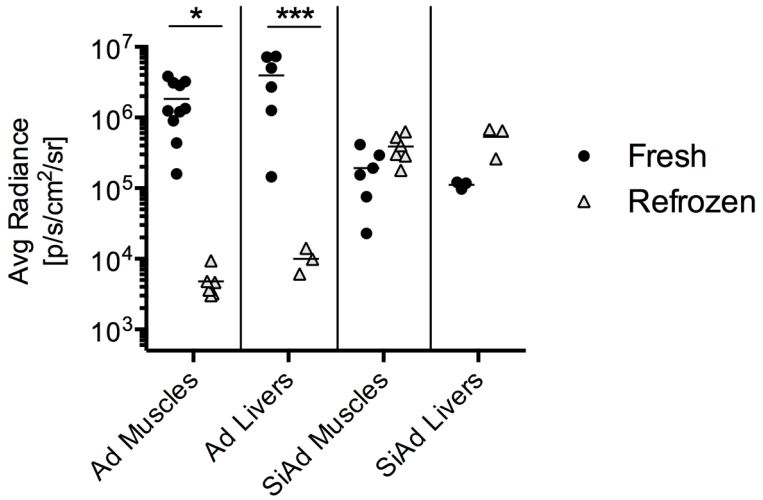

Figure 3.8: Comparing IM injections of $5x10^8$ PFU of Ad or SiAd in NSG mice from a vial stock that was had undergone a single freeze-thaw cycle (fresh) or one that had been thawed, refrozen, and thawed again (refrozen). SiAd rescues lost Ad activity.

We also tested the higher dose preparation in NSG mice. We found that mice injected with Ad had background levels of luciferase signal, but mice injected with SiAd had good signal. This is in contrast to the low dose data. For the first high dose experiment we used a vial of Ad-luc that had undergone one re-freeze cycle at -80C. It is known that Ad loses some activity from freeze thaw cycles and that Vector Biolabs recommends to avoid multiple freeze-thaw cycles. Fresh Ad is considered stock that

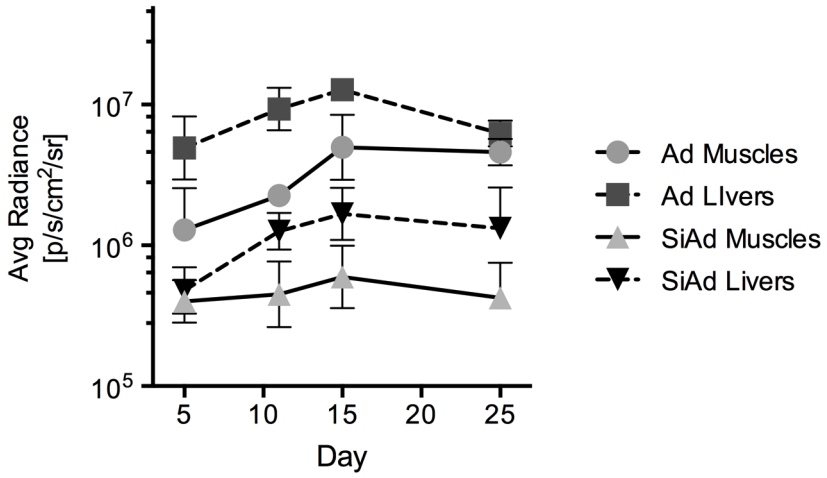

Figure 3.9: IM injections of 5x10^8 PFU of fresh Ad or SiAd made from a vial stock that had undergone a single freeze-thaw cycle in NSG mice.

was thawed at the time of use whereas refrozen Ad is considered stock that was thawed, refrozen at -80C, and thawed again for use. We observed this phenomenon, where muscles injected with refrozen Ad had background levels of luciferase signal (Figure 3.8).This is clear when comparing both the muscle and liver transduction of mice injected with either fresh Ad versus refrozen Ad (Figure 3.8). Interestingly, muscles injected with SiAd had robust signal. In contrast SiAd made with either fresh or refrozen Ad had comparable levels of both muscle and liver transduction (Figure 3.8). In this case, silica encapsulation is acting as a transfection reagent and suggests that the silica encapsulation procedure does coat all of the virions present as unencapsulated viral particles would have lost activity after freeze-thaw. Freeze thaw cycles effect the capsid protein structure leading to loss of transduction efficiency for naked Ad, but when performing the silica reaction the PLL still covers these aberrant capsids and allows for silica deposition. Thus, as long as the viral

DNA can be delivered to a cell then protein expression is likely. We performed a second experiment, where we IM injected fresh Ad and saw robust muscle and liver signal, which was greater than SiAd made with refrozen Ad (Figure 3.9).

3.1.4 Intravascular Injections

Though SiAd particles are somewhat large for effective intravascular (IV) delivery to tumors via the enhanced permeability and retention effect (EPR), we tested IV injections in tumor free NSG mice. EPR is based off the finding that growing solid tumors produce leaky vasculature where nanoparticles can passively accumulate [4]. Out of curiosity we tail vein injected SiAd and measured luciferase

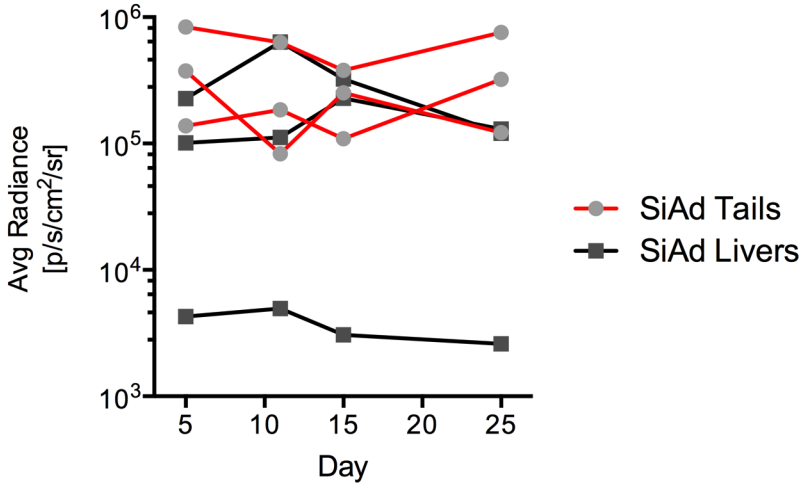

Figure 3.10: IV injections, tail vein, of $5x10^8$ PFU SiAd (n=3) in NSG mice.

signal over 25 days (Figure 3.10). As expected, tails injected with SiAd had strong signal. In two of the three mice, livers had comparable signal to tails and the liver of the third mice had no signal. This data confirms the hypothesis that SiAd particles

are retained and tend to stay at the site of injection. The liver transduction is attributed to SiAd particles that were cleared from the circulation.

3.1.5 Cancer Gene Therapy using TRAIL

To test the efficacy of delivering a therapeutic gene we purchased Ad expressing TNF-related apoptosis-inducing ligand (TRAIL) at both preparations, low and high dose (Vector Biolabs, Malvern, PA). TRAIL is ligand that binds receptors TRAIL-R1 and TRAIL-R2 and induces apoptosis through the death-inducing signaling complex (DISC) and downstream induction of caspase-8 [5]. It has been reported that TRAIL selectively induces apoptosis only in cancer cells and not healthy ones; thus, serves a good model for cancer gene therapy.

First, to confirm that TRAIL was capable of killing T98G cells we tested Ad and SiAd-TRAIL *in vitro*. Cells were treated with either Ad-TRAIL or SiAd-TRAIL at a MOI of 10 and 50. After 48 hours cells were stained with propidium iodide, which is a common intercalating dye which binds DNA and cannot cross live/intact cell membranes, and measured using flow cytometry. Cells were measured using flow cytometry and gated versus cells treated with PBS alone. At both MOI 10 and MOI 50, SiAd significantly killed more cells than Ad (Figure 3.11). Treated cells were also smeared on a slide and visualized with confocal microscopy (Figure 3.11). Even at a MOI 50, TRAIL induced apoptosis was inefficient with Ad-TRAIL killing only 8.5 $\pm$2.6% and SiAd-TRAIL killing 13.9 $\pm$0.2% of cells.

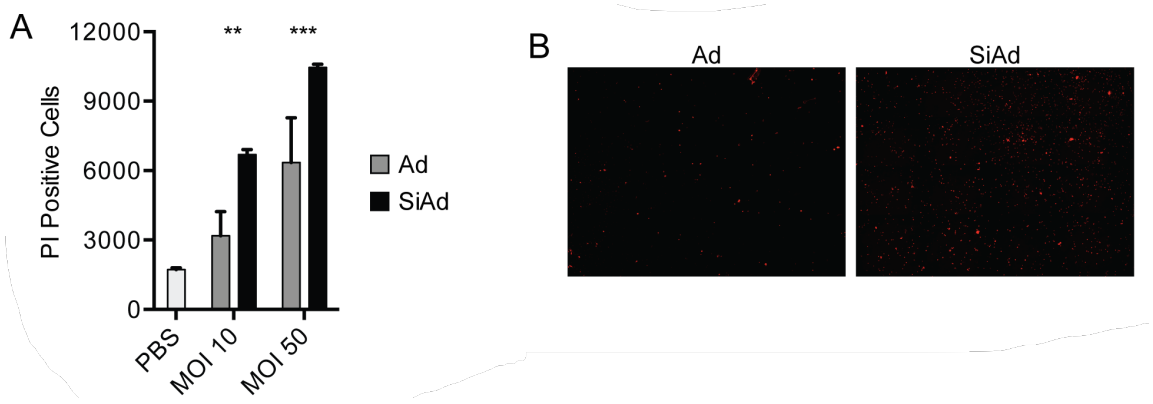

Figure 3.11: SiAd is significantly more potent than Ad *in vitro*. (A) T98G cells were treated with Ad or SiAd-TRAIL at different MOIs, stained with propidium iodide after 48hrs and measured using flow cytometry. (B) Stained cells visualized on a glass slide.***$p \leq 0.0005$

Once confirmed that T98G cells were susceptible to TRAIL induced apoptosis, we tested both low dose and high dose treatment on T98G xenografts. Xenografts were injected at the smallest size possible and tumor volume was measured at day 0, 2, 5, 7, 9 and 11. In addition, we injected at multiple time points to increase the effective dose of TRAIL and as is practiced in clinical trials. Tumor volume was calculated by measuring two dimensions of a tumor using a caliper where the third dimension is assumed to be the smaller of the two. Data is reported at % tumor volume change for each tumor normalized to the tumor volume pre-treatment. Both low dose and high dose treatment with SiAd significantly inhibited tumor growth compared to Ad, untreated and tumors treated with SiAd-luc (Figure 3.12). It was not surprising that tumor volume did not reduced in size or plateau since cell culture experiments showed that delivery of TRAIL even at a high MOI of 50 resulted only in 10% cell death. As mentioned previously, we are estimated to be delivering

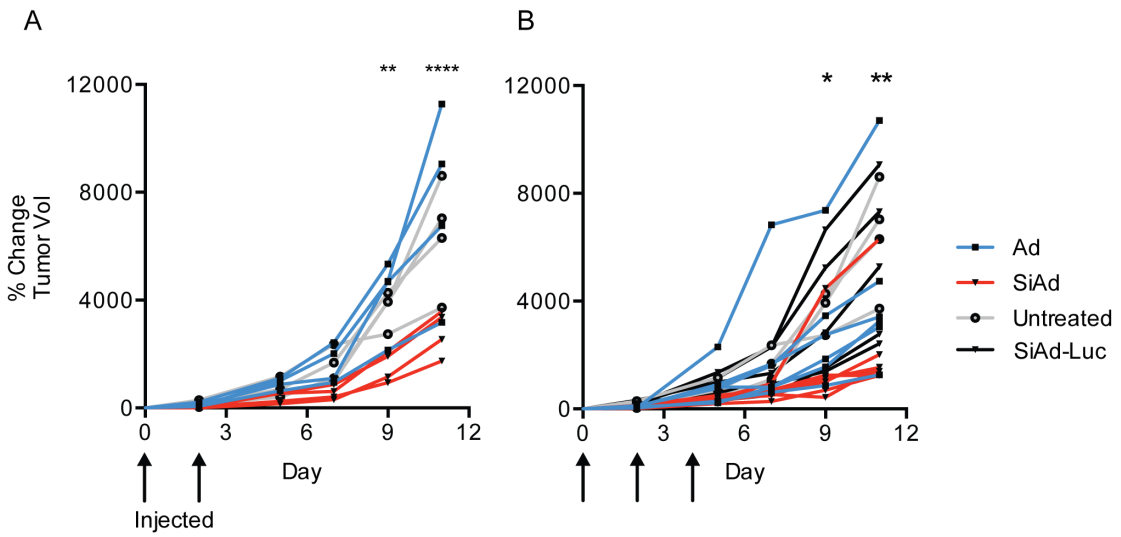

Figure 3.12: SiAd-TRAIL significantly inhibited tumor growth compared to controls. (A) Change in tumor volume with treatment Ad or SiAd at $5x10^7$ PFU. (B) Change in tumor volume with treatments Ad, SiAd, or SiAd-luc at $5x10^8$ PFU. ***$p \leq 0.0001$

around an MOI of 0.05-0.5 even with the higher dose preparation. In addition, we tested SiAd-luc (expressing luciferase) as a control to prove that TRAIL was cause of reduced tumor volume and not potential toxicity due to the silica coating.

To determine if multiple doses was effective, we performed a log-log transform of the data and linear regression analysis. From the log-log transform it is clear that all treatment groups have similar, non-significantly different, slopes, but the intercepts are significantly different (Figure 3.13). This suggests that only the first dose has an effect on reducing the overall tumor volume. This is due to the overall low dose of virus delivered. In order to induce stagnation of tumor growth, we would have to deliver a dose effective to kill at least 50% of the tumor cells present since tumors grow in an exponential manner.

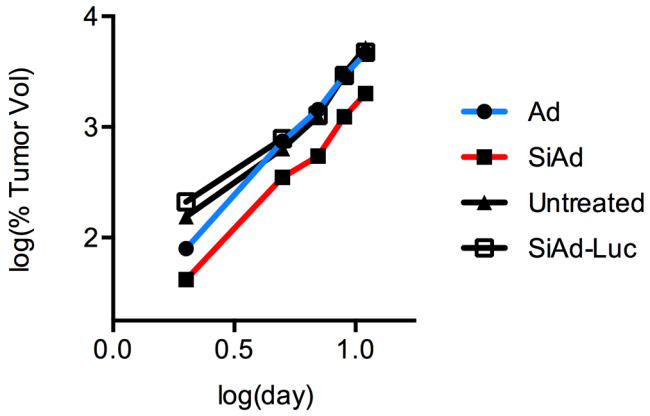

Figure 3.13: Log-log transform of all the TRAIL data shows that treatments have similar slopes, but are off-set from each other. This suggests that only the first dose is effective in killing cells.

Overall, this data shows that silica encapsulation of Ad can enhanced cancer gene therapy *in vivo* by transducing cells that have low CAR expression and by retaining particles at the site of interest. The experiments described above were performed on late passage T98G xenografts (P4, P5, and P8) which had reduced CAR expression compared to the original T98G cells (Figure 3.5).

3.2 Immune-competent Mice

Innate and adaptive immune responses to virions are one of the primary barriers to successful clinical outcomes. These responses occur on two different time scales, first the innate response happens within hours of injection and then the adaptive response occurs over days-weeks time. To study the immune response to SiAd, we used albino C57BL/6 (wild-type) mice purchased from Charles River (strain code 493).

3.2.1 Cytokine Panel to Measure Innate Response

Mice were IM injected in both hind limbs with either Ad or SiAd expressing luciferase at 5x10^8 PFU, high dose preparation. We choose IM injections because IM delivery is a common approach in the clinic for gene therapy and serves as a proxy for IT injections. For the first experiment, 5 mice each were injected with Ad or SiAd. Blood was collected retro-orbitally a few days prior to injection (to measure background levels of plasma cytokines), six hours after IM injection, and 5 days post-injection. Blood was centrifuged at 5000g for 10 minutes and approximately 50μl of plasma was collected and immediately stored at -20C. Once all the samples were collected, samples were thawed, centrifuged at 3,000 rpm for 10 minutes, and 50 μ supernatant was incubated with Luminex magnetic beads overnight and assayed as per manufacturer's instructions (Luminex Multiplex magnetic beads 20-plex Assay, LMC0006M, Life Technologies) in a black 96-well plate. This assay kit simultaneously measures 20 mouse cytokines: GM-CSF, IFN-γ, IL-1α, IL-1β, IL-2, IL-4, IL-5, IL-6, IL-10, IL-12, IL-13, IL-17, TNF-α, IP-10, KC, MCP-1, MIG, MIP-1α, FGF-basic and VEGF. This assay was measured in collaboration with Anupriya Agarwal, PhD.

Of the 20 cytokines measured, we chose 10 to report on. These ten (IP-10, IL-1β, MCP-1, IL-12, MIG, TNF-α, VEGF, IL-2, MIP-1α and IL-6) were significantly different than baseline levels independent of treatment and had greater than 75% of the data as measurable, within the standard curve for each cyotokine. For each

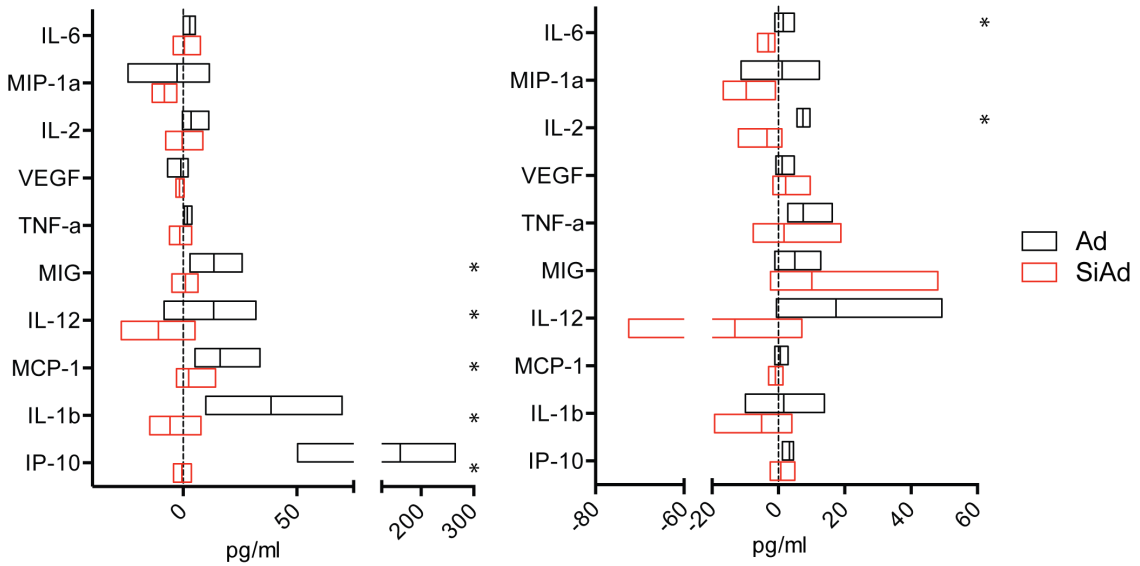

Figure 3.14: Plasma cytokine levels are reported as the difference between the (A) 6 hour or (B) 5 day measurement and the baseline signal for each mouse (n=5, each treatment). *p$\leq$0.05, multiple t-tests.

mouse, the difference between the signal at the time point measured and the baseline is reported. We found that IP-10, IL-1β, MCP-1, IL-12, and MIG were significantly higher in mice treated with Ad compared to SiAd at 6 hours, but at 5 days post-injection only IL-2 and IL-12 were significantly higher (Figure 3.14). To confirm that these results were not a result of delivering less viral load, but due to the silica coat we measured the luciferase signal from both muscles and livers as described previously. Luciferase expression was comparable and non-significantly different between Ad or SiAd treatments.

To confirm our findings we performed a second experiment in the same manner as the first. Five mice were IM injected in both hind limbs with either Ad or SiAd expressing luciferase at 5x10^8 PFU, high dose preparation. Plasma was collected

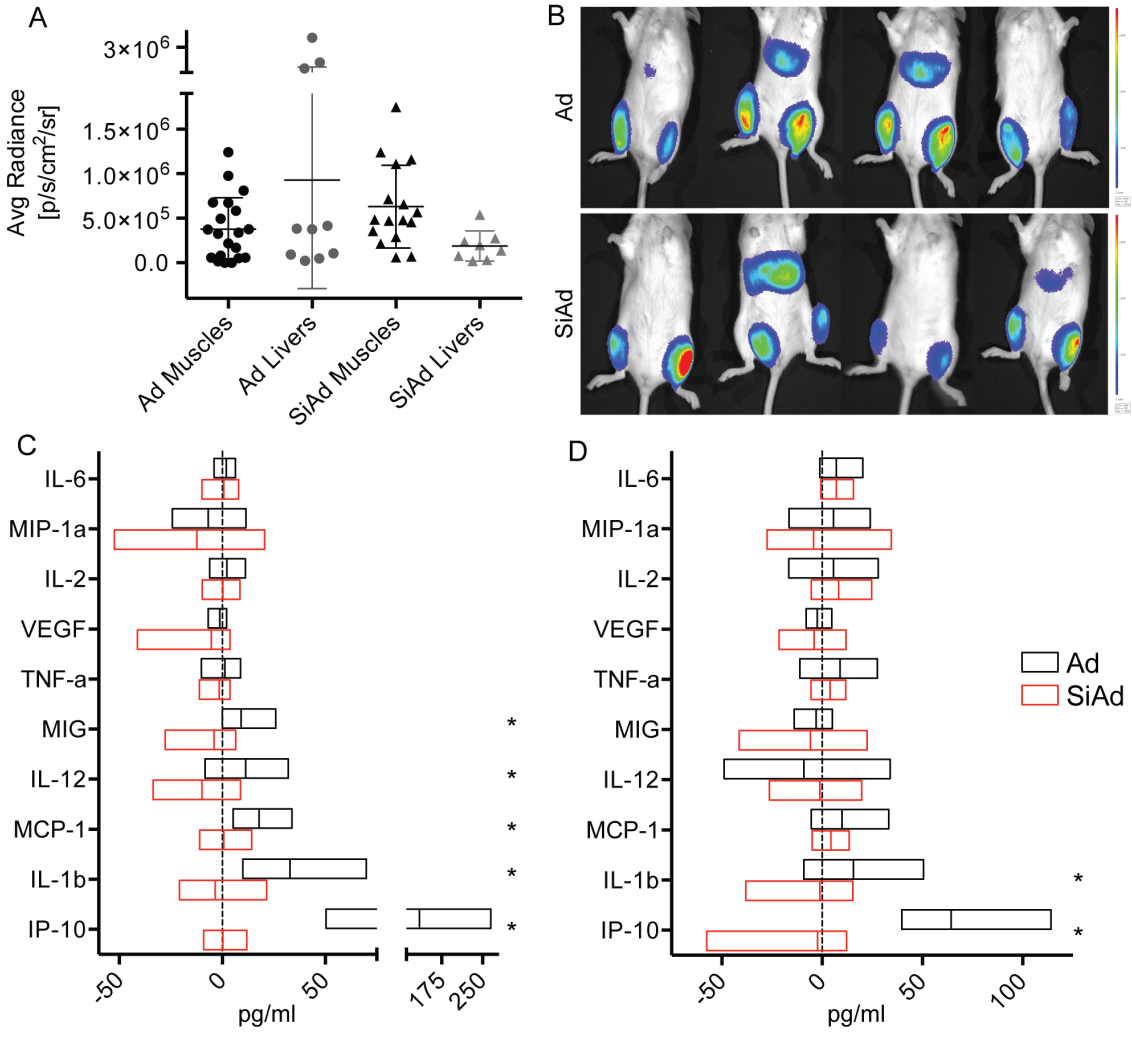

Figure 3.15: (A) Luciferase expression with Ad (n=10) or SiAd (n=10) treatment. (B) Representative images. (C) Cytokine levels 6-hours post IM injection normalized to background. (D) Cytokine levels 6-hours post second injection normalized to background. *p≤0.05, multiple t-tests.

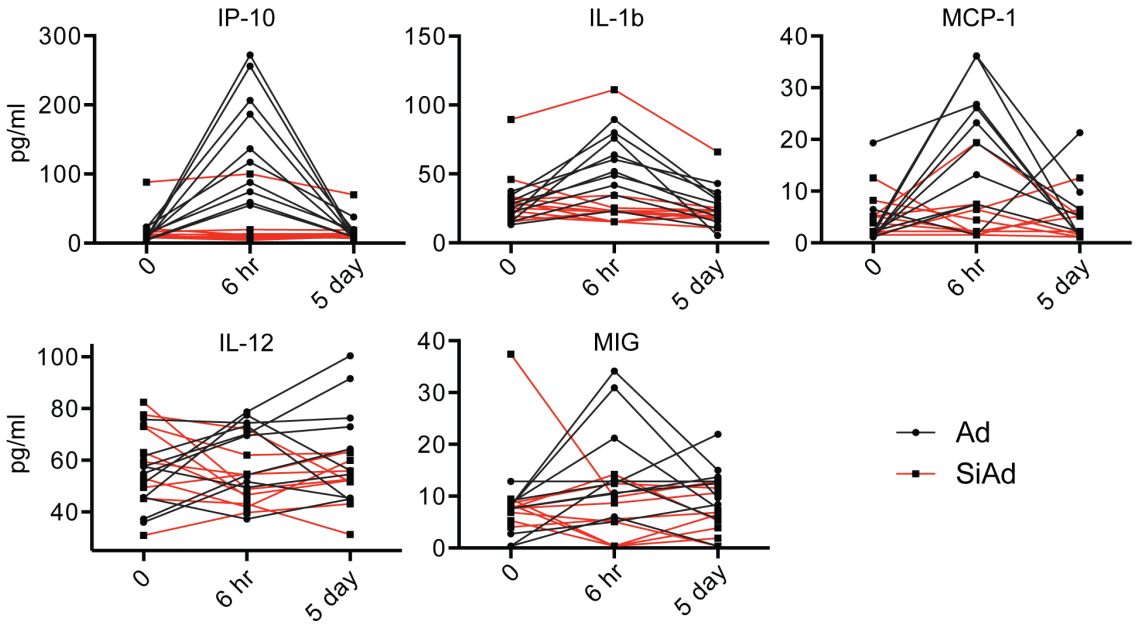

Figure 3.16: Raw values from cytokine panel for IP-10, IL-1β, MCP-1, IL-12, and MIG showing clear spike in levels at 6 hours with Ad treatment (n=10).

at baseline, 6 hours and 5 days post-injection. To test the effect of a second dose, we took plasma at 16 days post first injection as a new baseline. Then at 21 days post-injection, we re-administered Ad or SiAd in the same mice and took plasma 6 hours and 5 days post-injection. Again, we saw significant differences for IP-10 ($p \leq 0.0001$), IL-1β ($p \leq 0.0001$), MCP-1 ($p=0.0001$), IL-12 ($p=0.0025$), and MIG ($p=0.0058$) between Ad and SiAd at 6 hours post-injection (Figure 3.15C). Upon a second injection, the less robust where we only observed significant differences in IP-10 ($p \leq 0.00001$) and IL-1β ($p=0.0055$) (Figure 3.15D). When looking specifically at the raw data from both experiments with mice treated with a single injection for IP-10, IL-1β, MCP-1, IL-12, and MIG, we clearly see changes in cytokine levels between baseline (0 day), 6 hour and 5 days post injection (Figure 3.16). In mice

injected with Ad there is a spike in plasma cytokine levels at 6 hours which reduce to baseline at 5 days. We can also see the variability in baseline cytokine levels in mice. Luciferase expression was measured for all mice and representative images are shown (Figure 3.15 A & B). No significant differences were found in luciferase expression in muscles, however liver transduction was significantly reduced (p=0.04, ONE-way ANOVA).

We observed that SiAd did not induce any inflammatory cytokines. All of the elevated cytokines we found in Ad treated mice are involved in the innate immune response against viral particles. IP-10, also known as CXCL10, is a chemokine that induces chemotaxis and is associated with infections diseases [6]. It is being studied as a diagnostic marker for HIV infection and other inflammatory diseases [7]. The IL-1 family of molecules is another involved in both inflammation and immune response and is a simulator of T cells [8]. MCP-1, known as monocyte chemoattractant protein, is as the name implies is a chemokine that induces infiltration of macrophages [9]. IL-12 is secreted by antigen presenting cells in response to viral and bacterial infections to induce T cell responses [10]. It is implicated in clearing viral load. Most studies looking at innate immunity to Ad, have focused on IL-6, TNF-α, and IP-10. However we did not observe significant differences in IL-6 and TNF-α levels. Koizumi et al. found that the majority of serum cytokine levels are produced in the spleen and liver [11]. Though the spleen may accumulate Ad, it does not result in splenic transduction, which is in contrast to the liver where hepatocyte transduction can

occur. We did not observe transduction of the spleen, but in Ad treated mice there was significant liver transduction. Likely we did not deliver sufficient viral load to observe changes in IL-6 and TNF-α via the IM injection route. Overall, these results suggest that reduced liver transduction and silica cloaking of Ad can minimize the systemic innate immune response.

3.2.2 NSG vs. WT Transduction

Comparing the transduction efficiency in immune compromised and immune competent mice revealed some interesting findings (Figure 3.17). In both types of mice, mice were IM injected with $5x10^8$ PFU of Ad or SiAd-luc. Note that the NSG mice were injected with SiAd made from refrozen Ad stock. First, in WT mice

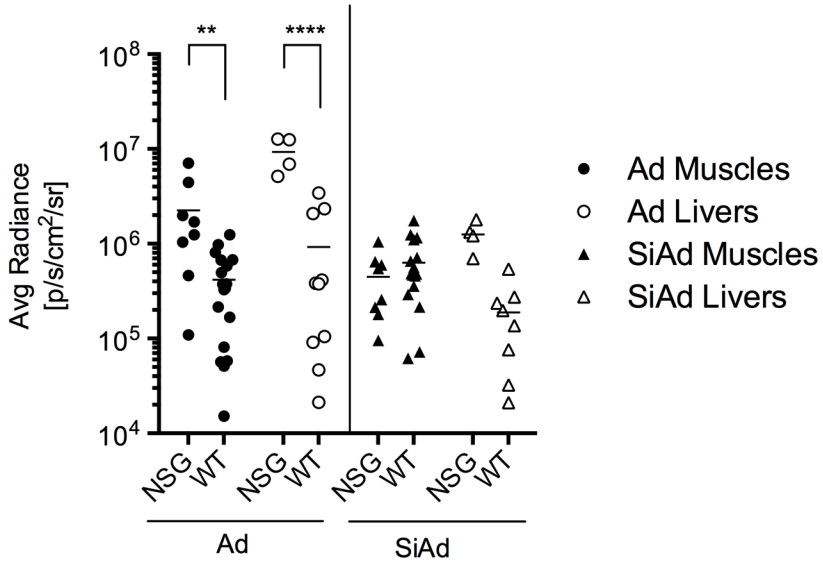

Figure 3.17: Comparison of muscle and liver transduction between NSG and WT mice IM injected with Ad or SiAd. **p≤0.005, 2way ANOVA.

treated with Ad, both muscles and livers had significantly reduced transduction

compared to NSG where on average muscle transduction was reduced by 5.4-fold and liver transduction was reduced by 10 fold (**p≤0.005, 2way ANOVA). Second, the transduction efficiency of SiAd was non-significantly different between NSG and WT mice for both muscles and livers. This data supports the hypothesis that in WT mice, innate immune components (outside of liver sequestration) are clearing naked Ad particles from the site of injection and circulation in WT mice. However, SiAd particles behaved similarly in NSG and WT mice and supports the finding that silica encapsulation does cloak virions from the innate immune system.

3.2.3 Reduced Production of Neutralizing Antibodies with SiAd Treatment

It is known that antibodies can be produced against foreign pathogens and materials in immune competent mice, specifically in c57bl/6 mice. This occurs on the time scale of weeks after exposure to the antigen. From the cytokine experiment, discussed previously, we had immune competent mice that had received multiple injections of Ad or SiAd over a 25 day period. plasma was collected from mice 44 days post primary injection with Ad or SiAd (n=10 total) and frozen at -20C. To detect the presence of neutralizing antibodies against Ad, a serial dilution neutralization assay was performed using Ad-luc. Sera were first heat inactivated at 56°C for 60min and serial 3-fold dilutions were performed starting at 1/100 to 1/218700 at 2x concentrated in DMEM. Next, 10ul of Ad-luc stock at $1x10^10$ PFU/ml was diluted to

5ml and 50ul of viral solution was added to each sera dilution and incubated at 37°C for 60min. Then, 100ul of sera dilution + viral solution was added to A549 cells, which resulted in a MOI 50 as this was in the linear range of luciferase expression. After 24 hours luciferase expression was measured using ONE-Glo Ex Luciferase Assay System (Promega) and Tecan Spark 20M. This procedure was adapted from Sprangers et al. [12].

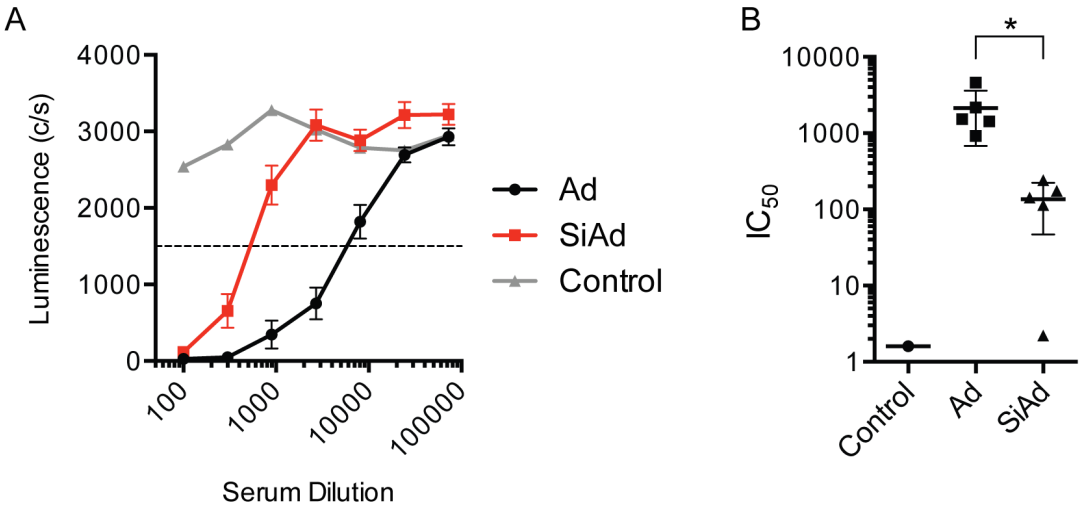

Figure 3.18: WT mice were injected with Ad or SiAd and plasma was collected. (A) plasma dilutions were tested for neutralizing antibodies using Ad-luc. (B) The 50% neutralization titer (IC_{50}) was 15-fold higher in mice treated with Ad verus SiAd. *p≤0.05, t-test.

To compare the amounts of neutralizing antibodies in plasma we plotted as luciferase expression vs. plasma diltuion (Figure 3.18A). Higher concentrations of antibody will neutralize Ad-luc and thus result in lower luciferase expression. The concentration of half max or the concentration at which 50% of virus present is neutralized (IC_{50}) was determined by linear regression analysis on the linear portion

of each plasma dilution. The IC_{50} titer for mice treated with SiAd was 135 ± 40, but the IC_{50} of mice treated with Ad was almost 15-fold higher at 2137 ± 652 (Figure 3.18B). The reduction in the concentration of plasma antibodies can be attributed to both the masking viral antigens by silica and to the overall reduced liver transduction. Mice injected with SiAd had about 8.5-fold less liver signal as measured by luciferase. Kuppfer cells in the liver can act as antigen presenting cells which are crucial to antigen presentation and antibody production. Transduction of tumor cells does not lead to antigen presentation is one method that tumors evade immune recognition. Overall, we found that mice treated with SiAd had lower concentrations of neutralizing antibodies against Ad and suggests that SiAd may extend the time for repeat injections.

3.3 Summary and Future Directions

The *in vivo* experiments performed above revealed some very interesting findings in both immune compromised and immune competent mice. IT injections in a T98G xenograft model showed that SiAd reduced off-target, liver, transduction by 210-fold and enhanced transduction of tumors by 23-fold. We found that tumor CAR expression changed with passage number, which had a significant impact of Ad transduction efficiency, but not on SiAd. As a model for cancer gene therapy we tested Ad or SiAd expressing TRAIL and found SiAd significantly inhibited tumor growth. In immune competent mice we performed IM injections and looked for plasma cytokines

as a marker for the innate immune response and plasma neutralizing antibodies as a measure of the adaptive immune response. There was a significant increase in five plasma cytokines (IP-10, IL-1β, MCP-1, IL-12, and MIG) when comparing Ad to SiAd at 6 hours post-injection. Not only was there a difference, but SiAd did not induce any inflammatory cytokines. In addition, we found that mice treated with SiAd had a significant reduction in plasma neutralizing antibodies against Ad. Overall this *in vivo* data shows that silica encapsulation of Ad can address some of the current barriers to clinical success and even enhance cancer gene therapy while reducing the overall immune response. In the future, higher doses of virus need to be tested, doses comparable to ones tested in the clinic. This goes in hand with developing a method which allows for scale-up of the encapsulation process. One potential method to assist in the synthesis of higher doses could be the use of microfluidic reactors, which have been used to synthesize other silica nanoparticles. Independent of scale-up methods, an actual oncolytic viral with replication capacity needs to be tested. Unfortunately, in the context of replicative viruses, silica encapsulation can only minimize innate and adaptive immune responses to the initial dose as progeny virions are un-encapsulated. More work needs to be done to show that SiAd directly reduces liver toxicity by looking at transaminase levels, which are elevated in Ad treatments and by looking for cytokine levels at the tissue scale using qPCR. In the context of oncolytic viral therapy, a true lytic virus could be enhanced with silica encapsulation by retaining the particles at the site of interest and minimizing loss to

the circulation and sequestration by the liver. Adenovirus is ideal model system, but the field is also focused on other viruses for gene therapy or oncolytic viral therapy. These other viruses such as herpes simplex or adeno-associated virus also subject to similar barriers to clinical success and could benefit from a nanoparticle formulation that enhances transduction while reducing immune responses and liver transduction.

In the context of non-lytic gene therapy, viral vectors can benefit from cloaking technologies as well to reduce immune responses and increase retention of particles at the site of injection. Again, delivery of a therapeutic gene needs to be tested. Mouse models of diseases caused by enzyme deficiencies are available, but the true test would be to use vectors already in clinical trials such as the AAV vector Glybera for LPLD. The next chapter describes preliminary work on transferring silica and other cloaking technology to AAV vectors.

3.4 Acknowledgements

None of the work described in this chapter would have been possible without the hard work of Jared Fischer, PhD. Jakki Martinez assited with some luciferase imaging. Theresa Nguyen performed the tissue staining for tumor CAR expression. Anupriya Agarwal, PhD assisted in running the cytokine assays.

The dissertation author was the primary investigator and author of this material. This chapter, in part, is being prepared for submission for publication as Sapre, Ajay; Yong, Gen; Yeh, Ya-san; Ruff, Laura; Sayar, Zeynep; Plaut, Justin; Mar-

tinez, Jacqueline; Nguyen, Theresa; Agawal, Anupriya; Liu, Yu-Tsueng; Messmer, Bradley; Esener, Sadik and Fischer, Jared. "Silica Cloaking of Adenovirus Enhances Gene Delivery while Reducing Immunogenicity."

3.5 References: Chapter 3

[1] S. Moghimi, A. Hunter, and T. Andresen, "Factors controlling nanoparticle pharmacokinetics: An integrated analysis and perspective," *Annual Review of Pharmacology and Toxicology*, vol. 52, no. 1, pp. 481–503, 2012. DOI: 10.1146/annurev-pharmtox-010611-134623. [Online]. Available: https://www.annualreviews.org/doi/abs/10.1146/annurev-pharmtox-010611-134623.

[2] S.-D. Li and L. Huang, "Pharmacokinetics and biodistribution of nanoparticles," *Molecular Pharmaceutics*, vol. 5, no. 4, pp. 496–504, 2008, ISSN: 1543-8384. DOI: 10.1021/mp800049w. [Online]. Available: https://doi.org/10.1021/mp800049w.

[3] U. Del Monte, "Does the cell number 10(9) still really fit one gram of tumor tissue?" *Cell Cycle*, vol. 8, pp. 505–6, 2009.

[4] Y. Nakamura, A. Mochida, P. L. Choyke, and H. Kobayashi, "Nanodrug delivery: Is the enhanced permeability and retention effect sufficient for curing cancer?" *Bioconjugate Chemistry*, vol. 27, no. 10, pp. 2225–2238, 2016, ISSN: 1043-1802. DOI: 10.1021/acs.bioconjchem.6b00437. [Online]. Available: https://doi.org/10.1021/acs.bioconjchem.6b00437.

[5] J. Lemke, S. von Karstedt, J. Zinngrebe, and H. Walczak, "Getting trail back on track for cancer therapy," *Cell Death Differ*, vol. 21, no. 9, pp. 1350–64, 2014, ISSN: 1476-5403 (Electronic) 1350-9047 (Linking). DOI: 10.1038/cdd.2014.81. [Online]. Available: http://www.ncbi.nlm.nih.gov/pubmed/24948009.

[6] M. Liu, S. Guo, J. M. Hibbert, V. Jain, N. Singh, N. O. Wilson, and J. K. Stiles, "Cxcl10/ip-10 in infectious diseases pathogenesis and potential therapeutic implications," *Cytokine & growth factor reviews*, vol. 22, no. 3, pp. 121–130, 2011, ISSN: 1359-6101 1879-0305. DOI: 10.1016/j.cytogfr.2011.06.001. [Online]. Available: http://www.ncbi.nlm.nih.gov/pmc/articles/PMC3203691/.

[7] L. Pastor, A. Casellas, J. Carrillo, S. Alonso, E. Parker, L. Fuente-Soro, C. Jairoce, I. Mandomando, J. Blanco, and D. Naniche, "Ip-10 levels as an accurate screening tool to detect acute hiv infection in resource-limited settings,"

Scientific Reports, vol. 7, no. 1, p. 8104, 2017, ISSN: 2045-2322. DOI: 10.1038/s41598-017-08218-0. [Online]. Available: https://doi.org/10.1038/s41598-017-08218-0.

[8] C. A. Dinarello, "Immunological and inflammatory functions of the interleukin-1 family," *Annual Review of Immunology*, vol. 27, no. 1, pp. 519–550, 2009, ISSN: 0732-0582. DOI: 10.1146/annurev.immunol.021908.132612. [Online]. Available: https://doi.org/10.1146/annurev.immunol.021908.132612.

[9] S. L. Deshmane, S. Kremlev, S. Amini, and B. E. Sawaya, "Monocyte chemoattractant protein-1 (mcp-1): An overview," *J Interferon Cytokine Res*, vol. 29, no. 6, pp. 313–26, 2009, ISSN: 1079-9907. DOI: 10.1089/jir.2008.0027.

[10] T. Komastu, D. D. Ireland, and C. S. Reiss, "Il-12 and viral infections," *Cytokine Growth Factor Rev*, vol. 9, no. 3-4, pp. 277–85, 1998, ISSN: 1359-6101 (Print) 1359-6101.

[11] N. Koizumi, T. Yamaguchi, K. Kawabata, F. Sakurai, T. Sasaki, Y. Watanabe, T. Hayakawa, and H. Mizuguchi, "Fiber-modified adenovirus vectors decrease liver toxicity through reduced il-6 production," *The Journal of Immunology*, vol. 178, no. 3, pp. 1767–1773, 2007. DOI: 10.4049/jimmunol.178.3.1767. [Online]. Available: http://www.jimmunol.org/content/jimmunol/178/3/1767.full.pdf.

[12] M. C. Sprangers, W. Lakhai, W. Koudstaal, M. Verhoeven, B. F. Koel, R. Vogels, J. Goudsmit, M. J. Havenga, and S. Kostense, "Quantifying adenovirus-neutralizing antibodies by luciferase transgene detection: Addressing preexisting immunity to vaccine and gene therapy vectors," *J Clin Microbiol*, vol. 41, no. 11, pp. 5046–52, 2003, ISSN: 0095-1137 (Print) 0095-1137.

Chapter 4

Cloaking of Adeno-associated Virus

The use of AAVs for gene addition and gene editing has become a common approach in the lab and clinic. Currently, there are over 70 clinical trials that are active or recruiting with an intervention using an AAV vector. Each serotype of AAV has associated tropism (see 1.2.3) though most studies have focused on AAV2 since it is well characterized and has relatively broad tropsim. Similar to Ad, the success of AAV vectors in the clinic are influenced by tropism, liver clearance, and immune responses. Thus we tested applying the knowledge from Chapter 2 for silica encapsulation of AAV. In addition, we tested a novel method of using exosome membranes as a cloaking mechanism to form exosome-AAV nanoparticles.

4.1 Exosome-AAV Nanoparticles

The use of liposomes to encapsulate drugs, proteins, and other biologics is widespread in biotechnology. Liposomes are spherical vesicles comprised of a one or more lipid bilayers with an aqueous core. These lipids come is variety of forms, natural or synthetic, and are composed of hydrophobic tail and a hydrophilic head group. The amphiphilic (both hydrophobic and hydrophilic) nature of lipids allows them to self assemble into vesicle structures where the hydrophilic head groups orient toward the inside and outside of the bilayer in aqueous media. In general liposome preparation consists of three steps: drying down lipids from an organic solvent phase, reconstituting lipids in an aqueous phase to form vesicles, and then purifying or extruding vesicles to obtain the desired size. Encapsulation of a desired entity is controlled through the second step where the aqueous media contains the protein/drug/enzyme of interest. When PEGylated, liposomes have show significantly enhance circulation half-life of drugs in humans and has resulted in a handful of FDA approved formulations [1]. In the context of transfection, cationic liposomes have been used to enhance delivery of nucleic acids. Cationic formulations can be very effective *in vitro*, but have significant issues in *in vivo* applications that stem from the positive surface charge [2]. Recently, extracellular vesicles (EVs), which are essentially naturally occurring liposomes, have been shown to be efficient carriers of cellular information (Figure 4.1). We sought to use the membranes of naturally

derived EVs to form liposome-like nanoparticles that contain or associate with AAVs to enhance transduction and serve as a cloaking mechanism.

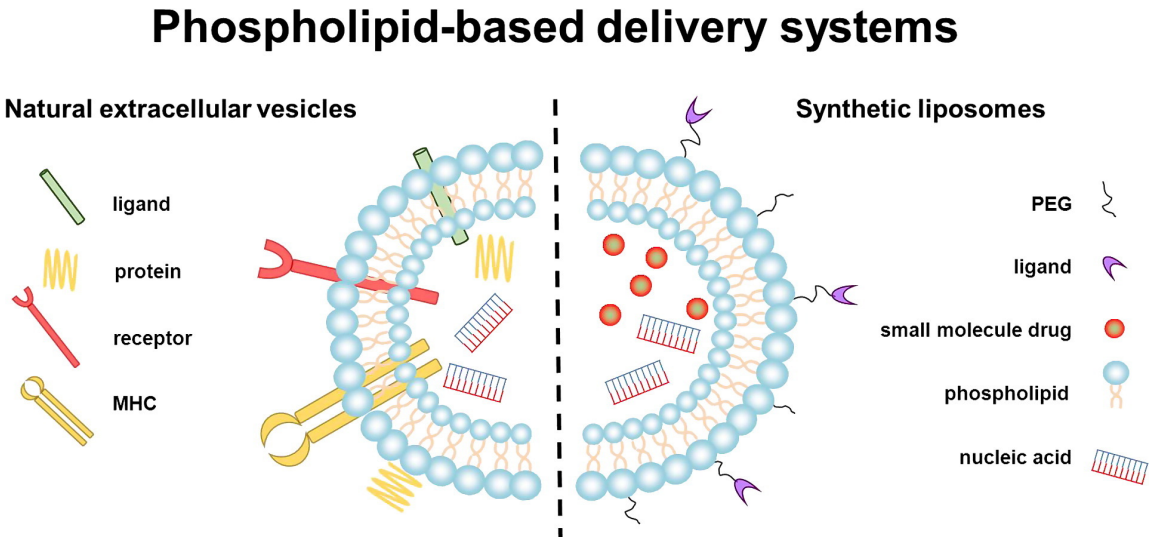

Figure 4.1: Natural exosomes and synthetic liposomes are similar. Reproduced with permission from [3], copyright Elsevier.

4.1.1 Exosomes

Exosomes are nanoscale vesicles which are a subset of extracellular vesicles (EVs) that are secreted by all cells. They are turning out to be interesting targets as therapeutic and diagnostic tools. Initially thought to be cellular debris, EVs have been found to contain RNA, proteins, and other signaling molecules [4]. Now the field classifies EVs as intercellular communicators that are capable of transmitting information from one cell to another and are implicated in tumorgenesis [5]. Recently, exosome associated AAVs have been found to enhance transduction of specific cells, both *in vitro* and *in vivo* [6]. These exosome associated AAVs were found during

the exosome purification process, which involves ultracentrifugation. Considering that AAVs (25 nm) and exosomes (25-100 nm) are similar in size, it is likely that these two entities are being collected together in the ultracentrifugation process and thus become "associated". Maguire et al. performed TEM on microvesicles and EVs that were collected from cells producing AAVs and also found AAVs associated with EVs, but it was not clear from the data published whether AAVs were physically encapsulated by EVs [7]. We sought to develop a technique to encapsulated AAVs in exosomes in a controlled manner by adapting methods used for the preparation of liposomes.

4.1.2 *Ex-vivo* Exosome-associated AAVs

First, we tested making exosome associated AAVs in a controlled manner *ex vivo*. Lyophilized exosomes derived from A549 cells was purchased from Galen Laboratory Supplies (HBM-A549-100/2). The product was diluted in 100μl sterile filtered water as a stock solution, which resulted in approximately 1x10^8 particles/μl. Each sample used 1μl of stock solution. For example, 1μl of stock solution was diluted in 10μl in water. To mimic exosome associated AAVs, we simply mixed reconstituted exosomes with AAV2 stock solutions and measured transduction. AAV2 was purchased from the Molecular Virology Support Core at Oregon Health Sciences University (Beaverton, OR) and was supplied at 4.9x10^{1}2 vg/ml stored in DPBS+35mM NaCl+5% glycerol. First, 11μl (1μl of stock solution diluted in 10μl water) of recon-

stituted exosomes were re-lyophilized to produce a pale white powder. This powder was reconstituted again using 10μl of AAV2 stock solution, hand mixed, and diluted to a final total volume of 50μl in PBS, sample labeled as ExoRecon. In addition, 11μl (1μl of stock solution diluted in 10μl water) of reconstituted exosomes was hand mixed with AAV2 stock solution and diluted in PBS, sampled labeled as ExoSTD. All samples were split and half of each sample was bath sonicated (QSonica, Newton, CT) on high power for 10 minutes. Samples were tested on A549 cells and transduction was measured using FACS (BD Aria Fusion) and confocal microscopy (Zeiss/Yokogawa CSU-X1) 48 hours post-transduction.

Hydrodynamic radius of each sample was measured using dynamic light scattering (DLS) (Figure 4.2). We found that ExoSTD AAV2 had a hydrodynamic radius of 67.3±2.7 nm and that ReconExo AAV2 had a radius of 76.7±2.7 nm. AAV2 alone was measured at 85.8±15.9 nm suggesting that without sufficient mixing, AAVs in 5% glycerol are slightly aggregated. Mixing of exosome membranes and AAVs did not result in large aggregates and these sub-100nm particles are ideal for transduction, possibly amenable to IV delivery.

We found that by simply mixing AAVs with exosomes or by reconstituting dried exosome content with an AAV2 solution resulted in enhanced transduction of cells (Figure 4.3 & 4.4). Sonication is a technique to disrupt lipid membranes and form unilamellar vesicles. In addition, it can be used to increase drug loading of liposomes. Here, we used sonication to disrupt reconstituted exosome membranes

		Size (d.nm):	% Intensity:	St Dev (d.nm):
Z-Average (d.nm): 273.7	Peak 1:	311.6	90.4	198.5
PdI: 0.357	Peak 2:	4507	9.6	887.7
Intercept: 0.901	Peak 3:	0.000	0.0	0.000
Result quality : Good				

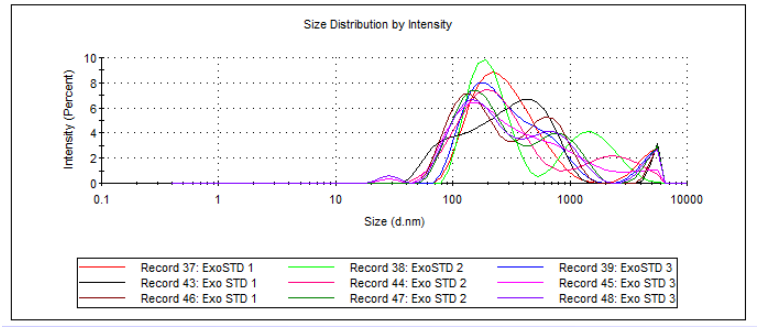

(a) Exosome standard in PBS

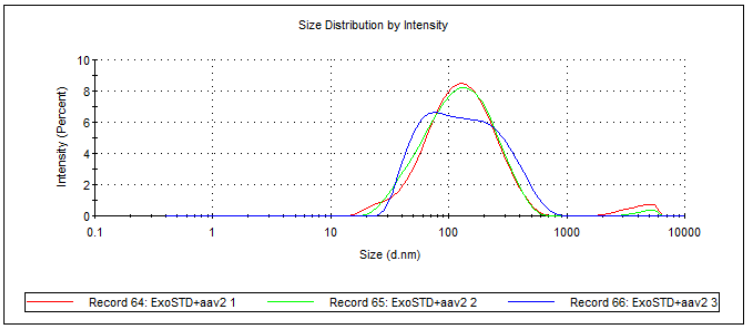

(b) Exosome standard mixed with AAV2

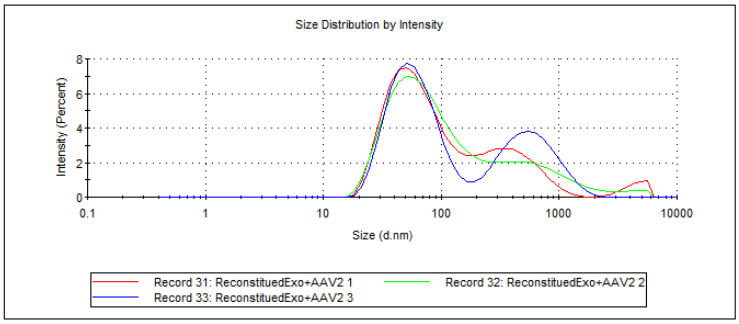

(c) Dried lyophilized exosomes reconstituted with AAV2

Figure 4.2: Hydrodynamic Radius of Exosome Associated AAV2

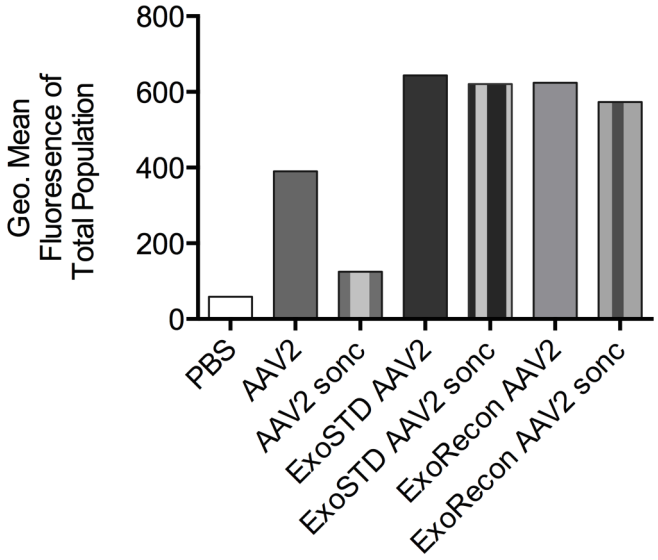

Figure 4.3: Exosome associated AAVs made *ex vivo* show enhanced transduction and protection against bath sonication measured with FACS. ExoSTD AAV2: reconstituted exosomes mixed with AAV2. ExoRecon AAV2: dried lyophilized exosomes mixed with AAV2.

and to potentially increase the association with AAVs. Interestingly, bath sonication of AAV2 alone significantly reduced transduction whereas sonication had little effect on exosome associated AAVs. This data suggests that sonication is powerful enough to disrupt AAV capsids, but for exosome associated AAVs the exosome membrane is shielding capsids from this effect. Further TEM analysis can reveal how AAVs are associated with exosomes using this simple method.

4.1.3 Exosome Membrane Liposomes with AAV2

Standard techniques to produce liposomes use lipids which are solubilized in organic solvents. The lipids are extracted by removing the solvent using a vacuum or simple evaporation and then further desiccated to remove all residual solvent.

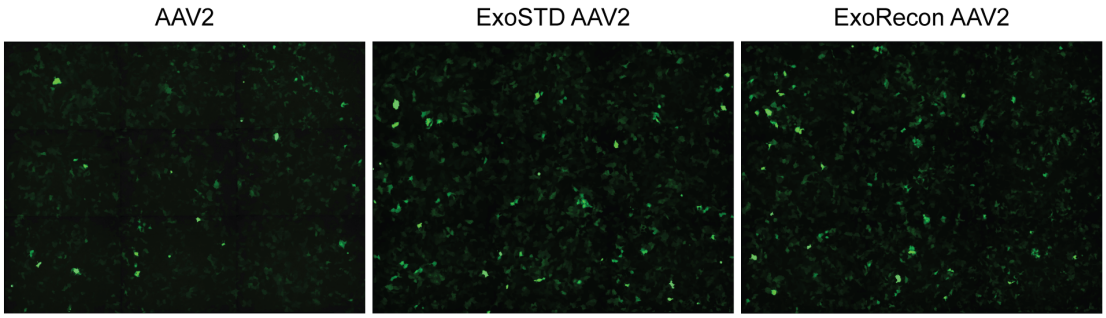

Figure 4.4: Exosome associated AAVs made *ex vivo* show enhanced transduction measured by confocal microscopy. ExoSTD AAV2: reconstituted exosomes mixed with AAV2. ExoRecon AAV2: dried lyophilized exosomes mixed with AAV2.

Drying of lipids results in the formation of a thin film, which can then be hydrated in aqueous media to form lipid vesicles [8]. We applied this simple technique to extract lipids and associated content from exosomes. Lyophilized exosomes derived from A549 cells was purchased from Galen Laboratory Supplies (HBM-A549-100/2). The product was diluted in 100μl sterile filtered water as a stock solution stored at 4C. To solubilize the lipids and exosomal contents, an aliquot of stock solution was lyophilized to a dry white powder in a glass vial. This powder was then dissolved in 50μl of either ethanol (EtOH) or chloroform (CHCl3). Both solvents are regularly used as a solvent for lipids and we found that exosomes were also soluble in both solvents with vortexing and bath sonication. The solvent was then removed under vacuum and further desiccated to produce a thin film. This film was then rehydrated with an AAV2 solution diluted in PBS and mixed by hand. Samples were tested on T98G cells and transduction was measured using confocal microscopy. Note that exosomes were derived from A549.

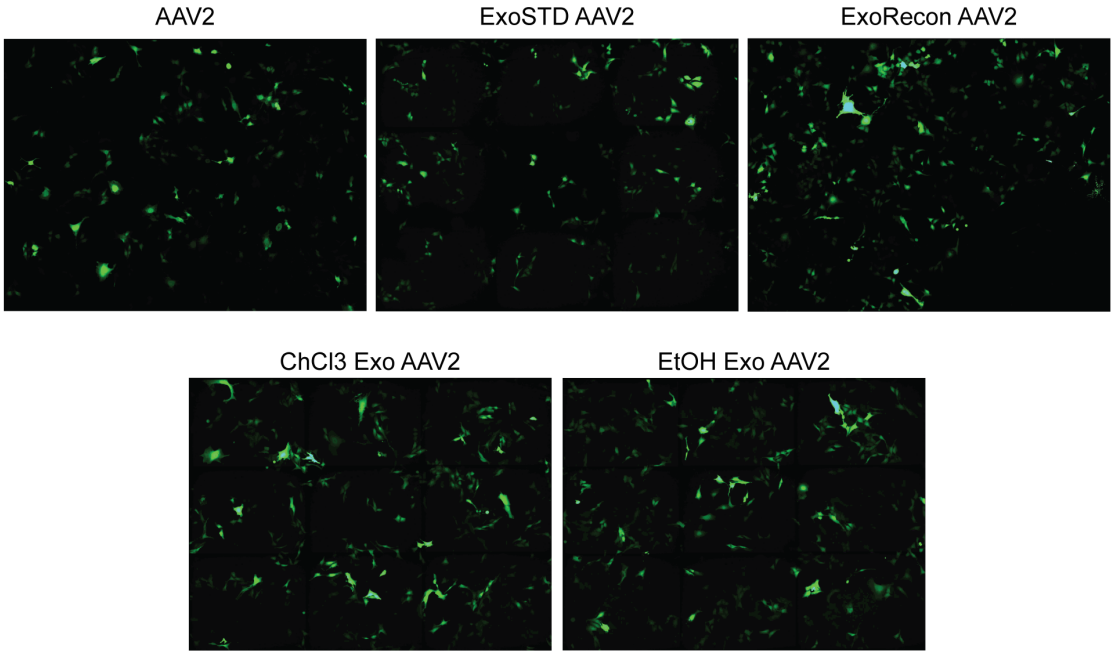

Figure 4.5: Transduction of rehydrated exosomes with AAV2 tested on T98G cells.

We found that rehydrating exosomal contents with an AAV2 solution enhanced transduction on T98G cells. AAV2 alone had low levels of transduction, grayscale mean = 2.1, which was slightly aided by mixing with exosomes in solution, grayscale mean = 7.3, see sample labeled "ExoSTD AAV2" (Figure 4.5). This is similair to exosome associated AAVs. Both samples generated from thin film hydration,"ExoEtOH AAV2" from ethanol and "ExoChCl3 AAV2" from choloroform, using an AAV2 solution showed enhanced transduction with grayscale mean values of 10.7 and 10.8, respectively (Figure 4.5). This suggests that thin film hydration allows the exosome membrane to encapsulate AAV virions and enhance cellular uptake. The literature suggests that exosomes can be very specific delivery vehicles, though here we saw that A549 exosomes are capable of delivering to T98G cells.

This is supported by other studies that showed there are degrees of specificity, where exosomes from one cell line are capable of transfecting other cell lines [9].

Overall, this preliminary data suggests that exosomes can enhance AAV transduction *in vitro* whether simply through association or as a liposomal formulation. Further studies need to be performed to show that AAVs are physically encapsulated in exosomes made as a liposomal formulation. An indirect measure of encapsulation would be to use an AAV that has narrower tropism and show that exosome encapsulation expands this tropsim to cells not normally transduced by AAV alone. In addition, the effect of solvents on exosome membrane proteins and exosome contents was unexplored. Potentially harsh solvents can denature proteins, rendering them non-functional though the results above suggest otherwise.

4.2 Silica-AAV Nanoparticles

Taking what we learned from silica encapsulation of adenovirus (Ad), we briefly tested silica encapsulation of AAVs using the same method as described in Chapter 2 of this dissertation. AAVs are composed of a pure capsid protein structure that is similar to Ad and thus can be used for template driven silica deposition. The zeta potential of AAV2 was measured as approximately -20 mV making it amenable to cationic PLL masking through electrostatic interactions. Similar to SiAd synthesis, 5μl of AAV2 stock solution at 4.9x10^{1}1 vg/ml (Oregon National Primate Research Center, Beaverton, OR) was incubated with 1.5μl PLL solution (300k+ MW 0.1% w/v) for 15 minutes and bath sonicated for 3 minutes on low power. TMOS was hydrolyzed to form silicic acid and 1.5 μl of 3.6% v/v silicic acid was added. The total reaction volume was diluted to 30μl in 0.05x PBS and vortexed at RT for 2.5 hours. Samples were tested on HeLa cells at various MOIs and fluorescence was measured using confocal microscopy (Zeiss/Yokogawa CSU-X1) at 48 hours post-transduction.

Characterization of particles using DLS and transmission electron microscopy (TEM) revealed conflicting results. By DLS (Zetasizer Nano) we measured the hydrodynamic radius of AAV2 at 43.5 $\pm$ 3nm and of SiAAV2 at 39.3 $\pm$ 1.8nm (Figure 4.6). Neat AAV2 theoretically has a diameter of about 25nm suggesting that AAV2 is slightly aggregated in solution. Surprisingly, SiAAV2 was measured as having a similar size by DLS, which at first suggested that silica encapsulation did not occur.

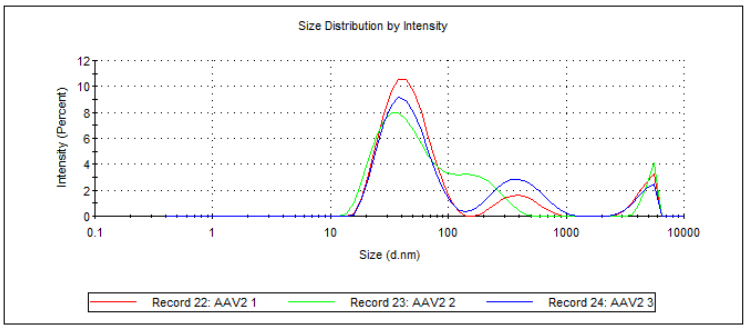

(a) Hydrodynamic Radius of AAV2

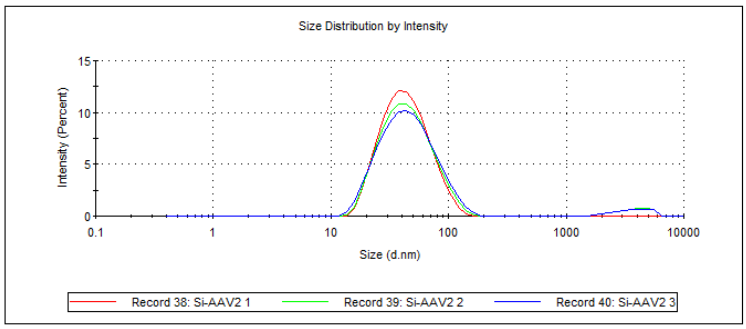

(b) Hyrdrodynamic Radius of SiAAV2

Figure 4.6: Hydrodynamic Radius of Silica Encapsulated AAV2

Using TEM we found large aggregates of particles for both AAV2 and SiAAV2 (Figure 4.7). These aggregates are possibly due to the drying of particles on the grid. Similar aggregate structures, on the order of hundreds on nanometers, with sinew-like connections were found in both samples. These large structures are in contrast to the DLS data above. Similar to previous TEM studies, imaging of AAV2 required the use of negative stain (uranyl acetate), however SiAAV2 was imaged without the use of negative stain, confirming that silica was present. Unlike proteins and lipids silica provides sufficient electron density for electron microscopy.

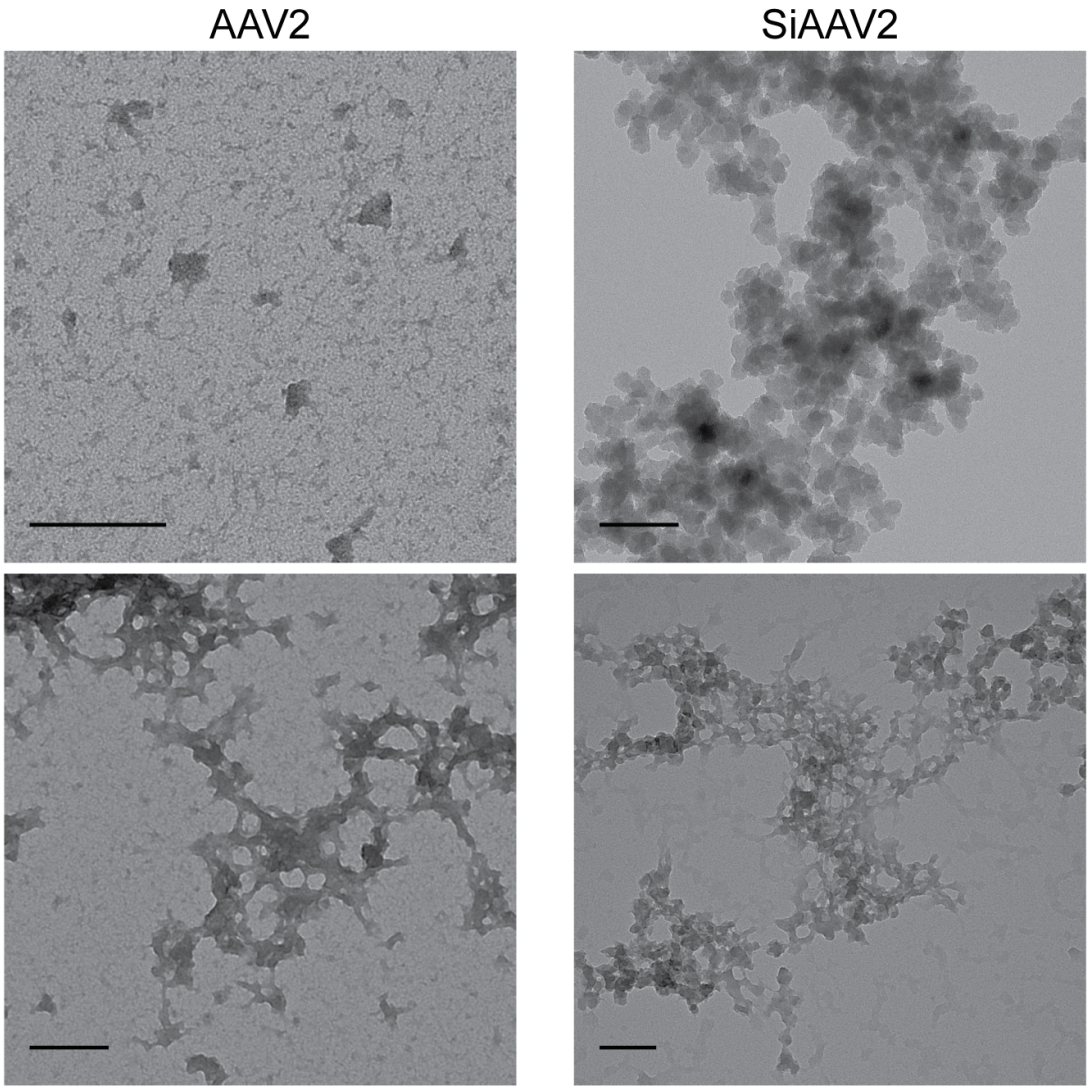

Figure 4.7: TEM of AAV2 stained with uranyl acetate and of SiAAV2 without the use of negative stain. Scale bars represent 100nm.

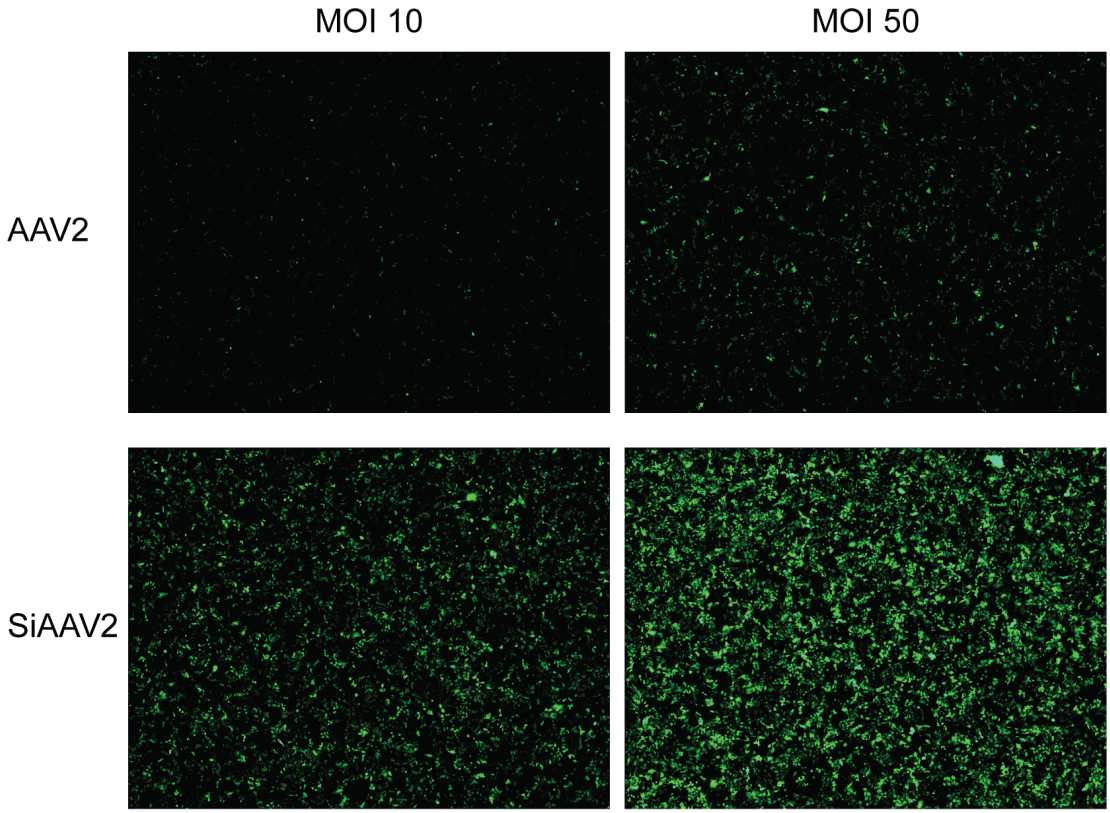

Figure 4.8: Enhanced transduction with SiAAV2 on HeLa cells as measured by confocal microscopy.

Particles were tested on HeLa cells and GFP fluoresence was measured at 48 hours. AAV2 is reported as having tropsim for HeLa [10]. We found that SiAAV2 significantly enhanced transduction at both MOIs tested (Figure 4.8). At the high MOI, mean grayscale values for AAV2 and SiAAV2 were 1.96 and 18.1, respectively. At the low MOI, mean grayscale values for AAV2 and SiAAV2 were 0.40 and 6.97, respectively. These preliminary experiments suggest that silica encapsulation of AAVs follows similar characteristics as encapsulation of Ads. Further optimization of silica reaction conditions needs to be explored.

4.3 Summary and Future Directions

The use of AAVs for gene therapy and for gene editing has exploded in the last ten years because AAVs have many ideal characteristics for *in vivo* applications. However, the barriers to clinical efficacy are similar to Ad: tropsim limits or defines AAV efficiency to cell types, liver clearance efficiently clears virions from the circulation, and immune responses both innate and adaptive limit the use of repeated injections, which are necessary. Encapsulation whether with an exosomal membrane or with silica was explored to address some of these challenges. Preliminary studies showed that both methods can enhance AAV transduction *in vitro*. The use of exosome membranes could allow for IV delivery without the use of PEG since exosomes are of human origin and can be patient derived. Future work will focus on testing CRISPR-CAS9 delivery using AAVs and showing efficacy in animal models. For gene editing *in vivo*, generally two viruses are used: one to deliver the Cas9 gene and another to deliver the guide RNA product and/or the donor DNA template. Either exosomal or silica encapsulation could enhance the delivery of both virions to the same cell and thus improve the efficiency of gene editing while reducing immunogenicity.

4.4 Acknowledgements

The dissertation author was the primary investigator and author of this material. I would like to thank Jonathan Flores for help with the TEM imaging of SiAAV2.

4.5 References: Chapter 4

[1] C. Zylberberg and S. Matosevic, "Pharmaceutical liposomal drug delivery: A review of new delivery systems and a look at the regulatory landscape," *Drug Delivery*, vol. 23, no. 9, pp. 3319–3329, 2016, ISSN: 1071-7544. DOI: 10.1080/10717544.2016.1177136. [Online]. Available: https://doi.org/10.1080/10717544.2016.1177136.

[2] S. A. L. Audouy, L. F. M. H. de Leij, D. Hoekstra, and G. Molema, "In vivo characteristics of cationic liposomes as delivery vectors for gene therapy," *Pharmaceutical Research*, vol. 19, no. 11, pp. 1599–1605, 2002, ISSN: 1573-904X. DOI: 10.1023/A:1020989709019. [Online]. Available: https://doi.org/10.1023/A:1020989709019.

[3] R. van der Meel, M. H. A. M. Fens, P. Vader, W. W. van Solinge, O. Eniola-Adefeso, and R. M. Schiffelers, "Extracellular vesicles as drug delivery systems: Lessons from the liposome field," *Journal of Controlled Release*, vol. 195, pp. 72–85, 2014, ISSN: 0168-3659. DOI: https://doi.org/10.1016/j.jconrel.2014.07.049. [Online]. Available: http://www.sciencedirect.com/science/article/pii/S0168365914005434.

[4] S. El Andaloussi, I. Mager, X. O. Breakefield, and M. J. A. Wood, "Extracellular vesicles: Biology and emerging therapeutic opportunities," *Nature Reviews Drug Discovery*, vol. 12, p. 347, 2013. DOI: 10.1038/nrd3978. [Online]. Available: http://dx.doi.org/10.1038/nrd3978.

[5] G. Camussi, M. C. Deregibus, S. Bruno, C. Grange, V. Fonsato, and C. Tetta, "Exosome/microvesicle-mediated epigenetic reprogramming of cells," *Am J Cancer Res*, vol. 1, no. 1, pp. 98–110, 2011, ISSN: 2156-6976 (Print) 2156-6976.

[6] B. Gyorgy, Z. Fitzpatrick, M. H. W. Crommentuijn, D. Mu, and C. A. Maguire, "Naturally enveloped aav vectors for shielding neutralizing antibodies and robust gene delivery in vivo," *Biomaterials*, vol. 35, no. 26, pp. 7598–7609, 2014,

ISSN: 0142-9612. DOI: https://doi.org/10.1016/j.biomaterials.2014.05.032. [Online]. Available: http://www.sciencedirect.com/science/article/pii/S0142961214005894.

[7] C. A. Maguire, L. Balaj, S. Sivaraman, M. H. Crommentuijn, M. Ericsson, L. Mincheva-Nilsson, V. Baranov, D. Gianni, B. A. Tannous, M. Sena-Esteves, X. O. Breakefield, and J. Skog, "Microvesicle-associated aav vector as a novel gene delivery system," *Mol Ther*, vol. 20, no. 5, pp. 960–71, 2012, ISSN: 1525-0016. DOI: 10.1038/mt.2011.303.

[8] H. Zhang, "Thin-film hydration followed by extrusion method for liposome preparation," *Methods Mol Biol*, vol. 1522, pp. 17–22, 2017, ISSN: 1064-3745. DOI: 10.1007/978-1-4939-6591-5_2.

[9] T. J. Smyth, J. S. Redzic, M. W. Graner, and T. J. Anchordoquy, "Examination of the specificity of tumor cell derived exosomes with tumor cells in vitro," *Biochimica et Biophysica Acta (BBA) - Biomembranes*, vol. 1838, no. 11, pp. 2954–2965, 2014, ISSN: 0005-2736. DOI: https://doi.org/10.1016/j.bbamem.2014.07.026. [Online]. Available: http://www.sciencedirect.com/science/article/pii/S000527361400279X.

[10] B. L. Ellis, M. L. Hirsch, J. C. Barker, J. P. Connelly, R. J. Steininger, and M. H. Porteus, "A survey of ex vivo/in vitro transduction efficiency of mammalian primary cells and cell lines with nine natural adeno-associated virus (aav1-9) and one engineered adeno-associated virus serotype," *Virology Journal*, vol. 10, pp. 74–74, 2013, ISSN: 1743-422X. DOI: 10.1186/1743-422X-10-74. [Online]. Available: http://www.ncbi.nlm.nih.gov/pmc/articles/PMC3607841/.

Appendix A

Final notes

We have shown that taking methods and materials from the nanoparticle field can augment the delivery viral vectors for therapeutic applications. In a sense these methods are allowing us to surpass viral evolution by enhancing transduction of cells independent of receptor-ligand transduction. There is still significant work to be done on further designing silica based coatings to not only enhance transduction, but also to add back desired specificity through silanol chemistry. We used adenovirus (Ad) as an ideal model system, but cloaking technologies can be applied to other clinically relevant viral vectors such as adeno-associated virus (AAV) or the integrating, enveloped vector lentivirus. Cloaking technologies are promising for minimizing immune responses associated with viral vectors. Here, we showed that silica cloaking of Ad elicited no inflammatory cytokines and reduced the production of neutralizing antibodies. This result is also important for and applicable to AAV vectors, which are commonly being tested for gene therapy therapies. For example, we can combine

multiple vectors into a single entity to improve efficiency with cloaking attributes. This is especially pertinent for therapies based off genome editing, which require multiple components to be delivered in a single cell. *In vivo* genome editing use AAVs is currently inefficient due to this factor. In addition, the production of neutralizing antibodies prevents re-administration of the vectors. The combination of synthetic and biologic components allows us to address issues associated with both and to exploit synergy for meaningful outcomes. This dissertation serves as a jumping off point for continuing work in this field and hopefully leads to advancements in the clinic.